Higgs potential in the type II seesaw model

A. Arhrib, R. Benbrik, M. Chabab, Gilbert Moultaka, M. C. Peyranere, L. Rahili, J. Ramadan

The Higgs Potential in the Type II Seesaw Model

A. Arhrib[1,2], R. Benbrik[2,3,4], M. Chabab[2],
G. Moultaka* [5,6], M. C. Peyranère[7,8], L. Rahili[2], J. Ramadan[2]

[1] *Département de Mathématiques, Faculté des Sciences et Techniques, Tanger, Morocco*
[2] *Laboratoire de Physique des Hautes Energies et Astrophysique*
Département de Physiques,Faculté des Sciences Semlalia,Marrakech, Morocco
[3] *Faculté Polydisciplinaire, Université Cadi Ayyad, Sidi Bouzid, Safi-Morocco*
[4] *Instituto de Fisica de Cantabria (CSIC-UC), Santander, Spain*
[5] *Université Montpellier 2, Laboratoire Charles Coulomb UMR 5221,*
F-34095 Montpellier, France
[6] *CNRS, Laboratoire Charles Coulomb UMR 5221, F-34095 Montpellier, France*
[7] *Université Montpellier 2, Laboratoire Univers & Particules de Montpellier UMR 5299,*
F-34095 Montpellier, France
[8] *CNRS/IN2P3, Laboratoire Univers & Particules de Montpellier UMR 5299,*
F-34095 Montpellier, France

July 7, 2011

Abstract

The Standard Model Higgs sector, extended by one weak gauge triplet of scalar fields with a very small vacuum expectation value, is a very promising setting to account for neutrino masses through the so-called type II seesaw mechanism. In this paper we consider the general renormalizable doublet/triplet Higgs potential of this model. We perform a detailed study of its main dynamical features that depend on five dimensionless couplings and two mass parameters after spontaneous symmetry breaking, and highlight the implications for the Higgs phenomenology. In particular, we determine *i)* the complete set of tree-level unitarity constraints on the couplings of the potential and *ii)* the exact tree-level *all directions* boundedness from below constraints on these couplings. When combined, these constraints delineate precisely the theoretically allowed parameter space domain within our perturbative approximation. Among the seven physical Higgs states of this model, the mass of the lighter (heavier) $\mathcal{CP}_{even}$ state h^0 (H^0) will always satisfy a theoretical *upper (lower) bound* that is reached for a critical value μ_c of μ (the mass parameter controlling triple couplings among the doublet/triplet Higgses). Saturating the unitarity bounds we find an upper bound $m_{h^0} < \mathcal{O}(0.7-1\text{TeV})$, while the upper bound for the remaining Higgses lies in the several tens of TeV. However, the actual masses can be much lighter. We identify two regimes corresponding to $\mu \gtrsim \mu_c$ and $\mu \lesssim \mu_c$. In the first regime the Higgs sector is typically very heavy and only h^0 that becomes SM-like could be accessible to the LHC. In contrast, in the second regime, somewhat overlooked in the literature, most of the Higgs sector is light. In particular, the heaviest state H^0 becomes SM-like, the lighter states being the $\mathcal{CP}_{odd}$ Higgs, the (doubly) charged Higgses and a decoupled h^0, possibly leading to a distinctive phenomenology at the colliders.

*corresponding author

1 Introduction

One of the major goals of the LHC is to uncover the mechanism underlying the electroweak symmetry breaking and thereby the origin of the weak gauge boson and fermion masses. Moreover, observation of neutrino oscillations has shown that neutrinos are massive (for a review see for instance [1] and references therein). Such masses do not necessarily require physics beyond the standard model (SM), since one can accommodate a (Dirac) mass through a Yukawa coupling assuming a right-handed neutrino similarly to the other massive fermions. However, the introduction of such a right-handed state, whose only role is to allow for non-zero neutrino masses while being neutral under all the SM interactions, might seem rather mysterious. Furthermore, in contrast with the other right-handed fermion states of the SM, the right-handed neutrino allows also for a Majorana mass that is invariant under the SM gauge group but violates lepton number. These features make plausible the existence of new flavor physics beyond the SM associated with the neutrino sector. Probably, one of the most attractive aspects is the ability to induce naturally the tiny neutrino masses from this new flavor physics sector [2]. The celebrated seesaw mechanism [3, 4, 5] relating directly the smallness of the neutrino masses to the presence of a large new scale Λ through $m_\nu \sim v^2/\Lambda$, when $\Lambda \gg v$ where v denotes the electroweak scale, is realized in a grand unified context (GUT) comprising right-handed neutrinos and often dubbed *type I seesaw*. It can also be achieved without right-handed neutrinos through an extended Higgs sector including an $SU(2)_L$ triplet scalar field, *type II seesaw* [6, 7, 8, 9, 10], or by including two extra matter multiplets in the adjoint of $SU(2)_L$, *type III seesaw* [11], or a hybrid type mixture of *type I* and *type III* [12, 13, 14, 15].

If such extended sectors are too heavy to be directly accessible to TeV scale experiments, they could still be indirectly probed through distinctive low energy effective operators in the neutrino sector [16]. In the present paper we will rather focus on the possibility of accessing directly the Higgs sector *per se* of the *type II* scenario, studying general dynamical constraints which originate from the potential that couples the Higgs doublet and the Higgs triplet. However, given the present theoretical uncertainties, we do not commit to any specific GUT or flavor physics scenarios beyond the SM. In particular mass parameters such as μ and M_Δ will not necessarily take large GUT scale values, even though such a configuration is included in the analysis. We will even consider regimes with very small μ ($\ll G_F^{-1/2}$). As noted in [17], such a small μ makes all the Higgs sector accessible to the LHC. Here we carry out a complete study, taking into account the full set of renormalizable operators present in the potential. The aim is to exhibit the various possible regimes consistent with the *dynamical constraints* dictated by the potential and their consequences on the phenomenology of the extended Higgs sector. Most of these operators are often neglected in the existing phenomenological studies of *type II seesaw*, based on the fact that after spontaneous symmetry breaking their effects are suppressed by the small Higgs triplet vacuum expectation value (VEV), v_t, when compared to the electroweak scale. This is, however, not justified when studying the small μ regimes just mentioned, where μ can be of order v_t. In this case the detailed dynamics leads to an interesting structure of the Higgs sector.

The paper is organized as follows: in section 2, we present the ingredients of the model, the physical Higgs states and mass spectrum, as well as a parameterization of the potential parameters in terms of the physical masses. In section 3, we discuss some of the phenomenological and theoretical constraints on the parameters related to precision measurements, the absence of tachyonic Higgs modes, as well as the presence of false vacua. In section 4, we provide a thorough study of the boundedness from below of the potential and

establish for the first time simple necessary and sufficient conditions on the couplings that are valid for *all field directions*. The unitarity constraints are analyzed in detail in section 5, through the study of all the scalar scattering channels. In section 6, we combine in an analytical compact form the constraints obtained in sections 4 and 5. Section 7 presents the behavior of the $\mathcal{CP}_{even}$ Higgs masses as functions of the potential parameters, highlighting theoretical upper and lower mass bounds and identifying different regimes that give better insight into the overall Higgs sector phenomenology, as well as the determination of unitarity mass bounds on the lightest Higgs. Section 8 is devoted to a short review of the salient features of the Higgs phenomenology at the colliders as well as to specific illustrations of our results. We conclude in section 9 and give some technical details in the appendices.

2 The model

We start by recalling the scalar potential and the main properties of the Higgs physical eigenstates after EWSB as well as the corresponding eigenmasses and mixing angles. We give the expressions without neglecting any of the couplings appearing in Eq. (2.4) nor making any specific assumption about the magnitudes of μ, m_H^2 and M_Δ^2 which would originate from the unknown underlying high energy theory. The results of this section fix the notations and will serve for the completely model-independent analysis carried out in the subsequent sections.

2.1 The Higgs potential

The scalar sector consists of the standard Higgs weak doublet H and a colorless scalar field Δ transforming as a triplet under the $SU(2)_L$ gauge group with hypercharge $Y_\Delta = 2$, so that $H \sim (1,2,1)$ and $\Delta \sim (1,3,2)$ under the $SU(3)_c \times SU(2)_L \times U(1)_Y$.

Under a general gauge transformation $\mathcal{U}(x)$, H and Δ transform as $H \to \mathcal{U}(x)H$ and $\Delta \to \mathcal{U}(x)\Delta\mathcal{U}^\dagger(x)$. One can then write the most general renormalizable and gauge invariant Lagrangian of this scalar sector as follows:

$$\mathcal{L} = (D_\mu H)^\dagger (D^\mu H) + Tr(D_\mu \Delta)^\dagger (D^\mu \Delta) - V(H,\Delta) + \mathcal{L}_{\text{Yukawa}} \tag{2.1}$$

where the covariant derivatives are defined by

$$D_\mu H = \partial_\mu H + igT^a W_\mu^a H + i\frac{g'}{2} B_\mu H \tag{2.2}$$

$$D_\mu \Delta = \partial_\mu \Delta + ig[T^a W_\mu^a, \Delta] + ig'\frac{Y_\Delta}{2} B_\mu \Delta \tag{2.3}$$

(W_μ^a, g), and (B_μ, g') denoting respectively the $SU(2)_L$ and $U(1)_Y$ gauge fields and couplings and $T^a \equiv \sigma^a/2$, with σ^a ($a = 1,2,3$) the Pauli matrices. The potential $V(H,\Delta)$ is given by,

$$\begin{aligned} V(H,\Delta) = &-m_H^2 H^\dagger H + \frac{\lambda}{4}(H^\dagger H)^2 + M_\Delta^2 Tr(\Delta^\dagger\Delta) + [\mu(H^T i\sigma^2 \Delta^\dagger H) + \text{h.c.}] \\ &+\lambda_1 (H^\dagger H) Tr(\Delta^\dagger\Delta) + \lambda_2 (Tr\Delta^\dagger\Delta)^2 + \lambda_3 Tr(\Delta^\dagger\Delta)^2 + \lambda_4 H^\dagger \Delta\Delta^\dagger H \end{aligned} \tag{2.4}$$

where Tr is the trace over 2×2 matrices. $\mathcal{L}_{\text{Yukawa}}$ contains all the Yukawa sector of the SM plus one extra Yukawa term that leads after spontaneous symmetry breaking to (Majorana) mass terms for the neutrinos, without requiring right-handed neutrino states,

$$\mathcal{L}_{\text{Yukawa}} \supset -Y_\nu L^T C \otimes i\sigma^2 \Delta L + \text{h.c.} \tag{2.5}$$

where L denotes $SU(2)_L$ doublets of left-handed leptons, Y_ν denotes neutrino Yukawa couplings, C the charge conjugation operator, and we have suppressed falvor indices for simplicity. Although part of the type II seesaw model, we will refer to the above model Eq. (2.1) as the doublet-triplet-Higgs-Model (DTHM) since in this paper we are mainly interested in the scalar sector, bringing up only occasionally the content of the Yukawa sector $\mathcal{L}_{\text{Yukawa}}$ and the related neutrino masses issue.

Defining the electric charge as usual, $Q = I_3 + \frac{Y}{2}$ where I denotes the isospin, we write the two Higgs multiplets in components as,

$$\Delta = \begin{pmatrix} \delta^+/\sqrt{2} & \delta^{++} \\ \delta^0 & -\delta^+/\sqrt{2} \end{pmatrix} \quad \text{and} \quad H = \begin{pmatrix} \phi^+ \\ \phi^0 \end{pmatrix} \tag{2.6}$$

where we have used for convenience the 2×2 traceless matrix representation for the triplet.[1]

The potential defined in Eq. (2.4) exhausts all possible gauge invariant renormalizable operators. For instance a term of the form $\lambda_5 H^\dagger \Delta^\dagger \Delta H$, which would be legitimate to add if Δ contained a singlet component, can actually be projected on the λ_1 and λ_4 operators appearing in Eq. (2.4) thanks to the identity $H^\dagger\Delta^\dagger\Delta H + H^\dagger\Delta\Delta^\dagger H = H^\dagger H Tr(\Delta^\dagger\Delta)$ which is valid because Δ is a traceless 2×2 matrix. This simply amounts to redefining λ_1 and λ_4 such as $\lambda_1 + \lambda_5 \to \lambda_1,\ \lambda_4 - \lambda_5 \to \lambda_4$. The potential thus depends on five independent dimensionless couplings λ and $\lambda_i, (i = 1, ...4)$ and three mass parameters, m_H^2, M_Δ^2 and μ. In the present paper we will assume all these parameters to be real valued. Indeed, apart from the μ term, all other operators in V are self-conjugate so that, by hermiticity of the potential, only the real parts of the λ's and the m_H^2, M_Δ^2 mass parameters will be relevant. As for μ, the only parameter that can pick up a would-be CP phase, this phase is unphysical and can always be absorbed in a redefinition of the fields H and Δ. One thus concludes that the DTHM Lagrangian is CP conserving (see also the discussion in [18]). Moreover, V depends on five complex (or ten real) scalar fields.

Assuming that spontaneous electroweak symmetry breaking (EWSB) is taking place at some electrically neutral point in the field space, and denoting the corresponding VEVs by

$$\langle\Delta\rangle = \begin{pmatrix} 0 & 0 \\ v_t/\sqrt{2} & 0 \end{pmatrix} \quad \text{and} \quad \langle H\rangle = \begin{pmatrix} 0 \\ v_d/\sqrt{2} \end{pmatrix} \tag{2.7}$$

one finds after minimization of the potential Eq.(2.4) the following necessary conditions :

$$M_\Delta^2 = \frac{2\mu v_d^2 - \sqrt{2}(\lambda_1+\lambda_4)v_d^2 v_t - 2\sqrt{2}(\lambda_2+\lambda_3)v_t^3}{2\sqrt{2}v_t} \tag{2.8}$$

$$m_H^2 = \frac{\lambda v_d^2}{4} - \sqrt{2}\mu v_t + \frac{(\lambda_1+\lambda_4)}{2}v_t^2 \tag{2.9}$$

Even though, as we noted above, CP symmetry is realized at the level of the Lagrangian, there remains in principle the possibility for a spontaneous breakdown of this symmetry,

[1]Note that the electric charge assignments for the upper and lower component fields are only conventional and can be interchanged by taking $Y_\Delta = -2, Y_H = -1$, entailing an exchange of the upper and lower components of the fermion weak doublets, without affecting the physical content. This seemingly trivial statement is important to keep in mind when discussing possible electric charge breaking minima of the potential.

an issue which we do not address in this paper. We can thus choose in the sequel v_d and v_t to be real valued; that is, we consider only CP conserving vacua for which complex valued v_d and/or v_t can always be rotated simultaneously to real values through some unphysical phase redefinition of the fields.

These equations, to which we will refer as the EWSB conditions, ensure that the vacuum corresponds to an extremum of the potential, [that is $\partial V/\partial \eta_i|_{\Delta=\langle\Delta\rangle,H=\langle H\rangle} = 0$ for each of the ten real-valued field components denoted here by $\eta_i, (i = 1, ...10)$], but one would still need to check that this extremum is indeed a stable, albeit local, minimum. The corresponding extra conditions are nothing else but the absence of tachyonic modes in the Higgs sector, to be considered in a later section. We just anticipate here that the latter conditions will enforce the signs of μ and v_t to be identical. We can thus choose in the sequel $v_t > 0$, $\mu > 0$ without loss of generality. Furthermore, the two free parameters m_H^2 and M_Δ^2 can now be traded for v_d and v_t through Eqs. (2.8, 2.9). In the rest of the paper we will take the eight parameters of the potential as being λ, $\lambda_i, (i = 1, ...4)$, μ, v_d and v_t; requiring the correct electroweak scale will put the further constraint $v \equiv \sqrt{v_d^2 + 2v_t^2} = 246\text{GeV}$ on v_d, v_t, reducing this set of free parameters down to seven.

Let us also note that the above EWSB conditions will not necessarily imply that the gauge symmetric vacuum (*i.e.* at $\eta_i = 0$) is unstable. Indeed the latter instability requires that $M_\Delta^2 < 0$ and/or $m_H^2 > 0$ which are not guaranteed by Eqs. (2.8, 2.9). Even more so, regimes with large μ will lead through the EWSB conditions to a very narrow gauge symmetric local minimum(!) so that metastability issues might have to be considered. [More comments about the structure of the vacua of the model will be deferred to section 3.3.]

On the other edge of the spectrum, very small values of μ could be favored if one requires the lepton number not to be strongly violated. Indeed, the μ term in Eq.(2.4) is the only source of lepton number violation at the Lagrangian level and *before* spontaneous EWSB. If this term is absent the Yukawa term Eq. (2.5) together with the other standard Yukawa terms imply a conserved lepton number (where the Δ and H Higgs fields carry respectively the lepton numbers $l_\Delta = -2$ and $l_H = 0$).[2] Then, from the lepton number assignment for H and Δ it follows that the μ term violates lepton number by two units. However, this violation is soft since the μ-induced lepton number violating processes (corresponding either to loop suppressed $2 \to 2$ processes or to propagator suppressed multi-particle processes) will have to involve both the standard and neutrino Yukawa couplings . These features suggest that if the two seemingly independent sources of lepton number violation, namely the Δ VEV and μ, are assumed to have a common origin such as some spontaneous symmetry breaking of an underlying flavor theory, then it is natural to expect $\mu = \mathcal{O}(v_t)$ up to possible Yukawa coupling factors.

2.2 Higgs masses and mixing angles

The 10×10 squared mass matrix

$$\mathcal{M}^2 = \frac{1}{2}\frac{\partial^2 V}{\partial \eta_i^2}|_{\Delta=\langle\Delta\rangle,H=\langle H\rangle} \tag{2.10}$$

can be recast, using Eqs.(2.8, 2.9), in a block diagonal form of one doubly-degenerate

[2]The processes mediated by Eq. (2.5) and involving Higgs triplet decay or exchange are sometimes misleadingly dubbed 'lepton number violating'. One can check that the net overall lepton number of any process, comprising such decays or exchange, is conserved. This global symmetry will be violated only spontaneously when Δ acquires a VEV, that is when the Majorana mass is induced from (2.5).

eigenvalue $m^2_{H^{\pm\pm}}$ and four 2×2 matrices denoted in the following by $\mathcal{M}^2_{\pm}, \mathcal{M}^2_{\mathcal{CP}_{even}}$ and $\mathcal{M}^2_{\mathcal{CP}_{odd}}$.

Mass of the doubly-charged field:

The double eigenvalue $m^2_{H^{\pm\pm}}$ corresponds to the doubly charged eigenstate $\delta^{\pm\pm}$ and could also be obtained directly by collecting all the coefficients of $\delta^{++}\delta^{--}$ in the potential. It reads

$$m^2_{H^{\pm\pm}} = \frac{\sqrt{2}\mu v_d^2 - \lambda_4 v_d^2 v_t - 2\lambda_3 v_t^3}{2v_t} \tag{2.11}$$

From now on we will denote the doubly charged mass eigenstates $\delta^{\pm\pm}$ by $H^{\pm\pm}$.

Mass of the singly-charged field:

The mass-squared matrix for the singly charged field is:

$$\mathcal{M}^2_{\pm} = (\sqrt{2}\mu - \frac{\lambda_4 v_t}{2}) \begin{pmatrix} v_t & -v_d/\sqrt{2} \\ -v_d/\sqrt{2} & v_d^2/2v_t \end{pmatrix}$$

This matrix is diagonalized by the following matrix $\mathcal{R}_{\beta'}$, given by :

$$\mathcal{R}_{\beta'} = \begin{pmatrix} \cos\beta' & -\sin\beta' \\ \sin\beta' & \cos\beta' \end{pmatrix} \tag{2.12}$$

where β' is a rotation angle. Among the two eigenvalues of $\mathcal{M}^2_{\pm}$, one is zero and corresponds to the charged Goldstone boson $G^{\pm}$ while the other corresponds to the singly charged Higgs boson $H^{\pm}$ and is given by

$$m^2_{H^{\pm}} = \frac{(v_d^2 + 2v_t^2)[2\sqrt{2}\mu - \lambda_4 v_t]}{4v_t} \tag{2.13}$$

The mass eigenstates $H^{\pm}$ and $G^{\pm}$ are rotated from the Lagrangian fields $\phi^{\pm}, \delta^{\pm}$ and defined by

$$G^{\pm} = \cos\beta' \phi^{\pm} + \sin\beta' \delta^{\pm} \tag{2.14}$$
$$H^{\pm} = -\sin\beta' \phi^{\pm} + \cos\beta' \delta^{\pm} \tag{2.15}$$

The diagonalization of $\mathcal{M}^2_{\pm}$ leads to the following relations involving the rotation angle β':

$$\frac{v_d^2}{2v_t}[\sqrt{2}\mu - \frac{\lambda_4 v_t}{2}] = \cos^2\beta' M^2_{H^{\pm}} \tag{2.16}$$
$$\frac{v_d}{\sqrt{2}}[\sqrt{2}\mu - \frac{\lambda_4 v_t}{2}] = \frac{\sin 2\beta'}{2} M^2_{H^{\pm}} \tag{2.17}$$
$$v_t[\sqrt{2}\mu - \frac{\lambda_4 v_t}{2}] = \sin^2\beta' M^2_{H^{\pm}} \tag{2.18}$$

These equations lead to a unique solution for $\sin\beta', \cos\beta'$ up to a global sign ambiguity. Indeed, Eq. (2.16) implies $\sqrt{2}\mu - \frac{\lambda_4 v_t}{2} > 0$ in order not have a tachyonic $H^{\pm}$ state and given

our convention of $v_t > 0$. Then it follows from Eq. (2.17) that $\sin\beta'$ and $\cos\beta'$ should have the same sign. One finds

$$\sin\beta' = \epsilon_{\beta'}\frac{\sqrt{2}v_t}{\sqrt{v_d^2+2v_t^2}} \quad , \quad \cos\beta' = \epsilon_{\beta'}\frac{v_d}{\sqrt{v_d^2+2v_t^2}} \tag{2.19}$$

with a sign freedom $\epsilon_{\beta'} = \pm 1$, and

$$\tan\beta' = \sqrt{2}\frac{v_t}{v_d} \tag{2.20}$$

Mass of the neutral fields:

The neutral scalar and pseudoscalar mass matrices read:

$$\mathcal{M}^2_{\mathcal{CP}_{even}} = \begin{pmatrix} A & B \\ B & C \end{pmatrix} \quad \text{and} \quad \mathcal{M}^2_{\mathcal{CP}_{odd}} = \sqrt{2}\mu \begin{pmatrix} 2v_t & -v_d \\ -v_d & v_d^2/2v_t \end{pmatrix} \tag{2.21}$$

where

$$A = \frac{\lambda}{2}v_d^2, \;\; B = v_d(-\sqrt{2}\mu + (\lambda_1+\lambda_4)v_t), \;\; C = \frac{\sqrt{2}\mu v_d^2 + 4(\lambda_2+\lambda_3)v_t^3}{2v_t} \tag{2.22}$$

These symmetric matrices are diagonalized by the following two orthogonal matrices :

$$\mathcal{R}_\alpha = \begin{pmatrix} \cos\alpha & -\sin\alpha \\ \sin\alpha & \cos\alpha \end{pmatrix} \quad \text{and} \quad \mathcal{R}_\beta = \begin{pmatrix} \cos\beta & -\sin\beta \\ \sin\beta & \cos\beta \end{pmatrix} \tag{2.23}$$

where α, β denote the rotation angles respectively in the $\mathcal{CP}_{even}$ and $\mathcal{CP}_{odd}$ sectors.[3] Upon diagonalization of $\mathcal{M}^2_{\mathcal{CP}_{even}}$ one obtains two massive even-parity physical states h^0 and H^0 defined by

$$h^0 = \;\; c_\alpha\, h + s_\alpha\, \xi^0 \tag{2.24}$$
$$H^0 = -s_\alpha\, h + c_\alpha\, \xi^0 \tag{2.25}$$

where h and ξ^0 are the real parts of the ϕ^0 and δ^0 fields shifted by their VEV values,

$$\phi^0 = \frac{1}{\sqrt{2}}(v_d + h + iZ_1) \quad \text{and} \quad \delta^0 = \frac{1}{\sqrt{2}}(v_t + \xi^0 + iZ_2). \tag{2.26}$$

The masses are given by the eigenvalues of $\mathcal{M}^2_{\mathcal{CP}_{even}}$ as follows,

$$m^2_{h^0} = \frac{1}{2}[A + C - \sqrt{(A-C)^2+4B^2}] \tag{2.27}$$
$$m^2_{H^0} = \frac{1}{2}[A + C + \sqrt{(A-C)^2+4B^2}] \tag{2.28}$$

[3]Hereafter, we will use the shorthand notations, $s_x \equiv \sin x$ and $c_x \equiv \cos x$, for all three angles α, β, β'.

so that $m_{H^0} > m_{h^0}$. Note that the lighter state h^0 is not necessarily the lightest of the Higgs sector (see section 7).

On the other hand, $\mathcal{M}^2_{\mathcal{CP}_{odd}}$ leads to one massive physical state A^0 and one massless Goldstone boson G^0 defined by:

$$A^0 = -s_\beta\, Z_1 + c_\beta\, Z_2 \tag{2.29}$$
$$G^0 = \quad c_\beta\, Z_1 + s_\beta\, Z_2 \tag{2.30}$$

with masses

$$m_A^2 = \frac{\mu(v_d^2 + 4v_t^2)}{\sqrt{2}v_t} \tag{2.31}$$

Knowing the above eigenmasses one can then determine the rotation angles α and β, which control the field content of the physical states, from the following diagonalization conditions:

1. $\underline{\mathcal{CP}_{even}}$:

$$C = s_\alpha^2 m_{h^0}^2 + c_\alpha^2 m_{H^0}^2 \tag{2.32}$$
$$B = \frac{\sin 2\alpha}{2}(m_{h^0}^2 - m_{H^0}^2) \tag{2.33}$$
$$A = c_\alpha^2 m_{h^0}^2 + s_\alpha^2 m_{H^0}^2 \tag{2.34}$$

2. $\underline{\mathcal{CP}_{odd}}$:

$$2\sqrt{2}\mu v_t = s_\beta^2 m_A^2 \tag{2.35}$$
$$\sqrt{2}\mu v_d = \frac{\sin 2\beta}{2} m_A^2 \tag{2.36}$$
$$\frac{\mu v_d^2}{\sqrt{2}v_t} = c_\beta^2 m_A^2 \tag{2.37}$$

Of course Eq. (2.32) should be equivalent to Eq. (2.34) upon use of $s_\alpha^2 + c_\alpha^2 = 1$ and Eqs. (2.27, 2.28), and similarly for Eqs. (2.35) and (2.37). Furthermore, $s_\alpha, c_\alpha, s_\beta, c_\beta$ will all be determined up to a global sign. There is however a difference between the two sectors. In the $\mathcal{CP}_{odd}$ sector s_β and c_β must have the same sign as can be seen from Eq.(2.36) and the fact that $\mu > 0$ (the latter being due to the absence of tachyonic A^0 state,Eq.(2.35)). One then obtains unambiguously

$$\tan\beta = \frac{2v_t}{v_d} \quad \text{and} \quad \tan 2\beta = \frac{4v_t v_d}{v_d^2 - 4v_t^2} \tag{2.38}$$

from Eqs. (2.35, 2.37), and

$$s_\beta = \epsilon_\beta \frac{2v_t}{\sqrt{v_d^2 + 4v_t^2}}\,, \qquad c_\beta = \epsilon_\beta \frac{v_d}{\sqrt{v_d^2 + 4v_t^2}} \tag{2.39}$$

with a sign freedom $\epsilon_\beta = \pm 1$.

In contrast, the relative sign between s_α and c_α in the $\mathcal{CP}_{even}$ sector depends on the values of μ as can be seen from Eqs.(2.33, 2.22). While they will have the same sign and $\tan\alpha > 0$ for most of the allowed μ and λ_1, λ_4 ranges, there will be a small but interesting

domain of small μ values and $\tan\alpha < 0$ which we discuss in detail in section 7. One obtains from Eqs. (2.32 - 2.34)

$$s_\alpha = -\frac{\epsilon_\alpha \epsilon}{\sqrt{2}}(1 + \frac{(A-C)}{\sqrt{(A-C)^2+4B^2}})^{1/2} \tag{2.40}$$

$$c_\alpha = \frac{\epsilon_\alpha}{\sqrt{2}}(1 - \frac{(A-C)}{\sqrt{(A-C)^2+4B^2}})^{1/2} \tag{2.41}$$

where $\epsilon_\alpha = \pm 1$ and $\epsilon \equiv \text{sign}[B]$, and

$$\tan 2\alpha = \frac{2B}{A-C} \tag{2.42}$$

Let us finally note that the angles β and β' are correlated since they depend exclusively on v_d and v_t. For instance one always has

$$\tan\beta = \sqrt{2}\tan\beta' \tag{2.43}$$

as can be seen from Eqs.(2.20, 2.38).

Lagrangian parameters from physical masses and couplings:

The full experimental determination of the DTHM would require not only evidence for the neutral and (doubly) charged Higgs states but also the experimental determination of the masses and couplings of these states among themselves as well as to the gauge and matter sectors of the model. Crucial tests would then be driven by the predicted correlations among these measurable quantities. For instance one can easily express the Lagrangian parameters μ and the λ's in terms of the physical Higgs masses and the mixing angle α as well as the VEV's v_d, v_t, using equations (2.31, 2.13, 2.11) and (2.32 - 2.34). One finds

$$\lambda_1 = -\frac{2}{v_d^2+4v_t^2}.m_A^2 + \frac{4}{v_d^2+2v_t^2}.m_{H^\pm}^2 + \frac{\sin 2\alpha}{2v_d v_t}.(m_{h^0}^2 - m_{H^0}^2) \tag{2.44}$$

$$\lambda_2 = \frac{1}{v_t^2}\{\frac{s_\alpha^2 m_{h^0}^2 + c_\alpha^2 m_{H^0}^2}{2} + \frac{1}{2}.\frac{v_d^2}{v_d^2+4v_t^2}.m_A^2 - \frac{2v_d^2}{v_d^2+2v_t^2}.m_{H^\pm}^2 + m_{H^{\pm\pm}}^2\} \tag{2.45}$$

$$\lambda_3 = \frac{1}{v_t^2}\{\frac{-v_d^2}{v_d^2+4v_t^2}.m_A^2 + \frac{2v_d^2}{v_d^2+2v_t^2}.m_{H^\pm}^2 - m_{H^{\pm\pm}}^2\} \tag{2.46}$$

$$\lambda_4 = \frac{4}{v_d^2+4v_t^2}.m_A^2 - \frac{4}{v_d^2+2v_t^2}.m_{H^\pm}^2 \tag{2.47}$$

$$\lambda = \frac{2}{v_d^2}\{c_\alpha^2 m_{h^0}^2 + s_\alpha^2 m_{H^0}^2\} \tag{2.48}$$

$$\mu = \frac{\sqrt{2}v_t}{v_d^2+4v_t^2}.m_A^2 \tag{2.49}$$

The remaining two Lagrangian parameters m_H^2 and M_Δ^2 are then related to the physical parameters through the EWSB conditions Eqs. (2.8, 2.9). To complete the determination in terms of physical quantities one should further extract the mixing angle α from the measurement of some couplings (see also Appendix C) and v_d and v_t from the W (or Z) masses. Using equations (3.53, 3.54, 2.38) one finds

$$v_d^2 = \frac{1}{(1+\frac{1}{2}\tan^2\beta)}\frac{\sin^2\theta_W\ M_W^2}{\pi\alpha_{QED}}\ , \qquad v_t^2 = \frac{\tan^2\beta}{(1+\frac{1}{2}\tan^2\beta)}\frac{\sin^2\theta_W\ M_W^2}{4\pi\alpha_{QED}} \tag{2.50}$$

or

$$v_d^2 = \frac{1}{(1+\tan^2\beta)}\frac{\sin 2\theta_W\ M_Z^2}{2\pi\alpha_{QED}}\ , \qquad v_t^2 = \frac{\tan^2\beta}{(1+\tan^2\beta)}\frac{\sin 2\theta_W\ M_Z^2}{8\pi\alpha_{QED}} \tag{2.51}$$

or

$$v_d^2 = \frac{\sin^2\theta_W}{\pi\alpha_{QED}}(2M_W^2 - \cos^2\theta_W M_Z^2)\ , \qquad v_t^2 = \frac{\sin^2\theta_W}{2\pi\alpha_{QED}}(\cos^2\theta_W M_Z^2 - M_W^2) \tag{2.52}$$

Using any of the above equations to substitute for v_d, v_t in Eqs. (2.44, 2.49) allows us to obtain the Lagrangian parameters solely in terms of experimentally measurable quantities. Although Eqs. (2.50)-(2.52) are theoretically trivially equivalent, they involve different sets of experimental observables and can thus lead to non equivalent reconstruction strategies depending on the achieved accuracies in the measurement of these observables. Similarly, trading $\tan\beta$ for $\tan\beta^{'}$ through Eq. (2.43) can be useful, depending on which of the two quantities is experimentally better determined through some coupling measurements. We should also note that Eqs. (2.44)-(2.52) not only allow to reconstruct the Lagrangian parameters from the measurable Higgs masses, α, β, M_Z and/or M_W, but can also serve as consistency checks among observable quantities for the model when the λ's and μ are determined independently through the measurement of couplings in the purely Higgs sector (see also Appendix C). Finally, as can be seen from Eq.(2.52), the magnitude of v_t entails the deviation of the ρ parameter from its SM tree-level value, a point we will discuss further in the following section.

3 Miscellaneous constraints

3.1 Constraints from electroweak precision measurements

In the Standard Model the custodial symmetry ensures that the ρ parameter, $\rho \equiv \frac{M_W^2}{M_Z^2\cos^2\theta_W}$ is equal to 1 at tree level. In the DTHM one obtains the Z and W gauge boson masses readily from Eq.(2.7) and the kinetic terms in Eq.(2.1) as

$$M_Z^2 = \frac{(g^2+g'^2)(v_d^2+4v_t^2)}{4} = \frac{g^2(v_d^2+4v_t^2)}{4\cos^2\theta_W} \tag{3.53}$$

$$M_W^2 = \frac{g^2(v_d^2+2v_t^2)}{4} \tag{3.54}$$

whence the modified form of the ρ parameter:

$$\rho = \frac{v_d^2+2v_t^2}{v_d^2+4v_t^2} \neq 1 \tag{3.55}$$

and actually $\rho < 1$ at the tree-level. Since we are interested in the limit $v_t \ll v_d$ we rewrite

$$\rho \simeq 1 - 2\frac{v_t^2}{v_d^2} = 1 + \delta\rho \tag{3.56}$$

with $\delta\rho = -2\frac{v_t^2}{v_d^2} < 0$ and $\sqrt{v_d^2 + 2v_t^2} = 246$ GeV. Thus the model will remain viable as far as the experimentally driven values of $\delta\rho$ are compatible with a negative number. The implication for the DTHM has already been studied in the literature [17]. Here we only discuss briefly this point taking into account the latest updates of the electroweak observables fits as reported by the PDG [19]. One should compare the theoretical value with the experimental value after having subtracted from the latter all the known standard model contributions to the ρ parameter. The quoted number after this subtraction, $\rho_0 = 1.0008^{+0.0017}_{-0.0007}$ obtained from a global fit including the direct search limits on the standard Higgs boson, is not compatible with a negative $\delta\rho$ and would exclude the DTHM. However at the 2 σ level, one obtains $\rho_0 = 1.0004^{+0.0029}_{-0.0011}$ [19], which is again compatible with $\delta\rho < 0$. Moreover, relaxing the Higgs direct limit leads to $\rho_0 = 1.0008^{+0.0017}_{-0.0010}$, again compatible with $\delta\rho < 0$. From the last two numbers one gets an upper bound on v_t of order $2.5-4.6$ GeV. In the present study we will thus be contented by the conservative assumption that an upper bound of 2.5 GeV guarantees consistency with the experimental constraints. We should note, though, that the tree-level DTHM value of $\delta\rho$ being of order 10^{-4}, it is legitimate to ask about the effects of radiative corrections to this quantity within the DTHM. As far as we know, radiative corrections to $\delta\rho$ are not available in the literature in the case of $Y_\Delta = 2$ that concerns us here, while several studies have been dedicated to this question in the framework of a $Y_\Delta = 0$ triplet Higgs [20, 21, 22, 23], In [20], it has been shown that the tree level bound on the triplet vev could be pushed to higher values by one-loop radiative corrections. Whether this happens also in our case is still to be investigated and deserves a study that is out of the scope of the present paper, including for that matter all other LEP/SLC SM observables.

3.2 Absence of tachyonic modes

From Eq. (2.31), the requirement that m_A^2 should be positive implies $\mu v_t > 0$. The same positivity requirement in the singly charged and doubly charged sectors, Eqs. (2.13, 2.11), together with our phase convention $v_t > 0$ discussed in section 2, lead to the following bounds on μ:

$$\mu > 0 \tag{3.57}$$

$$\mu > \frac{\lambda_4 v_t}{2\sqrt{2}} \tag{3.58}$$

$$\mu > \frac{\lambda_4 v_t}{\sqrt{2}} + \sqrt{2}\frac{\lambda_3 v_t^3}{v_d^2} \tag{3.59}$$

The tachyonless condition in the $\mathcal{CP}_{even}$ sector, Eqs. (2.27, 2.28), is somewhat more involved and reads

$$\sqrt{2}\mu v_d^2 + \lambda v_d^2 v_t + 4(\lambda_2 + \lambda_3)v_t^3 > 0 \tag{3.60}$$

$$-8\mu^2 v_t + \sqrt{2}\mu(\lambda v_d^2 + 8(\lambda_1 + \lambda_4)v_t^2) + 4(\lambda(\lambda_2 + \lambda_3) - (\lambda_1 + \lambda_4)^2)v_t^3 > 0 \tag{3.61}$$

The first of these two equations is actually always satisfied as a consequence of Eq. (3.57) and the boundedness from below conditions for the potential (see section 4 and Eq. (4.21)).

The second equation, quadratic in μ, will lead to new constraints on μ in the form of an allowed range

$$\mu_- < \mu < \mu_+ \tag{3.62}$$

The full expressions of $\mu_\pm$ and a discussion of their real-valuedness are given in appendix A. Here we discuss their behavior in the regime $v_t \ll v_d$. In this case one finds a vanishingly small μ_- given by

$$\mu_- = ((\lambda_1+\lambda_4)^2 - \lambda(\lambda_2+\lambda_3))\,\frac{2\sqrt{2}}{\lambda}\frac{v_t^3}{v_d^2} + \mathcal{O}(v_t^4) \tag{3.63}$$

and a large μ_+ given by

$$\mu_+ = \frac{\lambda}{4\sqrt{2}}\frac{v_d^2}{v_t} + \sqrt{2}(\lambda_1+\lambda_4)v_t + \mathcal{O}(v_t^2). \tag{3.64}$$

Depending on the signs and magnitudes of the λ's, one of the lower bounds (3.57 - 3.59) or μ_- will overwhelm the others. Moreover, these no-tachyon bounds will have eventually to be amended by taking into account the existing experimental exclusion limits. This is straightforward for $A^0, H^\pm$ and $H^{\pm\pm}$. We thus define for later reference

$$\mu_{\min} = \max\left[\begin{array}{c} \dfrac{\sqrt{2}\,v_t}{v_d^2+4v_t^2}\,(m_A^2)_{\exp}, \\ \dfrac{\lambda_4 v_t}{2\sqrt{2}} + \dfrac{\sqrt{2}\,v_t}{v_d^2+2v_t^2}\,(m_{H^\pm}^2)_{\exp}, \\ \dfrac{\lambda_4 v_t}{\sqrt{2}} + \sqrt{2}\dfrac{\lambda_3 v_t^3}{v_d^2} + \dfrac{\sqrt{2}\,v_t}{v_d^2}\,(m_{H^{\pm\pm}}^2)_{\exp} \end{array}\right] \tag{3.65}$$

where $(m_A)_{\exp}, (m_{H^\pm})_{\exp}, (m_{H^{\pm\pm}})_{\exp}$ denote some experimental lower exclusion limits for the Higgs masses. Eqs.(3.57 - 3.59) are then replaced by

$$\mu > \mu_{\min} \tag{3.66}$$

in order for the masses to satisfy these exclusion limits. Similar modifications on $\mu_\pm$ taking into account experimental exclusion limits in the $\mathcal{CP}_{even}$ sector are more involved and will be differed to section 7 after having established the theoretical upper (lower) bounds on the h^0 (H^0) masses. Furthermore, the upper bound μ_+ will be instrumental in determining the maximally allowed values of the six Higgs masses $m_{H^0}, m_A, m_{H^\pm}, m_{H^{\pm\pm}}$ as we will see in section 7.

3.3 The vacuum structure

Obviously, violation of any of the constraints discussed in the previous subsection is a signal that the would-be electroweak vacuum is not a minimum (but rather a saddle-point or a local maximum) for the given set of values $\lambda, \lambda_i, v_d, v_t$ when μ is either very small or very large. However, since Eqs.(2.8, 2.9) are non-linear in v_d, v_t, it could still be possible to find a different set of values v_d', v_t', for the same input values of m_H^2, M_Δ^2, where the true electroweak minimum is obtained at a lower point of the potential than the previous one. More generally, and depending on the values of the parameters of the potential, one expects on top of the electroweak minimum a rich structure of extrema that can

affect the interpretation and viability of this minimum and thus possibly lead to additional constraints on these parameters. A complete study of such extrema can be very involved since the potential depends on ten independent real fields. Here we only provide a partial qualitative discussion.

Upon use of Eqs.(2.7, 2.8, 2.9) in Eq.(2.4) one readily finds that the value of the potential at the electroweak minimum, $\langle V\rangle_{\rm EWSB}$, is given by:

$$\langle V\rangle_{\rm EWSB} = -\frac{1}{16}(\lambda v_d^4 + 4(\lambda_2+\lambda_3)v_t^4 + 4v_d^2 v_t((\lambda_1+\lambda_4)v_t - \sqrt{2}\mu)) \tag{3.67}$$

Since the potential vanishes at the gauge invariant origin of the field space, $V_{H=0,\Delta=0} = 0$, then spontaneous electroweak symmetry breaking would be energetically disfavored if $\langle V\rangle_{\rm EWSB} > 0$.[4] One can thus require as a first approximation the naive bound on μ

$$\mu < \mu_{\rm max} \equiv \frac{\lambda}{4\sqrt{2}}\frac{v_d^2}{v_t} + (\lambda_1+\lambda_4)\frac{v_t}{\sqrt{2}} + \mathcal{O}(v_t^2) \tag{3.68}$$

to ensure $V_{\rm EWSB} < 0$. As can be seen from Eq.(3.64) one has either $\mu_{\rm max} < \mu_+$ or $\mu_{\rm max} > \mu_+$ depending on the sign of $\lambda_1+\lambda_4$. But for all practical purposes $\mu_{\rm max} \simeq \mu_+$ in the regime $v_t/v_d \ll 1$, so that the proviso stated above concerning the relevance of the tachyonless conditions is weakened for the upper bound μ_+ which can be replaced by $\mu_{\rm max}$. There is, however, yet another critical value of μ. As mentioned at the end of section 2.1, M_Δ^2 and $-m_H^2$ can be both positive for sufficiently large values of μ thus making the gauge invariant point $H=0, \Delta=0$ a local minimum. This happens when $\mu > \mu_H$ where

$$\mu_H = \frac{\lambda}{4\sqrt{2}}v_d^2 + (\lambda_1+\lambda_4)\frac{v_t}{2\sqrt{2}}. \tag{3.69}$$

If $\lambda_1+\lambda_4 > 0$ then $\mu_H < \mu_{\rm max} < \mu_+$. To delineate some consistency constraints in this case, it would be necessary to look more closely at the decay rate from a metastable gauge invariant vacuum to the EWSB vacuum, if $\mu_H < \mu < \mu_{\rm max}$, and vice-versa, from a metastable EWSB vacuum to the gauge invariant vacuum when $\mu_{\rm max} < \mu < \mu_+$. Fortunately, however, these configurations altogether are already excluded if we take into account the experimental mass limits on the Standard Model Higgs. Indeed, as will be shown in sections 7 and 8, the lightest $\mathcal{CP}_{even}$ Higgs state h^0 becomes purely standard model-like for such large values of μ, irrespective of the values of the couplings λ, λ_i, while m_{h^0} becomes very small for these values (e.g. $m_{h^0} = \sqrt{3(\lambda_1+\lambda_4)}v_t$ for $\mu = \mu_H$) and thus experimentally excluded.

Nonetheless, the structure of the potential Eq.(2.4) is sufficiently rich to provide dangerous extrema configurations which are not excluded by the above mentioned experimental limits. We exhibit here, without much details, one example among a manifold of possibilities. There is an extremum in the field space direction defined by $\mathrm{Re}\,\phi^0 = \mathrm{Re}\,\phi^+ \equiv \frac{v_d^c}{\sqrt{2}}$ and $\mathrm{Re}\,\delta^0 = -\mathrm{Re}\,\delta^{++} \equiv \frac{v_t^c}{\sqrt{2}}$, and all other fields put to zero.

This requires

$$\mu = -\frac{\lambda_4 v_t^c}{\sqrt{2}} \tag{3.70}$$

$$m_H^2 = \frac{1}{2}(\lambda {v_d^c}^2 + (2\lambda_1-\lambda_4){v_t^c}^2) \tag{3.71}$$

$$M_\Delta^2 = -\lambda_1 {v_d^c}^2 - (2\lambda_2+\lambda_3){v_t^c}^2 \tag{3.72}$$

[4] We should, however, keep in mind the possibility that a long-lived metastable vacuum could still be physically acceptable, even when $\langle V\rangle_{\rm EWSB} > 0$, thus altering our constraints; these issues are not addressed further in the present paper.

Note that this direction, and thus the corresponding extremum, breaks spontaneously charge conservation. We will refer to this extremum as charge breaking (CB). Furthermore, in contrast with the EWSB point, Eqs.(2.8, 2.9), here μ is not a free parameter. We can then seek for a region in parameter space where this CB extremum coexists with an EWSB minimum, and check what happens at the gauge invariant extremum point as well. Requiring Eqs.(2.8, 2.9, 3.70 - 3.72) to be simultaneously satisfied leads to correlations among v_d, v_t, v_d^c, v_t^c. These lead in turn to constraints on the λ, λ_i parameter space in order for all these vev's to be real valued (modulo gauge transformations), together with the immediate constraint $\lambda_4 v_t^c < 0$ originating from Eq.(3.70) and $\mu > 0$.[5] The ensuing correlations allow to write $m^2_{h^0}, \langle V\rangle_{\rm EWSB}$ and $\langle V\rangle_{\rm CB}$ (the value of the potential at the CB extremum) in the following form:

$$\begin{aligned} m^2_{h^0} &= (\lambda(2\lambda_2+\lambda_3)+2\lambda_4^2+\lambda_1(\lambda_4-2\lambda_1))\frac{v_t v_t^c}{\lambda_4}+\mathcal{O}(v_t^2) \\ &= 2m_H^2+\mathcal{O}(v_t^2) \qquad (3.73) \\ \langle V\rangle_{\rm EWSB} &= -(\lambda(2\lambda_2+\lambda_3)+2\lambda_4^2+\lambda_1(\lambda_4-2\lambda_1))\times \\ &\qquad (\lambda(2\lambda_2+\lambda_3)+\lambda_1(-2\lambda_1+\lambda_4))\frac{v_t^2 v_t^{c\,2}}{4\lambda\lambda_4^2}+\mathcal{O}(v_t^3) \qquad (3.74) \\ \langle V\rangle_{\rm CB} &= (4\lambda_1^2-2\lambda(2\lambda_2+\lambda_3)-\lambda_4^2)\frac{v_t^{c\,4}}{4\lambda}+\mathcal{O}(v_t^2) \qquad (3.75) \end{aligned}$$

Various interesting conclusions can be drawn from the above equations. As can be seen from Eq.(3.73), a physical h^0, i.e. $m^2_{h^0} > 0$, implies a positive m_H^2 and thus an *unstable* gauge invariant point at the origin of the fields ($H = 0, \Delta = 0$). Furthermore, in the consistent (λ, λ_i) domain (given in footnote 2) $m^2_{h^0}$ is indeed positive and, furthermore, one finds from Eq.(3.74) that $\langle V\rangle_{\rm EWSB} < 0$. The EWSB vacuum is thus energetically favored over the gauge symmetry preserving one which lies at $V = 0$. It then remains to compare the EWSB point with the CB point. Close inspection of Eq.(3.75) shows that $\langle V\rangle_{\rm CB} > 0$ in all the (λ, λ_i) domain given in footnote 2, if and only if $\lambda_4 < 0$, in which case the EWSB is energetically favored over the CB. However, if $\lambda_4 > 0$ (and thus $v_t^c < 0$), there are regions in the (λ, λ_i) consistent domain where $\langle V\rangle_{\rm CB} < 0$, provided that $4\lambda_4^2 < \lambda(2\lambda_2+\lambda_3)$. Moreover, the potential at this CB point becomes much deeper than at the EWSB point since we are in the regime $v_t \ll |v_t^c|$. This is a dangerous configuration since it makes the EWSB vacuum potentially very short-lived due to tunneling effects [24, 25]. We stress here that this EWSB point is a true local minimum in this configuration, i.e. there are no tachyonic Higgs states which could have signaled its non-relevance beforehand. [This is easily seen from the fact that h^0 is non-tachyonic and is the lightest Higgs state when $\mu \sim |v_t^c| \gg v_t$; see also section 7.] Even more so, the potential is bounded from below, as can be shown by comparing the corresponding (λ, λ_1) domain with the boundedness from below constraints that we will derive in the following section. We have thus exhibited an example of a configuration where μ can be very large, consistent with the experimental h^0 mass limit, and *a fortiori* with all the non-tachyon constraints, corresponding locally to an acceptable EWSB vacuum, but still non-viable due to the existence of lower (charge breaking) points akin to what happens in two-Higgs-doublet models (see for instance [26]).

We end this section with a general comment concerning the neutrino mass see-saw mechanism. The common lore is to assume a GUT origin for μ and M_Δ, and taking

[5] Working in the regime $v_t \ll v_d, |v_t^c|, |v_d^c|$ and keeping only terms $\mathcal{O}(v_t)$, the constraint in the (λ, λ_i) space satisfying all these requirements is found to be $\lambda_1 < \frac{1}{4}(\lambda_4 - \sqrt{8\lambda(2\lambda_2+\lambda_3)+17\lambda_4^2})$. Note that $\lambda > 0$ and $2\lambda_2+\lambda_3 > 0$ for a bounded from below potential (see section 4).

$\mu \sim M_\Delta \sim \mathcal{O}(M_{\rm GUT})$ leads through Eq.(2.8) naturally to a tiny v_t. However, as noted in the introduction we do not commit in the present study to specific high energy physics scenarios, so that M_Δ and/or μ could be smaller than a hypothetical GUT scale. It is then interesting to note that even in this case a kind of see-saw is actually still at work model-independently due to the dynamics of the potential. This is simply due to the form of the μ upper bound μ_+, Eq.(3.64): the larger is μ the smaller should be v_t in order to avoid a tachyonic h^0. For instance, taking $\lambda \simeq 0.5$ and $\mu_+ \simeq 2\times 10^{12}$GeV leads to $v_t \simeq 1$eV and $M_\Delta \simeq 10^{13}$GeV.

4 Boundedness of the potential

A necessary condition for the stability of the vacuum comes from requiring that the potential given in Eq. (2.4) be bounded from below when the scalar fields become large in any direction of the field space. The constraints ensuring boundedness from below (BFB) of the DTHM potential have been studied in the literature so far only partially (see e.g. [18]), and at the tree-level. It would thus be somewhat premature to invoke possible quantum modifications of these constraints before fully settling first the tree-level issue. This section is devoted to this issue and aims at deriving, at the tree-level, the complete *necessary and sufficient* BFB conditions valid for *all* directions in field space.[6]

Obviously, at large field values the potential Eq. (2.4) is generically dominated by the part containing the terms that are quartic in the fields,

$$V^{(4)}(H,\Delta) = \frac{\lambda}{4}(H^\dagger H)^2 + \lambda_1 (H^\dagger H) Tr(\Delta^\dagger\Delta) + \lambda_2 (Tr\Delta^\dagger\Delta)^2 + \lambda_3 Tr(\Delta^\dagger\Delta)^2 + \lambda_4 H^\dagger\Delta\Delta^\dagger H \tag{4.1}$$

The study of $V^{(4)}(H,\Delta)$ will thus be sufficient to obtain the main constraints. To obtain BFB conditions it is common in the literature to pick up specific field directions or to put some of the couplings to zero. Consider for instance the two following cases:

1. in the absence of any coupling between doublet and triplet Higgs bosons, i.e. $\lambda_1 = \lambda_4 = 0$, it is obvious that

$$\lambda > 0 \ \ \& \ \ \lambda_2 > 0 \ \ \& \ \ \lambda_3 > 0 \tag{4.2}$$

   will ensure that the potential is bounded from below.

2. if one picks up the field space directions where only the electrically neutral components are non vanishing, one finds

$$V_0^{(4)} = \frac{\lambda}{4}|\phi^0|^4 + (\lambda_2+\lambda_3)|\delta^0|^4 + (\lambda_1+\lambda_4)|\phi^0|^2|\delta^0|^2 \tag{4.3}$$

   In order for the potential to be bounded from below in this sub-space, $V_0^{(4)}$ should be positive for any values of $|\phi^0|$ and $|\delta^0|$ including when one or the other is vanishing. The latter cases imply the necessary conditions $\lambda > 0$ and $\lambda_2 + \lambda_3 > 0$. It is then possible to rewrite Eq.(4.3) in the form

[6] We will thus not address in this paper the possibility that loop corrections could lift the potential in some otherwise unbounded from below directions, nor the issues related to metastability of the vacuum which could relax some of the constraints. See also section 3.3.

$$V_0^{(4)} = [\frac{\sqrt{\lambda}}{2}|\phi^0|^2 - \sqrt{\lambda_2+\lambda_3}|\delta^0|^2]^2 + (\lambda_1+\lambda_4+\sqrt{\lambda(\lambda_2+\lambda_3)})|\phi^0|^2|\delta^0|^2 \quad (4.4)$$

Since the first term is non-negative and vanishes in the direction $|\phi^0|^2/|\delta^0|^2 = 2\sqrt{(\lambda_2+\lambda_3)/\lambda}$, then the necessary and sufficient conditions for the BFB of the potential in *this* direction are

$$\begin{aligned} \lambda &> 0 \\ \lambda_2+\lambda_3 &> 0 \\ \lambda_1+\lambda_4+\sqrt{\lambda(\lambda_2+\lambda_3)} &> 0 \end{aligned} \quad (4.5)$$

As it will become clear later on in this section, the conditions in case 1 are sufficient but not necessary, even for this special case. Furthermore, while the conditions in case 2 are necessary and sufficient for the corresponding direction, they obviously remain necessary for the general potential but it is *a priori* not clear whether they can be sufficient. By looking at other special directions in 2-field and 3-field directions we will show that they are generally not sufficient. Before doing so, let us first point out a more convenient method to obtain positivity constraints like Eq.(4.5) directly from Eq.(4.3) rather than writing it first in the form of Eq.(4.4). The potential Eq.(4.3) can be cast in the form

$$V(\chi) = a + b\chi^2 + c\chi^4 \quad (4.6)$$

by the change of variable $\chi = |\phi^0|/|\delta^0|$. Since χ is by definition real valued and the moduli $|\phi^0|$ and $|\delta^0|$ can have any value, then the problem of finding the necessary and sufficient BFB conditions for Eq.(4.3) is equivalent to finding the conditions on a, b, c such that $V(\chi) > 0$ for any $\chi \in [0, \infty[$. Since $V(\chi)$ has no linear or cubic terms in χ it is easy to find these conditions by studying $V(\chi)$ as a bi-quadratic function:

$$\begin{aligned} a &> 0 \\ c &> 0 \\ b + 2\sqrt{ac} &> 0 \end{aligned} \quad (4.7)$$

Applied to Eq.(4.3) these conditions reproduce immediately Eq. (4.5). We can now easily study other field directions. For instance, the direction where only δ^{++} and ϕ^0 are non vanishing yields

$$V = (\lambda_2+\lambda_3)\,|\delta^{++}|^4 + \lambda_1\,|\delta^{++}|^2\,|\phi^0|^2 + \frac{\lambda}{4}\,|\phi^0|^4 \quad (4.8)$$

for which the BFB constraints are readily obtained from Eq.(4.7) as

$$\lambda > 0 \;\;\&\;\; \lambda_2+\lambda_3 > 0 \;\;\&\;\; \lambda_1+\sqrt{\lambda(\lambda_2+\lambda_3)} > 0. \quad (4.9)$$

Similarly, if we consider the field direction with non-vanishing δ^+ and ϕ^+, then

$$V = (\lambda_2+\frac{\lambda_3}{2})\,|\delta^+|^4 + (\lambda_1+\frac{\lambda_4}{2})\,|\delta^+|^2\,|\phi^+|^2 + \frac{\lambda}{4}\,|\phi^+|^4 \quad (4.10)$$

and the corresponding BFB conditions read

$$\lambda > 0 \ \ \& \ \ \lambda_2 + \frac{\lambda_3}{2} > 0 \ \ \& \ \ \lambda_1 + \frac{\lambda_4}{2} + \sqrt{\lambda(\lambda_2 + \frac{\lambda_3}{2})} > 0. \tag{4.11}$$

It is then obvious that these two sets of conditions are neither equivalent nor contained in the conditions of Eq.(4.5). This shows that the BFB conditions derived only from the neutral direction Eq.(4.3) are neither necessary nor sufficient to ensure boundedness from below of the full potential Eq.(2.4). In Appendix B we have listed the potentials for all the field directions with only two non-vanishing fields together with the corresponding BFB conditions. Adding these conditions we come closer to the real sufficient and necessary conditions. But one can get more conditions by going now to field directions where 3 fields are non-vanishing. We give the exhaustive list of all these 3-field directions potentials in Appendix B. In these more complicated configurations, an iteration of the method described above allowed to treat all of them, although the results become somewhat complicated and not so telling. For instance the 3-field direction with non-vanishing ϕ^0, ϕ^+, δ^+, see Eq.(B.24) yields some of the simplest BFB conditions

$$\begin{aligned} &\lambda > 0 \wedge 2\lambda_2 + \lambda_3 > 0 \wedge \sqrt{\lambda(4\lambda_2 + 2\lambda_3)} + 2\lambda_1 + \lambda_4 > 0 \wedge \\ &\qquad \Big(2\lambda(2\lambda_2 + \lambda_3) > (2\lambda_1 + \lambda_4)^2 \vee 2\lambda_1 + \lambda_4 > 0\Big) \end{aligned} \tag{4.12}$$

where $\wedge, \vee$ stand respectively for the logical AND, OR. These conditions are obtained by first defining the reduced variables $\chi_1 = |\phi^+|/|\phi^0|, \chi_2 = |\delta^+|/|\phi^0|$, and then using iteratively the constraints Eqs. (4.7). By the same method we could obtain even more complicated BFB conditions given in Eqs. (B.26 - B.35). Analyzing them numerically we confirm that Eqs. (4.5) are far from being the full story. However, and despite their apparently complicated structure the intersection of the regions they delineate in the space of the λ's has a form similar to equations (4.5) and (B.14). Moreover, the true BFB conditions will be obtained only if all field directions are taken into account, up to some arbitrary $SU(2)\times U(1)$ gauge transformations, but in this case the method used so far is not tractable anymore.

To proceed to the most general case, we adopt a different parameterization of the fields that will turn out to be particularly convenient to entirely solve the problem. Without loss of generality we can define:

$$r \equiv \sqrt{H^\dagger H + Tr\Delta^\dagger\Delta} \tag{4.13}$$
$$H^\dagger H \equiv r^2 \cos^2\gamma \tag{4.14}$$
$$Tr(\Delta^\dagger\Delta) \equiv r^2 \sin^2\gamma \tag{4.15}$$
$$Tr(\Delta^\dagger\Delta)^2/(Tr\Delta^\dagger\Delta)^2 \equiv \zeta \tag{4.16}$$
$$(H^\dagger\Delta\Delta^\dagger H)/(H^\dagger H Tr\Delta^\dagger\Delta) \equiv \xi \tag{4.17}$$

.

(where we adopted here a parameterization similar to the one used in [27] to study two-Higgs-doublet models, although for the latter models the problem is not fully solved by such a parameterization). Obviously, when H and Δ scan all the field space, the radius r scans the domain $[0, \infty[$ and the angle $\gamma \in [0, \frac{\pi}{2}]$. Moreover, one can show that

$$0 \leq \xi \leq 1 \text{ and } \frac{1}{2} \leq \zeta \leq 1 \tag{4.18}$$

With this parameterization it is straightforward to cast $V^{(4)}(H,\Delta)$ in the following simple form,

$$V^{(4)}(r,\tan\gamma,\xi,\zeta)=\frac{r^4}{4(1+\tan^2\gamma)^2}(\lambda+4(\lambda_1+\xi\lambda_4)\tan^2\gamma+4(\lambda_2+\zeta\lambda_3)\tan^4\gamma) \quad (4.19)$$

Due to the bi-quadratic dependence in $\tan\gamma$, one can indeed consider only the range $0\leq\tan\gamma<+\infty$ in accordance with the above stated range for γ. We have thus written $V^{(4)}$ in the form of Eq. (4.6). Boundedness from below is then equivalent to requiring $V^{(4)}>0$ *for all* $\tan\gamma\in[0,\infty[$ and *all* ξ,ζ satisfying Eq.(4.18). Now applying directly the conditions Eq.(4.7) one obtains

$$\lambda>0\ \ \&\ \ \lambda_2+\zeta\lambda_3>0\ \ \&\ \ \lambda_1+\xi\lambda_4+\sqrt{\lambda(\lambda_2+\zeta\lambda_3)}>0\ \ \forall\zeta\in[\frac{1}{2},1],\forall\xi[0,1] \quad (4.20)$$

Due to the monotonic dependence in ζ and ξ, it is easy to show that these conditions can be rewritten as,

$$\lambda>0\ \ \&\ \ \lambda_2+\lambda_3>0\ \ \&\ \ \lambda_2+\frac{\lambda_3}{2}>0 \quad (4.21)$$

$$\&\ \ \lambda_1+\sqrt{\lambda(\lambda_2+\lambda_3)}>0\ \ \&\ \ \lambda_1+\sqrt{\lambda(\lambda_2+\frac{\lambda_3}{2})}>0 \quad (4.22)$$

$$\&\ \ \lambda_1+\lambda_4+\sqrt{\lambda(\lambda_2+\lambda_3)}>0\ \ \&\ \ \lambda_1+\lambda_4+\sqrt{\lambda(\lambda_2+\frac{\lambda_3}{2})}>0 \quad (4.23)$$

We stress here that the above conditions ensure BFB for all possible directions in field space and thus provide the most general *all directions necessary and sufficient BFB conditions* that solve completely the issue at the tree-level. Note that all the 2-field directions conditions given in Eqs.(B.11 - B.15) are special cases of the above conditions. We also checked numerically that this is the case for all the ten 3-field directions conditions Eqs. (B.26 - B.35).

5 Unitarity constraints

Constraints on the scalar potential parameters can be obtained by demanding that tree-level unitarity be preserved in a variety of scattering processes: scalar-scalar scattering, gauge boson-gauge boson scattering and scalar-gauge boson scattering as was initially done for the SM [28, 29, 30]. The generalizations of such constraints to various extended Higgs sector scenarios have been studied in the literature, see for instance [31, 32, 33, 34]. Here we treat such constraints in the DTHM at the tree-level, limiting ourselves to 2-body scalar scattering processes dominated by quartic interactions. This is justified by the fact that we are interested in the leading unitarity constraints, that is in the limit where $\sqrt{s}$ is much larger than any other mass scale involved. In particular this means that we disregard here unitarity constraints that would involve the μ parameter when the latter is very large. Indeed, this parameter contributes to the scalar scattering processes through the cubic interactions entering the Feynman diagrams with scalar exchange in the s,t and u channels. Furthermore, the ratio μ/v_t controls the size of the exchanged scalar masses so

that some of the aforementioned diagrams can be important in the vicinity of the resonance pole in the limit of large $\sqrt{s} \sim \mu v_d/v_t$.

In order to derive the unitarity constraints on the scalar masses we adopt the basis of unrotated states, corresponding to the fields before electroweak symmetry breaking. The quartic scalar vertices have in this case a much simpler form than the complicated functions of λ_i, α and β obtained in the physical basis ($H^{\pm\pm}$, $H^{\pm}$, $G^{\pm}$, h^0, H^0, A^0 and G^0) of mass eigenstate fields. The S-matrix for the physical fields is related by a unitary transformation to the S-matrix for the unrotated fields. Close inspection shows that the full set of 2-body scalar scattering processes leads to a 35×35 S-matrix which can be decomposed into 7 block submatrices corresponding to mutually unmixed sets of channels with definite charge and CP states. One has the following submatrix dimensions, structured in terms of net electric charge in the initial/final states: $S^{(1)}(6 \times 6)$, $S^{(2)}(7 \times 7)$ and $S^{(3)}(2 \times 2)$, corresponding to 0-charge channels, $S^{(4)}(10 \times 10)$ corresponding to the 1-charge channels, $S^{(5)}(7 \times 7)$ corresponding to the 2-charge channels, $S^{(6)}(2 \times 2)$ corresponding to the 3-charge channels and $S^{(7)}(1 \times 1)$ corresponding to the unique 4-charge channel. The corresponding T-matrix submatrices $T^{(1)}, ..., T^{(7)}$ –with a momentum conservation factor $(2\pi)^4\delta^4(\sum \text{momenta})$ properly factored out– are then easily extracted using the pure scalar quartic interactions expressed in terms of the non-physical fields $\phi^{\pm}$, $\delta^{\pm}$, $\delta^{\pm\pm}$, h, ξ^0, and Z_i(i=1,2) as listed in Appendix C.

One can then in principle extract the unitarity constraints on each component of the T-matrix through the unitarity equation which we write here in a shorthand form as

$$-i(T - T^\dagger) \sim \int \text{“}TT^\dagger\text{”} \tag{5.1}$$

where $\int$ denotes symbolically the phase space integral over each intermediate state channel (see for instance [35]). However, it proves more efficient to define a modified matrix in such a way that its diagonalized form still satisfies Eq. (5.1). The usual unitarity bound on partial-wave amplitudes that is valid for *elastic* scattering would then apply readily to all the eigenvalues, thus encoding indirectly the bounds on all the components of the T-matrix.[7] The proper redefinition is a $\tilde{T}$-matrix having the same entries as T but with an extra $1/\sqrt{2}$ factor for each initial or final state channel having two identical particles. $\tilde{T}$ now satisfies Eq. (5.1) with the same phase space for *all* channels and a true matrix multiplication of $\tilde{T}$ by $\tilde{T}^\dagger$. Its diagonalized form will thus satisfy the same equation. Defining $\mathcal{M}_n \equiv i\tilde{T}^{(n)}$, with $n = 1, \cdots, 7$, we give hereafter the resulting submatrices whose entries correspond to the quartic couplings that mediate the $2 \to 2$ scalar processes. These submatrices are hermitian, thus the sought for eigenvalues will all be real-valued.

The first submatrix $\mathcal{M}_1$ corresponds to scattering whose initial and final states are one of the following: ($\phi^+\delta^-$,$\delta^+\phi^-$, hZ_2, $\xi^0 Z_1$, Z_1Z_2, $h\xi^0$). With the help of Appendix C one finds,

[7] This, however, cannot be achieved in general by simply diagonalizing T, since on the right-hand side of Eq. (5.1) the phase space factor is not the same for all the 2-particle channels, even in the high energy massless limit we are considering. It picks up a factor 1/2 only for internal states with identical particles so as to avoid double counting. The right-hand side of Eq. (5.1) is thus not a proper matrix multiplication of T by $T^\dagger$, a fact emphasized by the quotation marks in the equation.

$$\mathcal{M}_1 = \begin{pmatrix} \lambda_1 + \frac{\lambda_4}{2} & 0 & -\frac{i\lambda_4}{2\sqrt{2}} & \frac{i\lambda_4}{2\sqrt{2}} & \frac{\lambda_4}{2\sqrt{2}} & \frac{\lambda_4}{2\sqrt{2}} \\ 0 & \lambda_1 + \frac{\lambda_4}{2} & \frac{i\lambda_4}{2\sqrt{2}} & -\frac{i\lambda_4}{2\sqrt{2}} & \frac{\lambda_4}{2\sqrt{2}} & \frac{\lambda_4}{2\sqrt{2}} \\ \frac{i\lambda_4}{2\sqrt{2}} & -\frac{i\lambda_4}{2\sqrt{2}} & \lambda_{14}^+ & 0 & 0 & 0 \\ -\frac{i\lambda_4}{2\sqrt{2}} & \frac{i\lambda_4}{2\sqrt{2}} & 0 & \lambda_{14}^+ & 0 & 0 \\ \frac{\lambda_4}{2\sqrt{2}} & \frac{\lambda_4}{2\sqrt{2}} & 0 & 0 & \lambda_{14}^+ & 0 \\ \frac{\lambda_4}{2\sqrt{2}} & \frac{\lambda_4}{2\sqrt{2}} & 0 & 0 & 0 & \lambda_{14}^+ \end{pmatrix} \tag{5.2}$$

where $\lambda_{ij}^{\pm} = \lambda_i \pm \lambda_j$. We find that $\mathcal{M}_1$ has the following 3 double eigenvalues:

$$e_1 = \lambda_1 + \lambda_4 \tag{5.3}$$

$$e_2 = \lambda_1 \tag{5.4}$$

$$e_3 = \frac{1}{2}(2\lambda_1 + 3\lambda_4) \tag{5.5}$$

The second submatrix $\mathcal{M}_2$ corresponds to scattering with one of the following initial and final states: $(\phi^+\phi^-,\ \delta^+\delta^-,\ \delta^{++}\delta^{--},\ \frac{Z_1Z_1}{\sqrt{2}},\ \frac{Z_2Z_2}{\sqrt{2}},\ \frac{hh}{\sqrt{2}},\ \frac{\xi^0\xi^0}{\sqrt{2}})$, where the $\sqrt{2}$ accounts for identical particle statistics. Again, with the help of Appendix C, one finds that $\mathcal{M}_2$ is given by:

$$\mathcal{M}_2 = \begin{pmatrix} \lambda & \frac{\tilde{\lambda}_{14}}{2} & \lambda_{14}^+ & \frac{\lambda}{2\sqrt{2}} & \frac{\lambda_1}{\sqrt{2}} & \frac{\lambda}{2\sqrt{2}} & \frac{\lambda_1}{\sqrt{2}} \\ \frac{\tilde{\lambda}_{14}}{2} & 2\tilde{\lambda}_{23} & 2\lambda_{23}^+ & \frac{\tilde{\lambda}_{14}}{2\sqrt{2}} & \sqrt{2}\lambda_{23}^+ & \frac{\tilde{\lambda}_{14}}{2\sqrt{2}} & \sqrt{2}\lambda_{23}^+ \\ \lambda_{14}^+ & 2\lambda_{23}^+ & 4\lambda_{23}^+ & \frac{\lambda_1}{\sqrt{2}} & \sqrt{2}\lambda_2 & \frac{\lambda_1}{\sqrt{2}} & \sqrt{2}\lambda_2 \\ \frac{\lambda}{2\sqrt{2}} & \frac{\tilde{\lambda}_{14}}{2\sqrt{2}} & \frac{\lambda_1}{\sqrt{2}} & \frac{3}{4}\lambda & \frac{\lambda_{14}^+}{2} & \frac{\lambda}{4} & \frac{\lambda_{14}^+}{2} \\ \frac{\lambda_1}{\sqrt{2}} & \sqrt{2}\lambda_{23}^+ & \sqrt{2}\lambda_2 & \frac{\lambda_{14}^+}{2} & 3\lambda_{23}^+ & \frac{\lambda_{14}^+}{2} & \lambda_{23}^+ \\ \frac{\lambda}{2\sqrt{2}} & \frac{\tilde{\lambda}_{14}}{2\sqrt{2}} & \frac{\lambda_1}{\sqrt{2}} & \frac{\lambda}{4} & \frac{\lambda_{14}^+}{2} & \frac{3\lambda}{4} & \frac{\lambda_{14}^+}{2} \\ \frac{\lambda_1}{\sqrt{2}} & \sqrt{2}\lambda_{23}^+ & \sqrt{2}\lambda_2 & \frac{\lambda_{14}^+}{2} & \lambda_{23}^+ & \frac{\lambda_{14}^+}{2} & 3\lambda_{23}^+ \end{pmatrix} \tag{5.6}$$

where $\tilde{\lambda}_{14} = 2\lambda_1 + \lambda_4$ and $\tilde{\lambda}_{23} = 2\lambda_2 + \lambda_3$. Despite its apparently complicated structure, one can easily determine the seven eigenvalues of $\mathcal{M}_2$ as follows:

$$f_1 = \frac{\lambda}{2} \tag{5.7}$$
$$f_2 = 2\lambda_2 \tag{5.8}$$
$$f_3 = 2(\lambda_2 + \lambda_3) \tag{5.9}$$
$$a_\pm = \frac{1}{4}[\lambda + 4\lambda_2 + 8\lambda_3 \pm \sqrt{(\lambda - 4\lambda_2 - 8\lambda_3)^2 + 16\lambda_4^2}\ ] \tag{5.10}$$
$$b_\pm = \frac{1}{4}[3\lambda + 16\lambda_2 + 12\lambda_3 \pm \sqrt{(3\lambda - 16\lambda_2 - 12\lambda_3)^2 + 24(2\lambda_1 + \lambda_4)^2}\ ] \tag{5.11}$$

The third submatrix $\mathcal{M}_3$ corresponds to the basis $(hZ_1, \xi^0 Z_2)$ and is given by:

$$\mathcal{M}_3 = \begin{pmatrix} \frac{\lambda}{2} & 0 \\ 0 & 2\lambda_{23}^+ \end{pmatrix} \tag{5.12}$$

with eigenvalues $k_1 = f_1$ and $k_2 = f_3$.

The 1-charge channels occur for two-by-two body scattering between the 10 charged states ($h\phi^+$, $\xi^0\phi^+$, $Z_1\phi^+$, $Z_2\phi^+$, $h\delta^+$, $\xi^0\delta^+$, $Z_1\delta^+$, $Z_2\delta^+$, $\delta^{++}\delta^-$, $\delta^{++}\phi^-$). The 10×10 submatrix $\mathcal{M}_4$ obtained from the above scattering processes is given by:

$$\mathcal{M}_4 = \begin{pmatrix}
\frac{\lambda}{2} & 0 & 0 & 0 & 0 & \frac{\lambda_4}{2\sqrt{2}} & 0 & \frac{-i\lambda_4}{2\sqrt{2}} & \frac{-\lambda_4}{2} & 0 \\
0 & \lambda_1 & 0 & 0 & \frac{\lambda_4}{2\sqrt{2}} & 0 & \frac{i\lambda_4}{2\sqrt{2}} & 0 & 0 & 0 \\
0 & 0 & \frac{\lambda}{2} & 0 & 0 & \frac{i\lambda_4}{2\sqrt{2}} & 0 & \frac{\lambda_4}{2\sqrt{2}} & \frac{-i\lambda_4}{2} & 0 \\
0 & 0 & 0 & \lambda_1 & \frac{-i\lambda_4}{2\sqrt{2}} & 0 & \frac{\lambda_4}{2\sqrt{2}} & 0 & 0 & 0 \\
0 & \frac{\lambda_4}{2\sqrt{2}} & 0 & \frac{i\lambda_4}{2\sqrt{2}} & \frac{1}{2}\tilde{\lambda}_{14} & 0 & 0 & 0 & 0 & \frac{-\lambda_4}{2} \\
\frac{\lambda_4}{2\sqrt{2}} & 0 & \frac{-i\lambda_4}{2\sqrt{2}} & 0 & 0 & 2\lambda_{23}^+ & 0 & 0 & -\sqrt{2}\lambda_3 & 0 \\
0 & \frac{-i\lambda_4}{2\sqrt{2}} & 0 & \frac{\lambda_4}{2\sqrt{2}} & 0 & 0 & \frac{1}{2}\tilde{\lambda}_{14} & 0 & 0 & \frac{-i\lambda_4}{2} \\
\frac{i\lambda_4}{2\sqrt{2}} & 0 & \frac{\lambda_4}{2\sqrt{2}} & 0 & 0 & 0 & 0 & 2\lambda_{23}^+ & -i\sqrt{2}\lambda_3 & 0 \\
\frac{-\lambda_4}{2} & 0 & \frac{i\lambda_4}{2} & 0 & 0 & -\sqrt{2}\lambda_3 & 0 & i\sqrt{2}\lambda_3 & 2\lambda_{23}^+ & 0 \\
0 & 0 & 0 & 0 & \frac{-\lambda_4}{2} & 0 & \frac{i\lambda_4}{2} & 0 & 0 & \lambda_{14}^+
\end{pmatrix} \tag{5.13}$$

As one can see, this matrix contains many vanishing elements, and the 10 eigenvalues are straightforward to obtain analytically. They read as follows:

$$d_1 = e_1 \tag{5.14}$$
$$d_2 = e_2 \quad (twice) \tag{5.15}$$
$$d_3 = e_3 \tag{5.16}$$
$$d_4 = f_1 \tag{5.17}$$
$$d_5 = f_2 \tag{5.18}$$
$$d_6 = f_3 \tag{5.19}$$
$$d_7 = \lambda_1 - \frac{\lambda_4}{2} \tag{5.20}$$
$$d_\pm = a_\pm \tag{5.21}$$

The fifth submatrix $\mathcal{M}_5$ corresponds to scattering with initial and final states being one of the following 7 sates: ($\frac{\phi^+\phi^+}{\sqrt{2}}$,$\frac{\delta^+\delta^+}{\sqrt{2}}$,$\delta^+\phi^+$,$\delta^{++}\xi^0$, $\delta^{++}Z_2$, $\delta^{++}Z_1$, $\delta^{++}h$). It reads,

$$\mathcal{M}_5 = \begin{pmatrix} \frac{\lambda}{2} & 0 & 0 & 0 & 0 & 0 & 0 \\ 0 & \tilde{\lambda}_{23} & 0 & -\lambda_3 & -i\lambda_3 & 0 & 0 \\ 0 & 0 & \frac{\tilde{\lambda}_{14}}{2} & 0 & 0 & \frac{-i\lambda_4}{2} & \frac{-\lambda_4}{2} \\ 0 & -\lambda_3 & 0 & 2\lambda_2 & 0 & 0 & 0 \\ 0 & i\lambda_3 & 0 & 0 & 2\lambda_2 & 0 & 0 \\ 0 & 0 & \frac{i\lambda_4}{2} & 0 & 0 & \lambda_1 & 0 \\ 0 & 0 & \frac{-\lambda_4}{2} & 0 & 0 & 0 & \lambda_1 \end{pmatrix} \tag{5.22}$$

and possesses the following 7 distinct eigenvalues:

$$c_1 = e_1 \tag{5.23}$$
$$c_2 = e_2 \tag{5.24}$$
$$c_3 = f_1 \tag{5.25}$$
$$c_4 = f_2 \tag{5.26}$$
$$c_5 = f_3 \tag{5.27}$$
$$c_6 = d_7 \tag{5.28}$$
$$c_7 = 2\lambda_2 - \lambda_3 \tag{5.29}$$

There are also triply-charged states.The submatrix $\mathcal{M}_6$ corresponding to this case generates the scattering with initial and final states being one of the following ($\delta^{++}\phi^+$,$\delta^{++}\delta^+$), and is given by :

$$\mathcal{M}_6 = \begin{pmatrix} \lambda^+_{14} & 0 \\ 0 & 2\lambda^+_{23} \end{pmatrix} \tag{5.30}$$

with eigenvalues $k_1 = e_1$ and $k_2 = f_3$. Finally, it is easy to check that there is just one quadruply-charged state $\frac{1}{\sqrt{2}}\delta^{++}\delta^{++}$ leading to

$$\mathcal{M}_7 = f_3 \tag{5.31}$$

with f_3 as eigenvalue.

From the usual expansion in terms of partial-wave amplitudes a_J, we write, following our notations,

$$\mathcal{M}^{(kf)} = i\tilde{T}_{kf} = 16i\pi \sum_{J\geq 0} (2J+1)\, a_J^{(kf)}(s)\, P_J(\cos\theta) \tag{5.32}$$

where $\mathcal{M}^{(kf)}$ denotes the entries of the $\mathcal{M}$ matrix, the subscripts k and f run over all possible initial and final states of the above 35-state basis, θ denotes the scattering angle of the corresponding processes and the P_J's are the Legendre polynomials. Since we considered only the leading high energy (massless limit) contributions that are s and θ independent, all the partial waves with $J \neq 0$ vanish and one is left with

$$a_0^{(kf)} = -\frac{i}{16\pi}\mathcal{M}^{(kf)} \tag{5.33}$$

for each channel. The S-matrix unitarity constraint for elastic scattering $|a_0^{(kk)}| \leq 1$ (or alternatively $|Re(a_0^{(kk)})| \leq \frac{1}{2}$ [36, 37]) applies to the diagonal entries of $\mathcal{M}$. It encodes as well the constraints for non-elastic scattering, provided that it is applied to the eigenchannels of the 35-state basis as noted previously. Thus, this constraint translates through Eq. (5.33) directly to all the eigenvalues we determined above. We defer to the next section, Eqs. (6.4 - 6.13) the list of all the resulting constraints.

6 Combined unitarity and potential stability constraints

Let us first recall all the constraints obtained in sections 4 and 5.

BFB:

$$\lambda \geq 0 \;\;\&\;\; \lambda_2 + \lambda_3 \geq 0 \;\;\&\;\; \lambda_2 + \frac{\lambda_3}{2} \geq 0 \tag{6.1}$$

$$\&\;\; \lambda_1 + \sqrt{\lambda(\lambda_2+\lambda_3)} \geq 0 \;\;\&\;\; \lambda_1 + \sqrt{\lambda(\lambda_2+\frac{\lambda_3}{2})} \geq 0 \tag{6.2}$$

$$\&\;\; \lambda_1 + \lambda_4 + \sqrt{\lambda(\lambda_2+\lambda_3)} \geq 0 \;\;\&\;\; \lambda_1 + \lambda_4 + \sqrt{\lambda(\lambda_2+\frac{\lambda_3}{2})} \geq 0 \tag{6.3}$$

unitarity:

$$|\lambda_1 + \lambda_4| \leq \kappa\pi \tag{6.4}$$
$$|\lambda_1| \leq \kappa\pi \tag{6.5}$$
$$|2\lambda_1 + 3\lambda_4| \leq 2\kappa\pi \tag{6.6}$$
$$|\lambda| \leq 2\kappa\pi \tag{6.7}$$
$$|\lambda_2| \leq \frac{\kappa}{2}\pi \tag{6.8}$$
$$|\lambda_2 + \lambda_3| \leq \frac{\kappa}{2}\pi \tag{6.9}$$
$$|\lambda + 4\lambda_2 + 8\lambda_3 \pm \sqrt{(\lambda - 4\lambda_2 - 8\lambda_3)^2 + 16\lambda_4^2}\,| \leq 4\kappa\pi \tag{6.10}$$
$$|3\lambda + 16\lambda_2 + 12\lambda_3 \pm \sqrt{(3\lambda - 16\lambda_2 - 12\lambda_3)^2 + 24(2\lambda_1+\lambda_4)^2}\,| \leq 4\kappa\pi \tag{6.11}$$
$$|2\lambda_1 - \lambda_4| \leq 2\kappa\pi \tag{6.12}$$
$$|2\lambda_2 - \lambda_3| \leq \kappa\pi \tag{6.13}$$

where we introduced the parameter κ that takes the values $\kappa = 16$ or 8, depending on whether we choose $|a_0| \leq 1$ or $|Re(a_0)| \leq \frac{1}{2}$ as pointed out at the end of section 5.
Working out analytically these two sets of BFB and unitarity constraints, one can reduce them to a more compact system where the allowed ranges for the λ's are easily identified. One can obtain a necessary domain for $\lambda, \lambda_2, \lambda_3$ that does not depend on λ_1 and λ_4, by considering simultaneously Eqs.(6.7 - 6.13) together with Eq. (6.1). It then turns out that Eqs.(6.8, 6.9) as well as the lower part of Eq.(6.13) are weaker than the actually allowed domains for λ_2, λ_3, and similarly Eq.(6.7) is weaker than the constraint on λ coming from Eq.(6.11). We find,

$$0 \leq \lambda \leq \frac{2}{3}\kappa\pi \tag{6.14}$$

$$\lambda_2 + \lambda_3 \geq 0 \;\; \& \;\; \lambda_2 + \frac{\lambda_3}{2} \geq 0 \tag{6.15}$$

$$\lambda_2 + 2\lambda_3 \leq \frac{\kappa}{2}\pi \tag{6.16}$$

$$4\lambda_2 + 3\lambda_3 \leq \frac{\kappa}{2}\pi \tag{6.17}$$

$$2\lambda_2 - \lambda_3 \leq \kappa\pi \tag{6.18}$$

We stress here that the above constraints define the largest possible domain for $\lambda, \lambda_2, \lambda_3$ for any set of allowed values of λ_1, λ_4, although Eqs.(6.10, 6.11) have been used to determine this domain. It is noteworthy that the upper bound on λ Eq.(6.14) is reduced by a factor 3 with respect to the naive expectation Eq. (6.7). Studying further Eqs.(6.10, 6.11), one can rewrite them in the following simple form where the dependence on λ_1, λ_4 has been explicitly separated from that on $\lambda, \lambda_2, \lambda_3$:

$$|\lambda_4| \leq \min \sqrt{(\lambda \pm 2\kappa\pi)(\lambda_2 + 2\lambda_3 \pm \frac{\kappa}{2}\pi)} \tag{6.19}$$

$$|2\lambda_1 + \lambda_4| \leq \sqrt{2(\lambda - \frac{2}{3}\kappa\pi)(4\lambda_2 + 3\lambda_3 - \frac{\kappa}{2}\pi)} \tag{6.20}$$

where Eqs.(6.14, 6.18) have been used in deriving Eq.(6.20)[8]. Various comments are in order here. First, to obtain the full domain for λ_1, λ_4, one has to add to Eqs.(6.19, 6.20) equations (6.4 - 6.6, 6.12) as well as Eqs.(6.2, 6.3). Thus for each set of values of $\lambda, \lambda_2, \lambda_3$, the allowed domain for λ_1, λ_4 is easily determined as the overlap of a set of linear bands, as illustrated in Fig. 1.
As stated earlier, Eqs. (6.15 - 6.18) define the largest possible domain for λ_2, λ_3 allowed by the combined unitarity and BFB constraints. The reason is seen from Eqs. (6.19, 6.20) that are the only extra constraints on λ_2, λ_3 depending on the actual values of $\lambda, \lambda_1, \lambda_4$. As one can easily check, these constraints become trivially satisfied when $\lambda_1 = \lambda_4 = 0$ and thus correspond to the case of largest λ_2, λ_3 domain. For each set of non vanishing values for λ_1, λ_4 the domain of λ_2, λ_3 given by Eqs. (6.15 - 6.18) will be further reduced according to Eqs. (6.19, 6.20). We illustrate the largest (λ_2, λ_3) domain in Fig. 2.

[8] In writing Eq. (6.20) we relied on the fact that the minimum of $\sqrt{2(\lambda \pm \frac{2}{3}\kappa\pi)(4\lambda_2 + 3\lambda_3 \pm \frac{\kappa}{2}\pi)}$ is given by $\sqrt{2(\lambda - \frac{2}{3}\kappa\pi)(4\lambda_2 + 3\lambda_3 - \frac{\kappa}{2}\pi)}$ in all the domain allowed by $\lambda, \lambda_2, \lambda_3$. In contrast, $\min \sqrt{(\lambda \pm 2\kappa\pi)(\lambda_2 + 2\lambda_3 \pm \frac{\kappa}{2}\pi)}$ appearing in Eq. (6.19) cannot be written in a closed form in this domain.

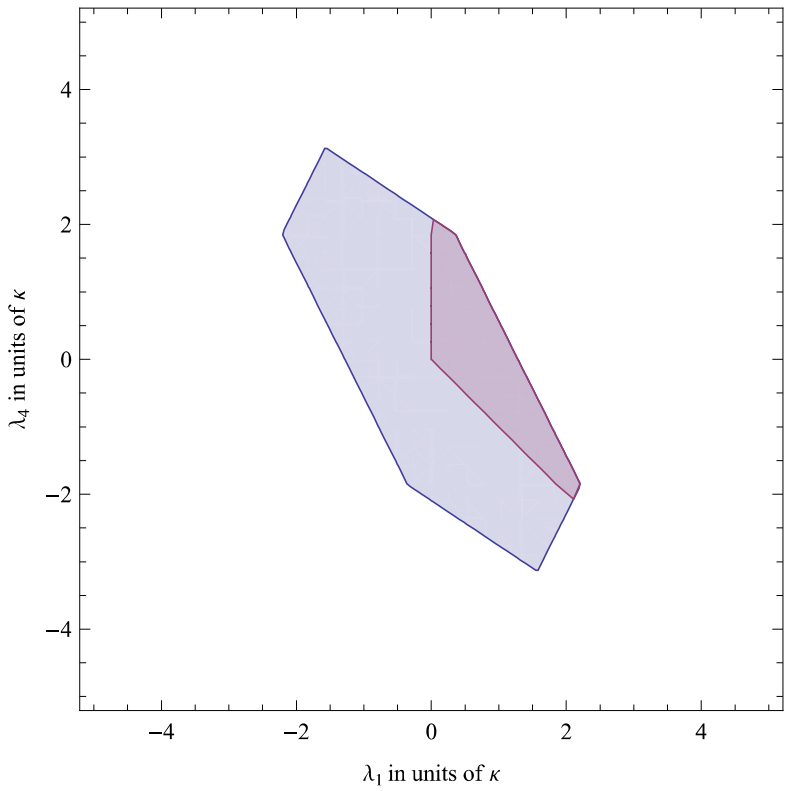

Figure 1: An illustration of a section of the (λ_1, λ_4) domain (blue) in units of κ as determined by Eqs. (6.4 - 6.6, 6.12, 6.19, 6.20), where we fixed $\lambda = \lambda_2 = \lambda_3 = 0$. Adding the BFB constraints Eqs.(6.2, 6.3) one obtains the reduced domain shown (light purple).

To summarize, the boundaries of the combined unitarity and general BFB domains for the five couplings are now given by the reduced set of equations (6.2 - 6.6, 6.14- 6.20) which moreover have an analytically simpler form. In particular, one readily finds from Eq. (6.20) that saturating the unitarity bound on λ, i.e. $\lambda = \frac{2}{3}\kappa\pi$, reduces the two-dimensional (λ_1, λ_4) domain to the one-dimensional (straight line) $\lambda_4 = -2\lambda_1$. This, as well as other features, will be useful in determining lower and upper bounds on the Higgs masses in the next section.

7 Higgs mass theoretical bounds

In this section we rely on the results of the previous sections to study the theoretically allowed ranges of the Higgs masses when varying the $\lambda_i's$ and the μ parameter in their allowed domains. Rather than assuming that μ is very large, i.e. of the order of the GUT scale together with $\mu \simeq M_\Delta$, we will study all the phenomenologically allowed range. We stress here that even very small values of μ are consistent with a tiny value of v_t necessary for realistic neutrino masses (and $\mathcal{O}(1)$ Yukawa couplings) provided that we take into account consistently Eq. (2.8).

Let us first describe qualitatively the generic behavior of the masses when μ is varied. We will show that, as a function of μ, the h^0 mass features a *maximum* $m_{h^0}^{\max}$ for a specific value $\mu = \mu_c$. This maximum will translate into an upper bound on m_{h^0} when the unitarity bound on λ is saturated. Similarly, the H^0 mass reaches a *minimum* $m_{H^0}^{\min}$ at a nearby value which we momentarily denote also $\mu = \mu_c$ for the sake of the qualitative discussion. In

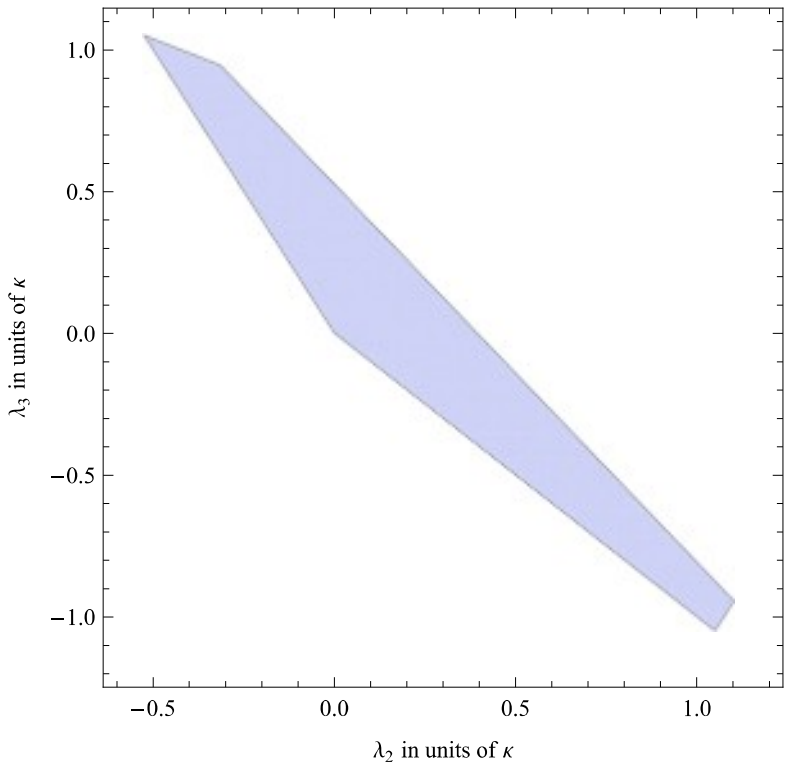

Figure 2: We illustrate here the *largest* $\lambda_2 - \lambda_3$ domain allowed by the combined unitarity and BFB constraints in units of κ. This domain corresponds to Eqs. (6.15 - 6.18) and is attained for $\lambda_1 = \lambda_4 = 0$ in which case Eqs. (6.19, 6.20) are trivially satisfied. As can be seen from Eqs. (6.19, 6.20), a smaller domain obtains as soon as λ_1 and/or λ_4 are non-zero, irrespecive of the value of λ satisfying Eq. (6.14).

the range $\mu < \mu_c$, H^0 is the heaviest among all the Higgses, decreasing very slowly with increasing μ towards its minimum value $m^{\rm min}_{H^0}$, while m_{h^0} increases very quickly with μ to $m^{\rm max}_{h^0}$. The other Higgs masses can have various hierarchies and in particular the unusual one where the $m_{H^{\pm\pm}}$ is the lightest state, $m_{H^{\pm\pm}} < m_{H^\pm} < m_A \simeq m_{h^0}$. In contrast, in the range $\mu_c < \mu < \mu_{\rm max}$, m_{H^0} now increases quickly with μ while m_{h^0} decreases very slowly from its maximal value. This sharply different behavior of m_{h^0} and m_{H^0} below and above μ_c can be traced back to the smallness of v_t. We illustrate numerically such a behavior in Fig. 3 where the seemingly constant $m^2_{h^0}$ for $\mu > \mu_c$ and constant $m^2_{H^0}$ for $\mu < \mu_c$ is an artifact of the very small ratio v_t/v_d. In fact, $m^2_{h^0}$ is decreasing very slowly to the right of μ_c and reaches zero when $\mu = \mu_+$, cf. section 3.2 and Appendix A, while $m^2_{H^0}$ starts off at $\mu = \mu_{\rm min}$ decreasing very slowly until its minimum value at $\mu = \mu_c$, then increases very slowly between μ_c and approximately $\mu = \bar{\mu} \simeq \lambda v_t/\sqrt{2}$, and increases very quickly afterwards. [9]

More quantitatively, we find that there are two different values of μ_c, that we dub $\mu_c^{(1)}$, $\mu_c^{(2)}$ that are uniquely determined in terms of v_d, v_t and the λ's. When one of these two critical values corresponds to $m^{\rm max}_{h^0}$ the other will correspond to $m^{\rm min}_{H^0}$, and vice versa, depending on the sign of the following quantity:

[9] The precise value is $\bar{\mu} = v_t(\lambda v_d^2 + 4(4\lambda_1 - \lambda_2 - \lambda_3 + 4\lambda_4)v_t^2)/\sqrt{2}(v_d^2 + 16 v_t^2)$. In fact $\bar{\mu}$ is the common value of μ at which the slopes of the variations of $m^2_{h^0}$ and $m^2_{H^0}$ as functions of μ experience a sudden change.

$$\mathcal{V}_\lambda \equiv (-\lambda + \lambda_1 + \lambda_4)\, v_d^2 + 4\,(\lambda_2 + \lambda_3)\, v_t^2 \tag{7.1}$$

Moreover, it turns out that at these extrema one of the two h^0 or H^0 states will correspond to a purely SM-like Higgs state, and this too is controlled by the sign of $\mathcal{V}_\lambda$. One can summarize the behavior analytically as follows:

i) $\underline{\mathcal{V}_\lambda > 0}$:

In this case m_{h^0} reaches a maximum given by

$$m^{2\ \max}_{h^0\ (1)} = m^2_{(1)} \equiv \frac{\lambda\, v_d^2}{2} \tag{7.2}$$

when μ takes the value

$$\mu = \mu_c^{(1)} \equiv (\lambda_1 + \lambda_4)\frac{v_t}{\sqrt{2}} \tag{7.3}$$

and $m^2_{H^0}$ reaches a minimum given by

$$\begin{aligned} m^{2\ \min}_{H^0\ (1)} = m^2_{(2)} &\equiv \frac{1}{2\,(v_d^2 + 16\, v_t^2)}(\lambda\, v_d^4 + 16\, v_t^2\,((\lambda_1 + \lambda_4)v_d^2 + 4(\lambda_2 + \lambda_3)\, v_t^2)) \\ &= \frac{\lambda\, v_d^2}{2} + \mathcal{O}(v_t^2) \end{aligned} \tag{7.4}$$

when μ takes the value

$$\mu = \mu_c^{(2)} \equiv \frac{v_t}{\sqrt{2}\,(v_d^2 + 16\, v_t^2)}((2\,\lambda - \lambda_1 - \lambda_4)\, v_d^2 + 8\,(2\,\lambda_1 + 2\,\lambda_4 - \lambda_2 - \lambda_3)\, v_t^2). \tag{7.5}$$

Expanding the Higgs masses squared around $\mu_c^{(1)}$ one finds

$$m^2_{h^0} = m^{2\ \max}_{h^0\ (1)} - \frac{4v_d^2}{\mathcal{V}_\lambda}\delta^2_{\mu 1} + \mathcal{O}(\delta^3_{\mu 1}) \tag{7.6}$$

$$\Delta^2_{H^0} = (-\lambda + \lambda_1 + \lambda_4)\frac{v_d^2}{2} + 2\,(\lambda_2 + \lambda_3)\, v_t^2 + \frac{v_d^2}{\sqrt{2}v_t}\delta_{\mu 1} + \mathcal{O}(\delta^2_{\mu 1}) \tag{7.7}$$

$$\Delta^2_{A^0} = (-\lambda + \lambda_1 + \lambda_4)\frac{v_d^2}{2} + 2\,(\lambda_1 + \lambda_4)\, v_t^2 + \frac{(v_d^2 + 4v_t^2)}{\sqrt{2}v_t}\delta_{\mu 1} + \mathcal{O}(\delta^2_{\mu 1}) \tag{7.8}$$

$$\Delta^2_{H^\pm} = (-\lambda + \lambda_1 + \frac{\lambda_4}{2})\frac{v_d^2}{2} + (2\lambda_1 + \lambda_4)\,\frac{v_t^2}{2} + \frac{(v_d^2 + 2v_t^2)}{\sqrt{2}v_t}\delta_{\mu 1} + \mathcal{O}(\delta^2_{\mu 1}) \tag{7.9}$$

$$\Delta^2_{H^{\pm\pm}} = (-\lambda + \lambda_1)\frac{v_d^2}{2} - \lambda_3 v_t^2 + \frac{v_d^2}{\sqrt{2}v_t}\delta_{\mu 1} + \mathcal{O}(\delta^2_{\mu 1}) \tag{7.10}$$

where $\Delta^2_X \equiv m^2_X - m^{2\ \max}_{h^0}$ denotes the various squared mass splittings from $m^{2\ \max}_{h^0}$ and $\delta_{\mu 1} \equiv \mu - \mu_c^{(1)}$.

ii) $\underline{\mathcal{V}_\lambda < 0}$:

In this case the reversed configuration occurs. m_{h^0} reaches a maximum, given by

$$m^{2\ \max}_{h^0\ (2)} = m^2_{(2)} \tag{7.11}$$

at $\mu = \mu_c^{(2)}$, while m_{H^0} reaches a minimum given by

$$m^{2\ \min}_{H^0\ (2)} = m^2_{(1)} \tag{7.12}$$

at $\mu = \mu_c^{(1)}$, where $m^2_{(1)}, m^2_{(2)}, \mu_c^{(1)}, \mu_c^{(2)}$ are as defined in Eqs.(7.2 - 7.5),

Again, expanding around $\mu_c^{(2)}$ we find

$$m^2_{h^0} = m^{2\ \max}_{h^0\ (2)} + \frac{4v_d^2}{\mathcal{V}_\lambda}\delta^2_{\mu 2} + \mathcal{O}(\delta^3_{\mu 2}) \tag{7.13}$$

and the squared mass splittings

$$\Delta^2_{H^0} = (\lambda - \lambda_1 - \lambda_4)\,\frac{v_d^2}{2} - 2(\lambda_2 + \lambda_3)\,v_t^2 + \frac{v_d^2}{\sqrt{2}v_t}\delta_{\mu 2} + \mathcal{O}(\delta^2_{\mu 2}) \tag{7.14}$$

$$\begin{aligned}\Delta^2_{A^0} = \frac{v_d^2}{(v_d^2 + 16\,v_t^2)}\,(\,&(\lambda - \lambda_1 - \lambda_4)\,\frac{v_d^2}{2} + 2\,(2\,(\lambda - \lambda_2 - \lambda_3) - \lambda_1 - \lambda_4)\,v_t^2\,) \\ &+ \frac{(v_d^2 + 4v_t^2)}{\sqrt{2}v_t}\delta_{\mu 2} + \mathcal{O}(\delta^2_{\mu 2}, v_t^4/v_d^2)\end{aligned} \tag{7.15}$$

$$\begin{aligned}\Delta^2_{H^\pm} = \frac{v_d^2}{(v_d^2 + 16\,v_t^2)}\,((\lambda - \lambda_1 - \frac{3}{2}\,\lambda_4)\,\frac{v_d^2}{2} + (2\,\lambda - \lambda_1 - 4\lambda_2 - 4\lambda_3 - \frac{11}{2}\lambda_4)\,v_t^2) \\ + \frac{(v_d^2 + 2v_t^2)}{\sqrt{2}v_t}\delta_{\mu 2} + \mathcal{O}(\delta^2_{\mu 2}, v_t^4/v_d^2)\end{aligned} \tag{7.16}$$

$$\begin{aligned}\Delta^2_{H^{\pm\pm}} = \frac{v_d^2}{(v_d^2 + 16\,v_t^2)}((\lambda - \lambda_1 - 2\,\lambda_4)\,\frac{v_d^2}{2} - (4\,\lambda_2 + 5\,\lambda_3 + 8\,\lambda_4)\,v_t^2 \\ + \frac{v_d^2}{\sqrt{2}v_t}\delta_{\mu 2} + \mathcal{O}(\delta^2_{\mu 2}, v_t^4/v_d^2)\end{aligned} \tag{7.17}$$

where $\delta_{\mu 2} \equiv \mu - \mu_c^{(2)}$.

Noting that $\mu_c^{(1)} - \mu_c^{(2)}$, $m^2_{(2)} - m^2_{(1)}$ and $\mathcal{V}_\lambda$ have the same sign, and defining

$$\mu_c^{\min} \equiv \min\{\mu_c^{(1)}, \mu_c^{(2)}\} \tag{7.18}$$

$$\mu_c^{\max} \equiv \max\{\mu_c^{(1)}, \mu_c^{(2)}\} \tag{7.19}$$

one can recast the results of Eqs.(7.2, 7.4, 7.11, 7.12) in a more compact form as

$$m^{2\ \max}_{h^0} = m^2_{h^0}(\mu = \mu_c^{\max}) = \min\{m^2_{(1)}, m^2_{(2)}\} \tag{7.20}$$

$$m^{2\ \min}_{H^0} = m^2_{H^0}(\mu = \mu_c^{\min}) = \max\{m^2_{(1)}, m^2_{(2)}\} \tag{7.21}$$

with an implicit reference to the two regimes *i)* and *ii)* if one keeps in mind that $m^2_{(i)}$ is reached for $\mu = \mu_c^{(i)}$.

The mixing pattern: for $\mu = \mu_c^{(1)}$, h^0 and H^0 become pure doublet or triplet states, since in this case $B = 0$ as can be seen from Eq.(2.22). However, a close inspection of Eq.(2.40) shows that in the regime *i)* (resp. *ii)*) one has $s_\alpha = 0$ (resp. $s_\alpha = 1$) for this value of μ. Thus, at $\mu = \mu_c^{(1)}$, h^0 becomes a pure SM-like Higgs in regime *i)*, but it is H^0 that becomes a pure SM-like Higgs in regime *ii)*. The fact that the SM-like state is not always associated with the lightest $\mathcal{CP}_{even}$ state is important when discussing the Higgs phenomenology and interpretation of the experimental limits and is consistent with the fact that $m^2_{(1)}$ is indeed the SM Higgs squared mass, Eq.(7.2). In fact, due to the smallness of v_t/v_d the behavior of the mixing angle α over the full range of the μ parameter follows closely the generic pattern discussed above: in both regimes *i)* and *ii)* one has essentially $s_\alpha \simeq \pm 1$ or $s_\alpha \simeq 0$ over most of the μ range, except for a very narrow region in the vicinity of $\bar{\mu}$ defined in footnote 9 and satisfying

$$\bar{\mu} = \frac{1}{2}(\mu_c^{(1)} + \mu_c^{(2)}) \tag{7.22}$$

where $|s_\alpha|$ changes quickly from $\simeq 0$ to $\simeq 1$. The generic dominance of no-mixing regimes can be understood from the asymptotic behavior at small and large μ values, i.e. $|\sin\alpha_{|\mu\to 0}| = 1 - 2\frac{(\lambda_1+\lambda_4)^2}{\lambda^2}(v_t^2/v_d^2) + \mathcal{O}(v_t^3)$ and $\sin\alpha_{|\mu\to\mu_+} = 2(v_t/v_d) + \mathcal{O}(v_t^2)$, together with the fact that $ds_\alpha/d\mu = \mathcal{O}(v_t^3)$. We illustrated this behavior in Fig. 5 adopting the sign convention $\epsilon_\alpha = +1$. As seen in Fig. 5.b, s_α remains positive in all the μ range since $B < 0$ (*cf.* Eq.(2.22, 2.40)). And in accordance with the asymptotic behavior, s_α tends to $\mathcal{O}(10^{-2})$ at large $\mu(> \bar{\mu})$ where h^0 is nearly SM-like, and to $\mathcal{O}(1)$ at small $\mu(< \bar{\mu})$ where H^0 is nearly SM-like. [Note that in this numerical example $\mu_c^{(1)}$ becomes negative and is never reached]. In contrast, for the regime illustrated in Fig. 5.a, s_α remains negative for $\mu < \mu_c^{(1)}$, crosses zero at $\mu_c^{(1)}$ and again tends to a positive value $\mathcal{O}(10^{-2})$ for $\mu \gg \mu_c^{(1)}$.

The exact magnitude of $|s_\alpha|$ at the three critical values of μ can be summarized as follows:

$$
\begin{array}{rccc}
 & \mathcal{V}_\lambda > 0: & & \mathcal{V}_\lambda < 0: \\
|s_\alpha(\mu=\mu_c^{(1)})| = & 0 & , & 1 \\
|s_\alpha(\mu=\bar{\mu})| = & \left(\frac{1}{2}-\frac{2v_t}{\sqrt{v_d^2+16v_t^2}}\right)^{1/2} & , & \left(\frac{1}{2}+\frac{2v_t}{\sqrt{v_d^2+16v_t^2}}\right)^{1/2} \\
= & \frac{1}{\sqrt{2}}-\sqrt{2}\frac{v_t}{v_d}+\mathcal{O}(\frac{v_t^2}{v_d^2}) & , & \frac{1}{\sqrt{2}}+\sqrt{2}\frac{v_t}{v_d}+\mathcal{O}(\frac{v_t^2}{v_d^2}) \\
|s_\alpha(\mu=\mu_c^{(2)})| = & \frac{v_d}{\sqrt{v_d^2+16v_t^2}} & , & \frac{4v_t}{\sqrt{v_d^2+16v_t^2}} \\
= & 1-8\frac{v_t^2}{v_d^2}+\mathcal{O}(\frac{v_t^3}{v_d^3}) & , & 4\frac{v_t}{v_d}+\mathcal{O}(\frac{v_t^3}{v_d^3})
\end{array}
\tag{7.23}
$$

Large mixing scenarios have been discussed previously in [18, 38] while here we quantify more precisely the regions where such a large mixing takes place.
For later analyses it is useful to characterize the μ range in the large $|s_\alpha|$ regime. One sees from the above equations that the size of this range is $\mathcal{O}(v_t)$. As a first approximation one can characterize it by the interval $0 < \mu < \mu_c^{\min}$, with $\mu_c^{\min}$ given by Eq. (7.18). However, depending on the values of λ and $\lambda_1+\lambda_4$, $|s_\alpha|$ can still be very close to 1 in the range $\mu_c^{\min} < \mu < \bar{\mu}$, especially that $\mu_c^{\min}$ is not positive definite [it becomes negative when $\lambda_1+\lambda_4 < 0$ or $2\lambda-(\lambda_1+\lambda_4) < 0$]. It is more sensible to base this characterization on the amount of deviation from the value $|s_\alpha| = 1$. Defining $\hat{\mu}$ in the vicinity of $\bar{\mu}$ in the form $\hat{\mu} \equiv \bar{\mu} - \delta \times v_t$, with δ strictly > 0, one finds $|s_\alpha(\hat{\mu})| = 1 - k(\delta)\frac{v_t^2}{v_d^2} + \mathcal{O}(\frac{v_t^3}{v_d^3})$. For each given *positive* value of k there corresponds a value of $\hat{\mu}$ given by

$$
\hat{\mu}_{(\pm)} = (\frac{\lambda}{\sqrt{2}} - \frac{\lambda-\lambda_1-\lambda_4}{\sqrt{2}\pm\sqrt{k}})v_t + \mathcal{O}(\frac{v_t^3}{v_d^2}) \tag{7.24}
$$

The two-fold ambiguity in this expression is resolved as follows: requiring consistently $\mu_c^{\min} \leq \hat{\mu} < \bar{\mu}$ to hold, one should take for $\mathcal{V}_\lambda > 0$, $\hat{\mu} = \hat{\mu}_{(-)}$ with $k \geq 8$, and for $\mathcal{V}_\lambda < 0$, $\hat{\mu} = \hat{\mu}_{(+)}$ for any $k \geq 0$.[10] In particular $\hat{\mu}$ reproduces respectively $\mu_c^{(1)}$ and $\mu_c^{(2)}$ for the special values $k = 0$ and $k = 8$ as expected, while $\bar{\mu}$ cannot be reached for any finite value of k [consistently with the fact that $|s_\alpha(\hat{\mu})| \simeq 1$ and $|s_\alpha(\hat{\mu})| \simeq 1/\sqrt{2}$ are not perturbatively close to each other in terms of powers of v_t/v_d].

With the above prescription one can characterize the μ range in the large $|s_\alpha|$ regime by $0 < \mu < \hat{\mu}(k)$, where k can now be interpreted as triggering the experimental sensitivity to the deviation of $|s_\alpha|$ from its maximal value $|s_\alpha| = 1$. Equation (7.24) shows that the lower the sensitivity to large $|s_\alpha|$ (i.e. the larger k), the lower the sensitivity of the size of the μ domain to $\lambda_1+\lambda_4$. We will come back to the above issues in the phenomenological

[10] Strictly speaking, in the case $\mathcal{V}_\lambda > 0$ one can still choose k in the interval $2 < k < 8$ if $\mathcal{V}_\lambda$ is sufficiently close to zero so that to ensure that $\mu_c^{\min} \leq \hat{\mu}$. In practice these details will not be important, since one does not expect an experimental sensitivity to the deviation from $|s_\alpha| = 1$ to be better than a few percent. A deviation of 1%, with $v_t = 1$GeV, puts the value of k already around 600 !

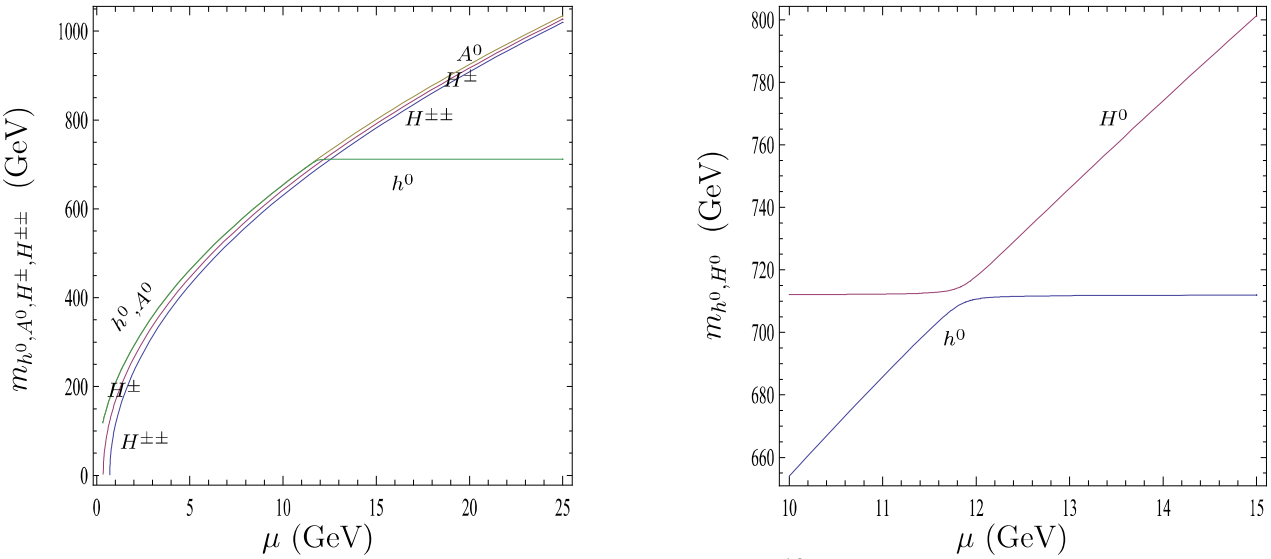

Figure 3: Illustration of the regime $\mathcal{V}_\lambda < 0$ with $\lambda = \frac{16\pi}{3}, \lambda_2 = 10^{-1}, \lambda_3 = 2\times 10^{-1}, \lambda_1 = -\frac{1}{2}, \lambda_4 = 1, v_t = 1$ GeV, $v = 246$ GeV, $v_d = \sqrt{v^2 - 2v_t^2}, \kappa = 8$, leading to $\mu_c^{(2)} \simeq 23$ GeV. see Eq. (7.5).

discussion of section 8.

Unitarity bounds: relying on the above properties we can now easily derive the theoretical upper bounds on the various Higgs masses. From Eq. (7.2), and using the maximal value allowed by the tree-level unitarity constraint for λ, Eq. (6.14), and $v_d \simeq 246$GeV, we determine an upper bound on m_{h^0},

$$m_{h^0} \lesssim 712\,\text{GeV (for } \kappa = 8) \tag{7.25}$$
$$\lesssim 1\,\text{TeV (for } \kappa = 16) \tag{7.26}$$

If Eq. (7.11) is used instead, then the saturation of unitarity and BFB bounds on $\lambda_1 + \lambda_4$ should be also considered. However, due to the smallness of v_t/v_d, this would lead to only a few GeV change in the above upper bounds. As far as m_{H^0} is concerned, the above bounds are essentially the minimally allowed values, as obvious from Eq. (7.20, 7.21), in the unitarity saturation limit. To obtain its theoretical upper bound as well as those of the other Higgs masses, one should rather take μ at its maximally allowed value, $\mu_{\max} \simeq \mu_+ \simeq \frac{\lambda}{4\sqrt{2}}\frac{v_d^2}{v_t}$, since all these masses increase monotonically with μ. For instance, with the set of parameters chosen in Figs. 3, 4 and $v_t = 1$ GeV one finds the upper bounds

$$m_{H^{\pm\pm}} \simeq m_{H^\pm} \simeq m_A \simeq m_{H^0} \simeq 88\,\text{TeV (for } \kappa = 8) \tag{7.27}$$
$$\simeq 124\,\text{TeV (for } \kappa = 16) \tag{7.28}$$

which are not phenomenologically compelling. Actually, somewhat lower bounds are obtained when taking into account the experimental exclusion limits on a light Higgs m_{h^0} but remain too high to be useful. In contrast, phenomenologically interesting scenarios with light charged, doubly charged, $\mathcal{CP}_{odd}$ and $\mathcal{CP}_{even}$ Higgses are possible for small values of μ. For instance as illustrated in Figs. 3, 4, such a light spectrum occurs when $\mu \ll \mu_c^{(2)} \simeq 23$ GeV. More generally, the analytical expressions given above for the mass splittings show

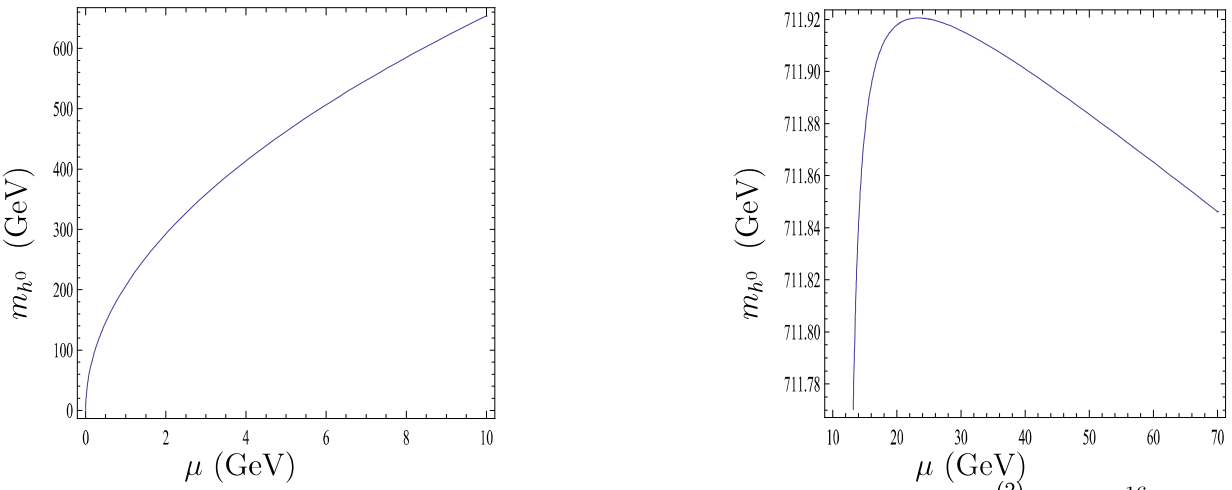

Figure 4: Zoom on the variation of m_{h^0} with μ in the vicinity of $\mu_c^{(2)}$; $\lambda = \frac{16\pi}{3}, \lambda_2 = 10^{-1}, \lambda_3 = 2\times 10^{-1}, \lambda_1 = -\frac{1}{2}, \lambda_4 = 1, v_t = 1$ GeV, $v = 246$ GeV, $v_d = \sqrt{v^2 - 2v_t^2}, \kappa = 8$, leading to $\mu_c^{(2)} \simeq 23$ GeV. see Eq. (7.5).

that in the vicinity of μ_c and in particular for $\mu < \mu_c$ the neutral $\mathcal{CP}_{even}$ h^0 is not necessarily the lightest Higgs.[11] The detailed patterns will depend on the actual values of the λ's and will be studied more thoroughly in the next section, but one can already see some generic features in regimes *i)* and *ii)* at $\mu \simeq \mu_c$. In regime *i)* where $-\lambda + \lambda_1 + \lambda_4 > 0$ one expects $H^{\pm\pm}$ to become the lightest Higgs if $-\lambda + \lambda_1 < 0$, that is when $\lambda_1 < \lambda < \lambda_1 + \lambda_4$. Similarly, in regime *ii)* where typically $\lambda - \lambda_1 - \lambda_4 > 0$ one again expects $H^{\pm\pm}$ to be the lightest Higgs when $\lambda_1 + \lambda_4 < \lambda < \lambda_1 + 2\lambda_4$. More generally, a close inspection of Eqs.(2.11, 2.27) shows that $m_{H^{\pm\pm}} < m_{h^0}$ when $\mu < \mu^\star = (\lambda + \lambda_4)v_t/\sqrt{2} + \mathcal{O}(v_t^3/v_d^2)$, and only if $\lambda_4 > 0$.[12] Furthermore, it immediately follows from Eqs.(2.13, 2.31) that $m_{H^{\pm\pm}} < m_{H^\pm} < m_A$ when $\lambda_4 > 0$ so that the necessary and sufficient condition for $H^{\pm\pm}$ to be the lightest Higgs is

$$\mu < \mu^\star \ \text{ with } \ \lambda_4 > 0. \tag{7.29}$$

Phenomenological bounds: in order to prepare for a phenomenological study, we discussed in section 3.2 the modification on the tachyonic bounds of μ when experimental exclusion limits are available for $m_{A^0}, m_{H^\pm}$ and $m_{H^{\pm\pm}}$, *cf.* Eqs.(3.65, 3.66). Here we address the same question concerning m_{h^0} and m_{H^0}. Given some experimental exclusion *lower* bounds $(m_{h^0})_{\rm exp}$, (resp. $(m_{H^0})_{\rm exp}$) there corresponds two values $\mu_\pm^{h^0}$ (resp. $\mu_\pm^{H^0}$), namely

$$\begin{aligned}\mu_\pm^{h^0} = & \frac{1}{8\sqrt{2}v_t}(\lambda v_d^2 + 8(\lambda_1+\lambda_4)v_t^2 - 2(m_{h^0}^2)_{\rm exp} \\ & \pm 2\left[(m_{(1)}^2 - (m_{h^0}^2)_{\rm exp})(m_{(2)}^2 - (m_{h^0}^2)_{\rm exp})\right]^{\frac{1}{2}}(1 + 16\frac{v_t^2}{v_d^2})^{\frac{1}{2}})\end{aligned} \tag{7.30}$$

(and similarly for $\mu_\pm^{H^0}$ with $(m_{h^0})_{\rm exp}$ replaced by $(m_{H^0})_{\rm exp}$), for which m_{h^0} reaches $(m_{h^0})_{\rm exp}$ (resp. m_{H^0} reaches $(m_{H^0})_{\rm exp}$). Note that in the limit of no experimental bounds, i.e.

[11] We have kept in these expressions subleading terms of $\mathcal{O}(v_t^2)$ in order to handle as well the small parts of the λ_i's parameter space where the leading $\mathcal{O}(v_d^2)$ are suppressed.

[12] Although this expression of $\mu^\star$ is well-defined for $\lambda_4 < 0$, one finds that the splitting $m_{H^{\pm\pm}}^2 - m_{h^0}^2$ is negative only in the domain defined by $\mu < (\lambda + 2\lambda_4)v_t/\sqrt{2} + \mathcal{O}(v_t^3/v_d^2)$ and $-\lambda_4 v_d^2/(4\sqrt{2}v_t) + \mathcal{O}(v_t) < \mu < (\lambda+\lambda_4)v_t/\sqrt{2} + \mathcal{O}(v_t^3/v_d^2)$, which is clearly non-empty only for $\lambda_4 > 0$.

$(m^2_{h^0,H^0})_{\rm exp} \to 0$, Eq.(7.30) gives back Eq.(A.1). Furthermore, relying on the fact that m_{h^0} has a maximum and m_{H^0} has a minimum as functions of μ, *cf.* Eq. (7.20, 7.21), the phenomenological bounds read

$$\begin{array}{c} \mu_-^{h^0} \leq \mu \leq \mu_+^{h^0} \quad \text{assuming} \quad (m_{h^0})_{\rm exp} \leq m_{h^0}^{\rm max} \\ \text{and} \\ \mu \leq \mu_-^{H^0} \text{ or } \mu_+^{H^0} \leq \mu \quad \text{assuming} \quad (m_{H^0})_{\rm exp} \geq m_{H^0}^{\rm min} \end{array} \tag{7.31}$$

Obviously $(m_{h^0})_{\rm exp} > m_{h^0}^{\rm max}$ would be an inconsistent assumption, while $(m_{H^0})_{\rm exp} < m_{H^0}^{\rm min}$ would be an empty assumption not leading to any constraint as far as μ is concerned.

In summary, the experimental lower bounds on the various Higgs masses will typically constrain the μ parameter to lie in a finite domain defined by the combination of Eqs.(3.66, 7.31).

8 Higgs phenomenology

Although previous studies in the literature assumed typically the triplet mass M_Δ and the mass parameter μ to be much larger than the electroweak scale, $M_\Delta \gg v_d$, attention has been paid more recently to the possibility of having $M_\Delta, \mu \lesssim 1$ TeV where the Higgses of the DTHM might be accessible at the Tevatron and the LHC [17, 39, 40, 41, 42, 43, 44, 45, 46]. In this spirit, the results obtained in the previous sections help defining educated strategies to extract constraints on the physical Higgs masses and model parameters from experimental data, rather than performing merely blind (and CPU time consuming) scans on these parameters. The existing experimental exclusion limits on the SM Higgs particle are readily translated into constraints on the DTHM in the parameter space region where h^0 becomes SM-like, i.e. when the mixing between the doublet and the triplet is very small. However, even when far from this region, existing exclusion limits for an extended Higgs sector (such as in two Higgs doublets models or in the minimal supersymmetric extension of the SM) can also be partially adapted to h^0, H^0, A^0 and $H^\pm$, while of course $H^{\pm\pm}$ has a distinctive experimental search.

In this section we give a quick overview of the Higgs sector phenomenology and experimental searches (for an extended overview on the phenomenology of triplet models see Ref. [47]), followed by a preliminary analysis using our results. A detailed study taking into account all present-day experimental limits lies out of the scope of this paper and will be presented elsewhere.

Doubly charged Higgs

Observation of the doubly charged Higgs $H^{\pm\pm}$ would signal unambiguously physics beyond Higgs doublets, let alone physics beyond the SM Higgs sector. Owing to charge conservation, it is obvious that $H^{\pm\pm}$ cannot couple to a pair of quarks, therefore, its possible decay modes are:

i) same sign charged lepton pair $H^{\pm\pm} \to l^\pm l^\pm$ that proceed via lepton number violating coupling,

ii) a pair of $W^\pm$ gauge bosons $H^{\pm\pm} \to W^\pm W^\pm$,

iii) $H^{\pm\pm} \to W^\pm H^\pm$,

iv) a pair of charged Higgs bosons $H^{\pm\pm} \to H^{\pm} H^{\pm}$.

We emphasize also that the doubly charged Higgs couples to the photon and to the Z boson through gauge couplings Eqs. (C.17, C.18), while its couplings to a pair of $W^{\pm}$ is proportional to the triplet vev v_t, see Eqs. (C.15). Therefore the decay channel ii) will be suppressed for $v_t \ll v_d$. The decay channel iv) will also be suppressed for small v_t as can be seen from the form of the coupling of $H^{\pm\pm}$ to a pair charged Higgses $H^{\pm}$, Eq. (C.16). Indeed, one has $\cos\beta' \simeq 1$ and $\sin\beta' \sim v_t/v_d$ from Eq. (2.19), and furthermore, the $\mu \sin^2\beta'$ is also of order v_t due to the μ upper bound $\mu_+ \sim v_d^2/v_t$, *viz* Eq. (A.1). In contrast, the coupling $H^{\pm\pm}W^{\pm}H^{\pm}$ is proportional to the gauge coupling and has no suppression factors. The decay channel ii) will thus contribute substantially if kinematically open. Depending on the size of the Yukawa couplings of the leptons, the doubly charged Higgs can decay dominantly either to a pair of leptons or to $W^{\pm}$ and $H^{\pm}$, and subdominantly to a pair of $W^{\pm}$ and/or a pair of $H^{\pm}$ if kinematically allowed.

In e^+e^- collisions, the doubly charged Higgs can be pair produced through γ and Z s-channel[13] $e^+e^- \to \gamma^*, Z^* \to H^{\pm\pm}H^{\mp\mp}$ [48, 49, 50, 51]. One can have also access to the associate production of $H^{\pm}$ with $W^{\mp}$ through s-channel Z exchange [52, 53, 54]. If the e^-e^- option is available at ILC, then the doubly charged Higgs can be produced in $W^{\pm}W^{\pm}$ fusion through $e^-e^- \to W^{-*}W^{-*} \to e^-e^-H^{++}$. Even if $H^{\pm\pm}W^{\mp}W^{\mp}$ has a v_t suppression, the rate for $W^{\pm}W^{\pm}$ fusion could be substantial especially at higher energies options for e^-e^- [49].

At the Tevatron or the LHC, the two production mechanisms with potentially large cross sections are $p\bar{p}/pp \to \gamma^*, Z^* \to H^{\pm\pm}H^{\mp\mp}X$ or a single production through WW fusion $p\bar{p}/pp \to W^{\pm *}W^{\pm *} \to H^{\pm\pm}X$ [55, 56]. The latter process as well as the s-channel $p\bar{p}/pp \to W^{\pm *} \to W^{\mp}H^{\pm\pm}$ depend on the coupling $H^{\pm\pm}W^{\mp}W^{\mp}$ which is proportional to the triplet vev. However, the suppression due to the small value of v_t is somewhat compensated by the fact that $W^{\pm}W^{\pm}$ fusion could be substantial at high energy. Those processes have to be supplemented by the associate production of singly and doubly charged Higgs bosons $p\bar{p}/pp \to H^{\pm\pm}H^{\mp}X$ which could have a comparable cross section to $p\bar{p}/pp \to H^{\pm\pm}H^{\mp\mp}X$ [57], [58].

Such doubly charged Higgs have been subject to many experimental searches. At LEP-II, the experiments L3, OPAL and Delphi [59],[60], [61] performed a search for doubly charged Higgs boson assuming that $H^{\pm\pm}$ decay dominantly to a pair of leptons $H^{\pm\pm} \to l^{\pm}l^{\pm}$. Four leptons final states have been analyzed at L3, OPAL and Delphi. L3 performed a search for the six possibilities: ee, $\mu\mu$, μe, $\mu\tau$, $e\tau$ and $\tau\tau$. No excess has been found and lower limits in the range 95-100 GeV at 95% confidence level on the doubly charged Higgs boson mass are derived. Those lower limits depend on the doubly charged Higgs decay modes. For example, if $H^{\pm\pm} \to e^{\pm}e^{\pm}$ is the dominant decay, then the lower limit is 100 GeV while if $H^{\pm\pm} \to \mu^{\pm}\tau^{\pm}$ is the dominant decay then the lower limit is about 95 GeV.
At the Tevatron, DØ[62],[63] and CDF [64], [65] have searched for $p\bar{p} \to \gamma^*, Z^* \to H^{\pm\pm}H^{\mp\mp}X$ with $H^{\pm\pm} \to l^{\pm}l^{\pm}$. DØ measurement [62] represents the first doubly charged Higgs search with the decay $H^{\pm\pm} \to \mu^{\pm}\mu^{\pm}$. Note that DØ search was limited to $H^{\pm\pm} \to \mu^{\pm}\mu^{\pm}$ that is an almost background free signal, while CDF explored the three final states $e^{\pm}e^{\pm}, \mu^{\pm}\mu^{\pm}$ and $e^{\pm}\mu^{\pm}$. Both DØ and CDF excluded a doubly charged Higgs with a mass in the range $100 \to 150$ GeV. We stress that all those bounds assume a 100% branching ratio for $H^{\pm\pm} \to l^{\pm}l^{\pm}$ decay, while in realistic cases one can easily find scenarios where $H^{\pm\pm} \to l^{\pm}l^{\pm}$

[13] the t-channel mediated by a lepton is in general suppressed by the small Yukawa coupling

is suppressed while $H^{\pm\pm} \to W^{\pm *} W^{\pm *}$ is substantial [17, 39, 66, 67] which could invalidate partially the CDF and D$\emptyset$ limits. However, the LHC has the capability to extend the above limits up to a mass about 1 TeV for high luminosity option [17, 40, 56, 68]. Observation of doubly charged Higgs bosons at the LHC and measurement of its leptonic branching ratios will shed also some light on the neutrino mass pattern [17, 39, 51, 58, 66, 67, 69, 70, 44].

Finally, indirect limits on the mass and the bileptonic couplings of the doubly charged Higgs boson can be extracted from low energy lepton flavor violating processes, such as $\mu \to e\gamma$, $\mu \to 3e$, $\tau \to 3l$,... (see for instance [41, 45]).

Singly charged Higgs

Let us now discuss briefly the couplings of the singly charged Higgs and its decay modes. The charged Higgs coupling to lepton and neutrino is proportional to $\approx m_\nu/v_t \approx Y_\nu$ [17] which could be of the order $\mathcal{O}(1)$ if v_t is very small. Similarly, the charged Higgs coupling to a pair of quark u and d is proportional to $\tan\beta'$ which is suppressed by v_t/v_d [17]. In the case of $H^-\bar{t}b$, this coupling could enjoy some enhancement from Yukawa coupling of the top quark. The suppression of the coupling $H^-\bar{t}b$ has three consequences:

- Given the suppression factor of the order v_t/v_d for $H^-\bar{t}b$, the charged Higgs mass can not be subject to $b \to s\gamma$ constraint, similarly to the two Higgs doublet model type I where the coupling is suppressed by $1/\tan\beta$.
- Some of the conventional mechanisms for charged Higgs production at Hadron colliders such as $bg \to tH^+$ and $gg \to tbH^+$ will be suppressed.
- Since the charged Higgs search at the Tevatron is based on the top decay $t \to H^+b$, given the suppression of $H^+t\bar{b}$ coupling the branching ratio of $t \to bH^+$ would also be suppressed. One concludes then that the CDF limit does not apply in this case.

Besides those processes which are suppressed, one can still produce charged Higgses through the associate production of singly and doubly charged Higgs $pp/p\bar{p} \to W^* \to H^{\pm\pm}H^\mp$ [57, 58] with a spectacular signature from $H^{\pm\pm} \to l^\pm l^\pm$. Other mechanisms are: the Drell-Yan process $pp/p\bar{p} \to \gamma^*, Z^* \to H^\pm H^\mp$, the associate production of charged Higgs and neutral Higgs $pp/p\bar{p} \to W^* \to H^\pm h^0$, $pp/p\bar{p} \to W^* \to H^\pm H^0$, $pp/p\bar{p} \to W^* \to H^\pm A^0$ and the associate production of charged Higgs with W gauge boson $pp/p\bar{p} \to Z^* \to W^\pm H^\mp$. Note that among the latter processes, the ones with $W^\pm H^\mp$ or $H^\mp h^0$ final states are suppressed by a v_t/v_d factor as compared to the Drell-Yan and the two other associate production processes that are controlled by gauge couplings, cf. Eqs. (C.10, C.13) and Eqs. (C.11, C.12).

If the charged Higgs decays dominantly to leptons (for small v_t) we can apply the LEP mass lower bounds that are of the order of 80 GeV [71], [72]. For large v_t, i.e. much larger than the neutrino masses but still well below the electroweak scale, the dominant decay is either $H^+ \to t\bar{b}$ or one of the bosonic decays $H^+ \to W^+Z$, $H^+ \to W^+h^0/W^+A^0$. For the first two decay modes there has been no explicit search neither at LEP nor at the Tevatron, while for the $H^+ \to W^+A^0$ decay (and possibly for $H^+ \to W^+h^0/$ if h^0 decays similarly to A^0), one can use the LEPII search performed in the framework of two Higgs doublet models. In this case the charged Higgs mass limit is again of the order of 80 GeV [72].

Neutral Higgses

The lighter $\mathcal{CP}_{even}$ Higgs boson h^0 is fully dominated by the doublet component (i.e the mixing $|s_\alpha| \ll 1$) when $\mu > \bar{\mu}$, as discussed in section 7 and illustrated on Fig. 5. In this case the coupling of h^0 to a pair of neutrinos is suppressed being proportional to s_α. Such Higgs will completely mimic the SM Higgs boson and then the LEP and the recent Tevatron limits would apply. In this scenario of very small mixing, the other neutral Higgses H^0 and A^0 would be fermiophobic to all charged leptons and quarks but their coupling to a pair of neutrinos that is proportional to $\cos\alpha Y_\nu \approx Y_\nu = m_\nu/v_t$ could be enhanced for small v_t. Then the dominant decay mode for H^0 and A^0, for small v_t, would be a pair of neutrinos [17].

Note that A^0, being $\mathcal{CP}_{odd}$, does not couple to a pair of gauge bosons while the couplings H^0ZZ and H^0WW in the small mixing case are suppressed by v_t/v_d, Eqs.(C.4, C.6). Thus the W and Z Higgsstrahlung productions of H^0 and A^0 are expected to be small. Furthermore, while the H^0A^0Z vertex is controlled by the gauge coupling, Eq. (C.8), h^0A^0Z has an extra v_t/v_d suppression, Eq. (C.7). This implies that in the small mixing case, one can still produce A^0 and H^0 through the Drell-Yan process $e^+e^-/pp/p\bar{p} \to Z^* \to H^0A^0$. For very small v_t, A and H^0 would decay essentially into a pair of neutrinos. At LEP, the signal would then be a photon (from initial state radiation) and missing energy in the final state. A lower bound on m_H and m_A of the order of 55 GeV can be extracted in this case from LEPII data, assuming mass degeneracy between A^0 and H^0 [73]. [In the non degenerate case the lower bound translates into $m_H + m_A \geq 110$ GeV.] Increasing v_t well above the neutrino masses decreases significantly $H^0/A^0 \to \nu\nu$, and the decay channels $H^0 \to b\bar{b}$, $A^0 \to b\bar{b}$, as well as $H^0 \to ZZ$, $A^0 \to Zh^0$ if open, see Eqs. (C.4, C.7), can become dominant. If $H^0 \to b\bar{b}$, $A^0 \to b\bar{b}$ dominate, the LEPII Higgs search through $e^+e^- \to H^0A^0$ in the two Higgs doublet Model can apply to the DTHM in this case, and the limit is roughly $m_H + m_A \geq 185$ GeV [74]. There is however a distinctive feature in the DTHM related to the $H^0h^0h^0$ coupling, Eq. (C.9), the latter becoming substantial for increasing μ and thus for heavier H^0. The $H^0 \to h^0h^0$ decay mode would then be important in both the large and small (with respect to the neutrino masses) v_t regimes.

In the case of maximal mixing $|s_\alpha| \approx 1$ which occurs for $\mu < \bar{\mu}$, see Fig. 5, the roles of h^0 and H^0 are interchanged. H^0 is fully doublet and h^0 is fully triplet. Taking into account this interchange, the previous discussion applies here to H^0. However, since h^0 remains the lighter Higgs which can be now far from SM-like, one expects weaker experimental constraints on its mass than the ones quoted above.

Top decay into charged Higgs

A light charged Higgs of the order $100 \to 200$ GeV is still allowed by theoretical constraints as well as by experimental search. If the charged Higgs satisfies $m_{H^\pm} \leq m_t - m_b$, one could ask whether the decay $t \to bH^+$ can have a significant branching ratio to be observed at the LHC. As mentioned before, the coupling H^+tb has a v_t/v_d suppression and the branching ratio for $t \to bH^+$ is expected to be small. We perform a systematic scan over the DTHM parameters space looking for charged Higgs masses that allow the $t \to bH^+$ decay to be open. In Fig. 6 we show the branching ratio for $t \to bH^+$ where we included $t \to bW^+$ and $t \to sW^+$ decay channels and the QCD corrections. It is obvious that a large effect on $t \to bH^+$ would appear for the largest possible values of v_t that are allowed by EW precision constraints and the theoretical constraints. Indeed for a triplet vev v_t in the range $0.1 \to 3.5$ GeV and a charged Higgs mass less than 165 GeV, one finds $\mathrm{Br}(t \to bH^+)$ in

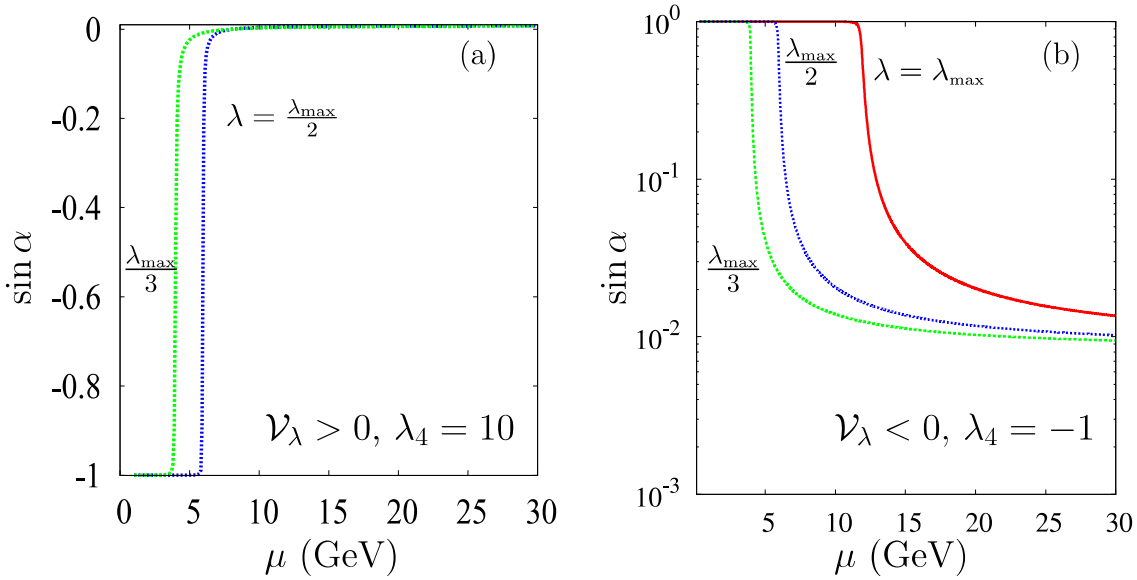

Figure 5: The mixing angle as a function of μ, in the regimes $\mathcal{V}_\lambda > 0$ (a) and $\mathcal{V}_\lambda < 0$ (b); the other parameters are given by $v_t = 1$ GeV, $\lambda_{max} = 16\pi/3$, $\lambda_2 = \lambda_3 = 0.1$, $\lambda_1 = 0.5$ and $\epsilon_\alpha = +$. The log scale in (b) shows the asymptotic values at large μ. The same asymptotic values apply in (a); see text for further discussion.

the range $10^{-5} \to 10^{-4}$.

However, it is well known that the LHC will act as a top factory. With low luminosity 10fb^{-1}, 8 million $t\bar{t}$ pairs per experiment per year will be produced. This number will increase by one order of magnitude with the high luminosity option. Therefore, the properties of top quarks can be examined with significant precision at LHC. For instance, it has been shown that for top decays through flavor changing neutral processes, it is possible to reach $\text{Br}(t \to cH^0) \leq 4.5 \times 10^{-5}$ at the LHC [75]. For $t \to bH^+$, no such studies are available. But it is clear that if we let one top decay to bW and the other one decay to bH with a branching ratio in the range $10^{-5} \to 10^{-4}$, this would lead to $800 \to 8000$ raw $bW^+\bar{b}H^-$ (or $\bar{b}W^-bH^+$events in the case of high luminosity option which may be enough to extract charged Higgs and measure its coupling to the top. Note also that high sensitivity to the charged or neutral Higgses of top decays through loop induced flavor changing neutral currents, can also be attained at the ILC [76, 77, 78].

DTHM spectrum and theoretical constraints

We illustrate, in Figs. 7.a and 8.a, the correlations among μ, $\sin\alpha$ and v_t for fixed values of the λ_i's and λ, and in Figs. 7.b, 8.b and 8.c, the correlations among μ, $\sin\alpha$ and the $\mathcal{CP}_{even}$ Higgs masses (or equivalently λ), for fixed values of the λ_i's and v_t, where we take into account the boundedness from below and unitarity constraints discussed in the previous sections. Note that the chosen numbers in the figures are such that $\mathcal{V}_\lambda < 0$ in Figs. 7 and $\mathcal{V}_\lambda > 0$ in Fig.8.a, while Figs.8.b and 8.c interpolate between these two regimes, see Eq. (7.1). For fixed μ, increasing the magnitude of v_t decreases m_{h^0} and increases the mixing parameter $|s_\alpha|$ as can be seen from Figs. 7.a and 8.a. The upper-left white areas

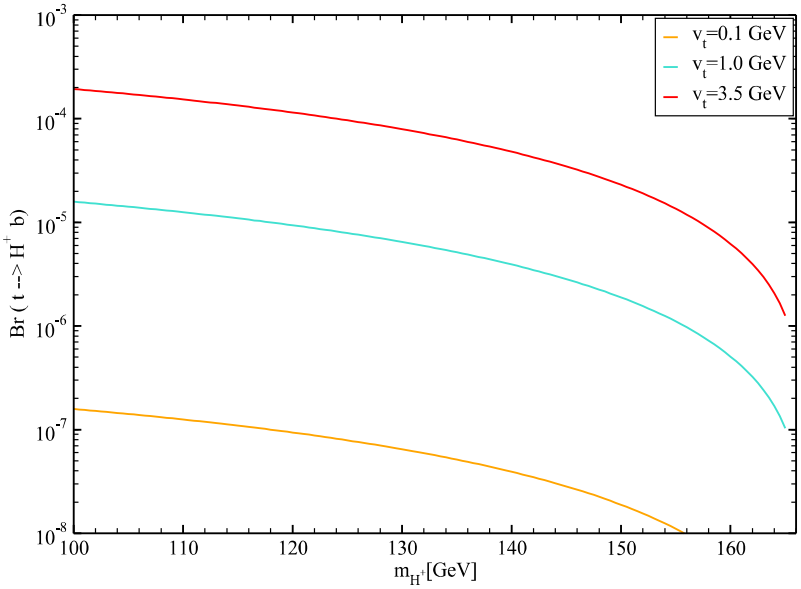

Figure 6: Branching ratio for $t \to bH^+$ as a function of charged Higgs mass for three values of the triplet vev v_t.

in these plots correspond to $m_{h^0} \lesssim 115$GeV where we took the latter value as a fiducial lower bound for a standard-model like Higgs. Such a bound corresponds to $\lambda^{\rm SM} \simeq 0.44$, for $v_t < 1$GeV, while the upper bound for m_{h^0} is around 120GeV, corresponding to the value $\lambda = 0.48$ chosen in the figures, cf. Eqs. (7.2, 7.4). It thus follows that the colored areas in the plots, indicating mainly very small s_α values, i.e. h^0 behaving like a SM Higgs, correspond to the small Higgs mass range 115GeV $\leq m_{h^0} \lesssim$ 120GeV. Increasing the value of λ, keeping $\lambda^{\rm SM}$ fixed, would result in an increase of the Higgs mass range as well as of the regions with larger $|s_\alpha|$ (the red areas on the plots). In fact, there are two regions corresponding to $m_{h^0} \lesssim 115$GeV, the white area in the upper-left corner corresponding to small values of μ delimited by the red thin area, and another region at very large values of μ ($\gtrsim \mathcal{O}(1) - \mathcal{O}(10^3)$TeV), which are out of the scope of the μ range shown on the plots, that are delimited by green-blue areas. One should note that, in the former region, $|s_\alpha|$ reaches quickly 1, so that h^0 carries essentially a triplet component and is thus not excluded by a fiducial SM-like Higgs mass lower bound, even if it is lighter than this bound. In contrast, in the latter region where $|s_\alpha|$ remains very small, a SM Higgs mass lower bound applies to h^0. It follows that such a bound does not put lower bounds on μ, while it leads typically to very large upper bounds on μ as a function of v_t. In the small μ region, H^0 carries mainly the SM-like component and should respect a SM Higgs mass lower bound. However, due to the very low sensitivity to μ in this regime (see Fig. 3), such a bound will translate merely into a lower bound on λ. Therefore, exclusion of very small values of μ can only originate from exclusion limits on the lightest non-SM-like $\mathcal{CP}_{even}$ or $\mathcal{CP}_{odd}$ Higgses, which could be extracted for instance from existing limits for the the minimal supersymmetric extension of SM in the non-decoupling regime [79].

Complementary features, now with a fixed v_t and varying λ, are illustrated in figures 7.b, 8.b and 8.c. The gross features of Figs. 7.b and 8.b are in agreement with the previous discussion on the phenomenological bounds, related to Eqs. (7.30, 7.31). They illustrate how an information on m_{h^0} constrains the allowed range for μ without any prior knowledge

on λ. For a given m_{h^0}, the allowed range of λ is theoretically bounded from below by some $\lambda_{\min}$, in order to satisfy $m_{h^0} \leq m_{h^0}^{\max}$, see Eq. (7.31). Then for each value of λ in the domain $\lambda_{\min} \leq \lambda \leq \lambda_{\max} \equiv \frac{16\pi}{3}$ there corresponds two values of μ consistent with a given m_{h^0}, according to Eq.(7.30). Then it is easy to see, from the shape of the $m_{h^0}(\mu)$ plots shown in Fig. 3, that the largest spread between $\mu_+^{h^0}$ and $\mu_-^{h^0}$ is reached for $\lambda = \lambda_{\max}$, since increasing λ results in shifting upwards these plots . The two branches of the envelop of the domains in Figs. 7.b, 8.b correspond to $\mu_\pm^{h^0}(\lambda_{\max})$. Furthermore, increasing m_{h^0} with fixed $\lambda = \lambda_{\max}$ results in an increase of μ_- and decrease of μ_+, as can be again seen from the shape of $m_{h^0}(\mu)$ plots shown in Fig. 3, till the two branches join and terminate when m_{h^0} reaches its unitarity bound Eq. (7.26). With the numbers chosen on the plots, μ is bounded to lie between $\mu_- \approx 0.3$ GeV and $\mu_+ \approx 10^5$ GeV. One can see that for small $\mu \leq 1$ GeV, m_{h^0} must be less than about 200 GeV. The latter bound on m_{h^0} increases quickly to reach the unitarity bound Eq. (7.26) when μ increases from 1 GeV to 10 GeV. Above, $\mu = 10$ GeV, m_{h^0} can be any number between the LEP limit (114 GeV) and this unitarity bound. As noted previously, one should take into account the actual doublet content of h^0 when reading out exclusion domains from these plots. In the plot, we have illustrated the size of $|s_\alpha|$. In most of the cases the mixing angle is very small (blue to green areas), which means that h^0 is dominated by doublet component. In these regions where a SM Higgs exclusion limit can be readily applied, one might still need to combine this information with the search limits for the other charged, doubly-charged and $\mathcal{CP}_{odd}$ Higgs states, in order to reduce further the otherwise large allowed domain for μ, see Eq. (3.65). However, due to the v_t suppression in Eq. (3.65) of the lower bound $\mu_{\min}$, such a reduction is not expected to be significant unless the experimental lower bounds, $(m_{H^{\pm\pm}})_{\exp}$ or $(m_{H^\pm})_{\exp}$ or $(m_{H^{A^0}})_{\exp}$, become sufficiently higher than the electroweak scale. In contrast, bounds on m_{h^0} alone would shrink significantly the spread of the μ range whenever $|s_\alpha| > 10^{-2}$ (the green/red areas), reducing as well the order of magnitude of the size of μ. In such a regime of small μ one starts being sensitive to values of the λ_i's, as can be seen through the slight difference, in the green area, between Fig. 7.b and Fig. 8.b. This effect will of course increase for higher values of the λ_i's consistent with unitarity and BFB constraints.

Figure 8.c illustrates the behavior of m_{H^0} as a function of μ and λ which, as compared to Fig. 8.b, shows a striking difference from the behavior of m_{h^0}. According to the previous discussion on neutral Higgses (see also Fig. 5), $|s_\alpha|$ is essentially either very small or very close to 1. Thus, the red area corresponds to an H^0 behaving essentially like the SM Higgs. The dual sizes of the red areas in both plots can be understood again from the mass shapes of Fig. 3: for small $\mu(< \bar{\mu})$, m_{h^0} changes very quickly with μ while m_{H^0} is almost insensitive to μ. It follows that a variation of λ, that amounts to shifting upwards or downwards these mass shapes in Fig. 3, results in a small change in μ for a fixed m_{h^0} and a big change in μ for a fixed m_{H^0}, whence the narrow red strip in Fig. 8.b and the large red area in Fig. 8.c. (One can understand similarly the dual sizes of the blue and green areas for large $\mu(> \bar{\mu})$.) These features suggest a useful complementary strategy when using present or future exclusion limits, depending on whether one interprets these limits in the small or large $|s_\alpha|$ regimes. We discuss this strategy only qualitatively here, summarizing its main points as follows:

-I- in the *small* $|s_\alpha|$ regime, akin to moderate to large μ values, the typical Higgs spectrum features a $\mathcal{CP}_{even}$ lightest state h^0 behaving like a SM-Higgs, the remaining Higgs states being much heavier as illustrated in Fig. 3 and Fig. 9.a. Interpreting the exclusion limits within this regime amounts to applying a SM Higgs mass lower bound $m_h^{(\mathrm{SM})}$ to m_{h^0} that leads to a lower bound on λ, see Eq. (7.31). To any λ above this bound will correspond a

lower, $\mu_-^{h^0}$, and an upper, $\mu_+^{h^0}$, bound on μ. The lower bound $\mu_-^{h^0}$ is, however, typically too small to be consistent with the small $|s_\alpha|$ regime and should be superseded by a larger value $\mathcal{O}(\max\{\mu_c^{(1)}, \mu_c^{(2)})\})$. Furthermore, one should keep in mind that $\mu_+^{h^0}$ is extremely sensitive to m_{h^0} and decreases quickly with increasing m_{h^0}. This implies the important feature that a slight improvement of the exclusion limit $m_h^{(\mathrm{SM})}$ results in a substantial *decrease* of the upper bound on μ. The heavier $\mathcal{CP}_{even}$ state H^0 is not expected to bring significant constraints. Indeed, in the considered regime, this state carries essentially the triplet component with suppressed couplings to the SM sector. Its mass can thus be bounded only by $m_h^{(\mathrm{non-SM})}$, the exclusion mass limit on non-SM-like Higgs particles. Since such an exclusion mass limit is expected to be weaker than the SM-like limit due to lower statistics, that is $m_h^{(\mathrm{non-SM})} < m_h^{(\mathrm{SM})}$, then taking into account that one has theoretically $m_{H^0} > m_{h^0}$, one is trivially lead to $m_h^{(\mathrm{non-SM})} < m_{H^0}^{\min}$ which implies no new constraints (cf. the discussion following Eq. (7.31)). As stated previously, exclusion limits on the remaining Higgs states can also be used independently to improve the lower bound on μ based on Eq. (3.65). One can, however, get further information within the present regime depending on whether these exclusion limits are higher or lower than $m_h^{(\mathrm{SM})}$. In particular if $(m_{H^{\pm\pm}})_{\exp} \gtrsim m_h^{(\mathrm{SM})}$, which excludes an $H^{\pm\pm}$ lighter than h^0, then one excludes all the $\lambda_4 > 0$ region, or else, puts a stronger lower bound on μ, namely $\mu > \mu^*$. (see Eq. (7.29) and discussion thereof.) In the case where $(m_{H^{\pm\pm}})_{\exp} \lesssim m_h^{(\mathrm{SM})}$, which is the present experimental situation, there is a small window $\mu_{min} < \mu < \mu^*$ with $\lambda_4 > 0$, otherwise $\mu^* < \mu < \mu_+^{h^0}$ irrespective of the sign of λ_4, and for all the allowed values of λ discussed above. We have illustrated in Fig. 9.b a case where $H^{\pm\pm}$ can be the lightest Higgs state.

-II- in the *large* $|s_\alpha|$ regime, akin to small μ values, H^0 is the heaviest among all the Higgs states of the model and behaves like a SM-Higgs. This is a rather unusual configuration that should help constrain more efficiently, or perhaps exclude, this regime. Also in this small μ regime, and in contrast with the previous regime where only λ was playing a role, there can be now a somewhat increased sensitivity to the λ_i's as well, in particular $\lambda_1 + \lambda_4$. The reason is that the size of the μ domain is of order $\hat{\mu}$, Eq. (7.24), where in the latter λ_1, λ_4 do not suffer a v_t suppression as compared to λ. However, as discussed in section 7, the parameter k will characterize the sensitivity to the deviation of H^0 from a pure SM-Higgs state, which can lead, for realistic experimental sensitivities, to a significant reduction of the sensitivity on $\lambda_1 + \lambda_4$.

One then has to consider two cases:

a) $m_h^{(\mathrm{SM})} < m_{H^0}^{\min}$: this case implies essentially a lower bound on λ through Eq. (7.21), but no constraint on μ apart from the defining region in this regime, namely $0 < \mu \leq \hat{\mu}$, whose size depends mainly on λ and to a lesser extent on $\lambda_1 + \lambda_4$. The latter couplings are bounded by the combined unitarity and BFB constraints of section 6, so that there is an indirect sensitivity to λ_2 and λ_3 as well. The red area in Fig. 8.c gives an illustration of this least constrained case. The μ domain extends over all the red area, while the vertical boundary of this area is determined by the maximal value of $\lambda = \frac{16\pi}{3}$ given by unitarity. This boundary corresponds to the unitarity upper bound on the SM-Higgs mass as well as the one on m_{h^0}, Eq. (7.26). Of course H^0 can escape this bound but at the expense of switching consistently to the small $|s_\alpha|$ regime as seen on Fig. 8.c.

b) $m_h^{(\mathrm{SM})} \gtrsim m_{H^0}^{\min}$: in this case not only do we have an upper bound on λ through Eq. (7.21), but actually also a lower bound. Indeed, a too small λ, leading to a

too low $m^{\min}_{H^0}$ with respect to $m_h^{(\mathrm{SM})}$, will eventually put $m_h^{(\mathrm{SM})}$ just above all the values of m_{H^0} corresponding to the *large* $|s_\alpha|$ regime thus ruling out this regime altogether. Furthermore, this configuration will immediately rule out the *small* $|s_\alpha|$ regime as well, since $m_h^{(\mathrm{SM})}$ is by definition applicable only to SM-like states and we have $m_h^{(\mathrm{SM})} \gtrsim m^{\min}_{H^0} > m_{h^0}$ for all m_{h^0}. Consequently, a too small λ would exclude the whole μ parameter space. One concludes that λ should lie in a very narrow strip such that $m^{\min}_{H^0} \lesssim m_h^{(\mathrm{SM})} \lesssim m_{H^0}(\mu = 0)$. This strip is essentially giving the lower bound on λ of case a) and thus does not provide significantly new information. [Note, though, that for values of $\lambda_1 + \lambda_4$ close to its unitarity bound, and taking for instance $m_h^{(\mathrm{SM})} \simeq 114\mathrm{GeV}$ and $v_t = 1\mathrm{GeV}$, case b) can still reduce the lower bound on λ, from $\lambda \simeq 0.43$ to $\lambda \simeq 0.38$. But the effect will be smaller for smaller values of v_t.] One should, however, keep in mind that due to the high flatness of m_{H^0} as a function of μ in the region $0 < \mu \leq \hat{\mu}$, the slightest variation of λ within the above noted strip would result in the exclusion of significant parts of the $0 < \mu \leq \hat{\mu}$ region. For instance, with $\lambda_1 = 1.5$, $\lambda_2 = \lambda_3 = 0.1$, $\lambda_4 = -1$ and taking the SM-Higgs lower bound $m_h^{(\mathrm{SM})} = 114\mathrm{GeV}$, if one reduces the lower bound of λ (for which the whole range $0 < \mu \leq \hat{\mu} \approx 0.3$ of the *large* $|s_\alpha|$ regime is allowed) by just 1‰, then the SM-Higgs lower bound would imply $\mu < -5\mathrm{GeV}$ or $\mu > 0.3\mathrm{GeV}$ thus ruling out the whole *large* $|s_\alpha|$ regime!

For all practical purposes and barring the fine-tuned effects just mentioned, the above discussion of cases a) and b) shows that an experimental lower bound on the SM-like Higgs mass cannot by itself cut into the *large* $|s_\alpha|$/small μ regime; it either excludes it or allows all of it, depending on whether λ is respectively below or above the value $\bar{\lambda}$ that satisfies $m_h^{(\mathrm{SM})} = m^{\min}_{H^0}(\lambda = \bar{\lambda})$. Thus, the size of the μ domain $[0, \hat{\mu}]$ that is controlled mainly by λ [but can also be sensitive to $\lambda_1 + \lambda_4$] for each given value of v_t, see Eq. (7.24), will not be reduced by the actual value of the experimental bound $m_h^{(\mathrm{SM})}$. Moreover, an extra constraint from an experimental lower bound on the mass of a non-SM-like $\mathcal{CP}_{even}$ Higgs state would have a marginal effect since m_{h^0} decreases very quickly in the region $\mu \lesssim \hat{\mu}$. An efficient reduction of the μ domain can come only from experimental lower bounds on the masses of the charged, doubly-charged and $\mathcal{CP}_{odd}$ Higgs states. Indeed, these bounds translate into a lower bound on μ typically of the same size as $\hat{\mu}$, Eq. (3.65). As far as these experimental bounds are of the same order, $(m^2_{A^0})_{\mathrm{exp}} \simeq (m^2_{H^\pm})_{\mathrm{exp}} \simeq (m^2_{H^{\pm\pm}})_{\mathrm{exp}}$, the relevant bound will be given by A^0 (resp. $H^{\pm\pm}$) when $\lambda_4 < 0$ (resp. $\lambda_4 > 0$).

Comparing $\mu_{\min}$ and $\hat{\mu}$, one determines easily the necessary and sufficient conditions for which the *large* $|s_\alpha|$ regime would be excluded. They read:

$(m^2_{A^0})_{\mathrm{exp}} \geq (k\lambda - 2(\lambda_1 + \lambda_4) - \sqrt{2k}|\lambda - \lambda_1 - \lambda_4|)\dfrac{v_d^2}{2(k-2)} + \mathcal{O}(v_t^2)$, for $\lambda_4 < 0$, and

$(m^2_{H^{\pm\pm}})_{\mathrm{exp}} \geq (k(\lambda - \lambda_4) - 2\lambda_1 - \sqrt{2k}|\lambda - \lambda_1 - \lambda_4|)\dfrac{v_d^2}{2(k-2)} + \mathcal{O}(v_t^2)$, for $\lambda_4 > 0$, where we have taken into account the two-fold structure as discussed after Eq. (7.24).

9 Conclusion

We have carried out a detailed study of the renormalizable Higgs potential relevant to the type II seesaw model, keeping the full set of the seven free parameters of the potential. We determined analytically the unitarity constraints on the various scalar couplings and fully solved the *all directions* conditions for boundedness from below. These combined

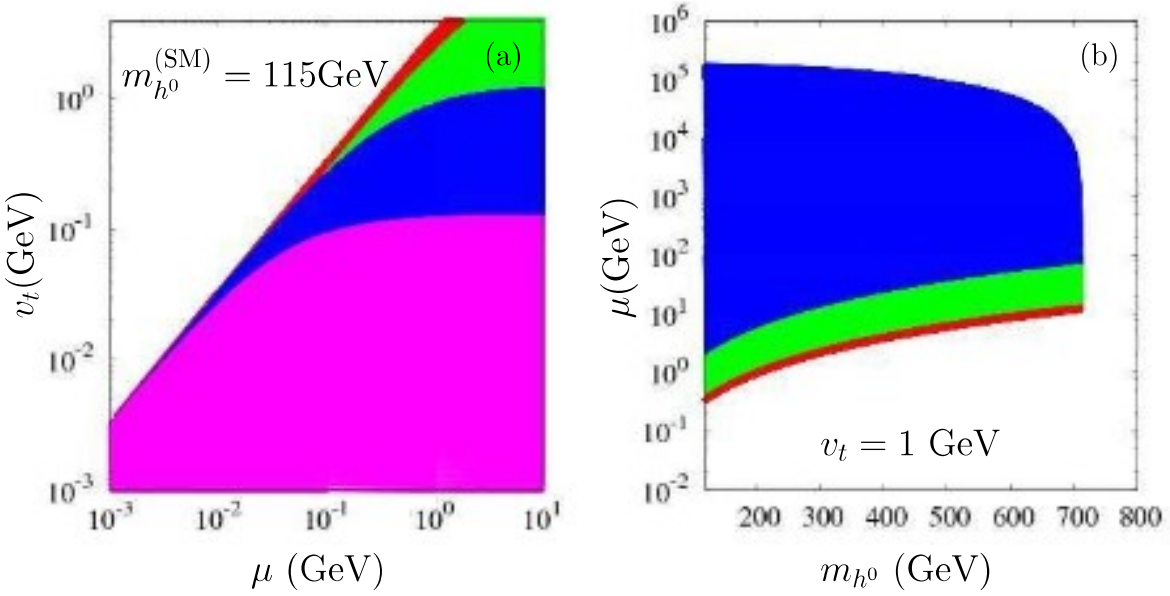

Figure 7: (a) correlation between μ and v_t with $m_{h^0} > m_{h^0}^{(\mathrm{SM})} = 115\mathrm{GeV}$ and $\lambda = 0.48$, (b) correlation between μ and m_{h^0}, scanning over λ in the range $0.44 \leq \lambda \leq 16\pi/3$, with $v_t = 1\mathrm{GeV}$; color code: $10^{-1} \leq s_\alpha \leq 1$ (red), $10^{-2} \leq s_\alpha \leq 10^{-1}$ (green), $10^{-3} \leq s_\alpha \leq 10^{-2}$ (blue) and $s_\alpha \leq 10^{-3}$ (magenta). The other parameters are $\lambda_1 = -\lambda_4 = 1$, $\lambda_2 = \lambda_3 = 0$ and $\kappa = 8$. $\mathcal{V}_\lambda < 0$ for both figures.

theoretical constraints delineate efficiently the physically allowed regions of the parameter space and should be taken into account in phenomenological studies. We also examined the vacuum structure of the potential and determined general consistency constraints on the μ parameter, as well as theoretical upper (resp. lower) bounds on the lighter (resp. heavier) $\mathcal{CP}_{even}$ Higgs particle mass that can constrain further the phenomenological analyses. We also identified two distinct regimes respectively for large and small μ. In the first regime the lightest Higgs particle is the h^0, behaving as a SM-like Higgs, the remaining Higgses being typically too heavy to be of any phenomenlogical relevance. In the second regime, it is the heaviest Higgs H^0 that behaves as a SM-like Higgs, the lighter charged, doubly charged and $\mathcal{CP}_{odd}$ states become accessible to the colliders, with possibly the $H^{\pm\pm}$ being the lightest state, while the lighter $\mathcal{CP}_{even}$ decouples quickly from the SM sector. We also initiated the study of possible consequences from existing experimental exclusion limits.

Although we did not commit to any underlying GUT assumptions, thus allowing μ to vary between a few GeV and possibly the GUT scale, we do retrieve, as a consequence of the (model-independent) dynamical constraints on μ, a seesaw-like behavior that leads to tiny v_t if μ is taken very large.

Finally, the results of this study having been obtained at the tree-level, one should keep in mind that modifications due to quantum corrections to the effective potential can possibly be substantial in some cases. The inclusion of such corrections is, however, beyond the scope of the present paper given the non-trivial form of the constraints already at the tree-level.

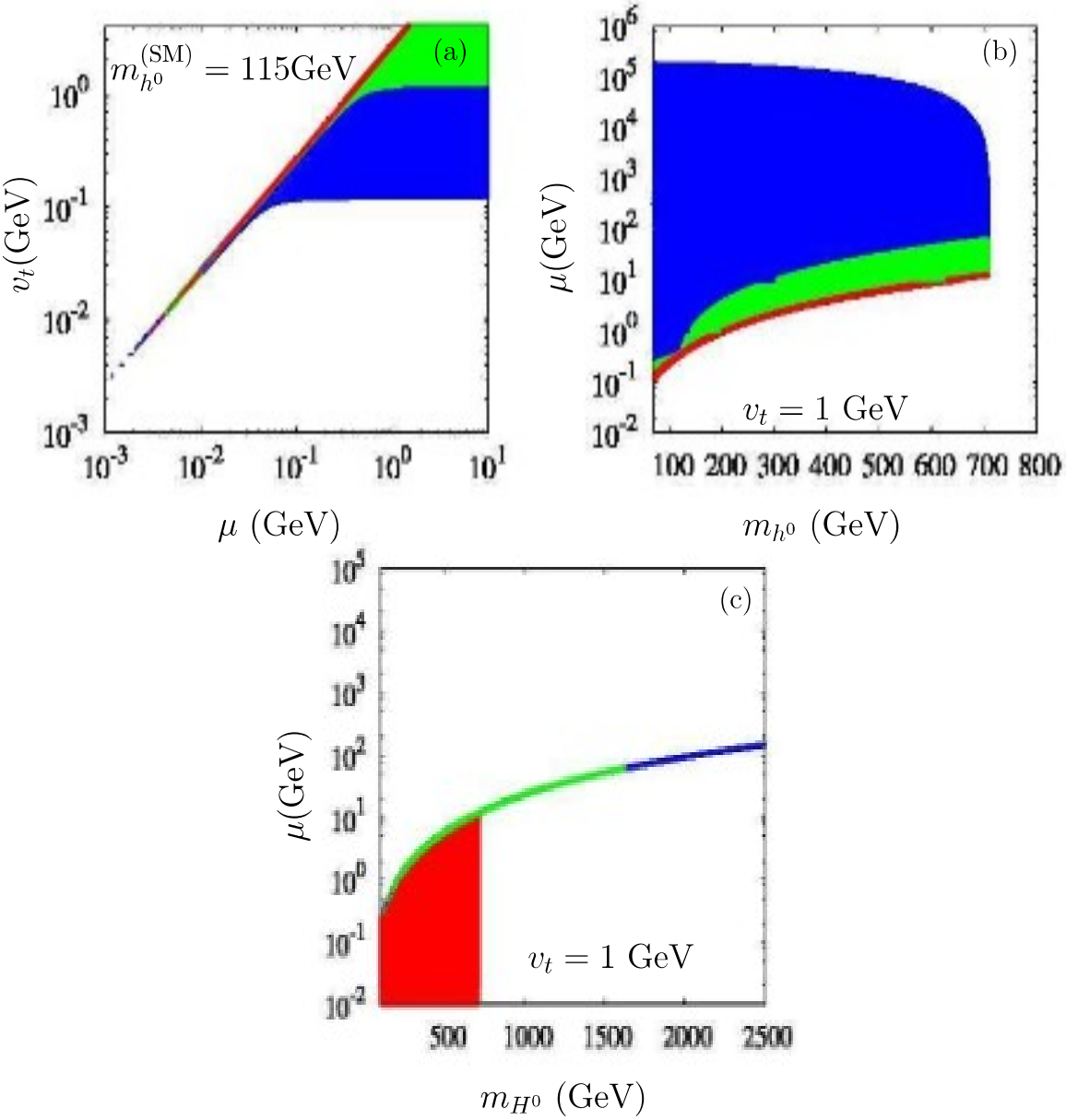

Figure 8: (a) correlation between μ and v_t with $m_{h^0} > m_{h^0}^{(\mathrm{SM})} = 115\mathrm{GeV}$ and $\lambda = 0.48$, (b) correlation between μ and the light $\mathcal{CP}_{even}$ Higgs mass, (c) between μ and the heavy $\mathcal{CP}_{even}$ Higgs mass, scanning over λ in the range $0.44 \leq \lambda \leq 16\pi/3$, with $v_t = 1\mathrm{GeV}$; color code: $10^{-1} \leq |s_\alpha| \leq 1$ (red), $10^{-2} \leq |s_\alpha| \leq 10^{-1}$ (green), $10^{-3} \leq |s_\alpha| \leq 10^{-2}$ (blue) and $|s_\alpha| \leq 10^{-3}$ (white bottom area in (a)). The other parameters are given by $\lambda_1 = 1.5$, $\lambda_2 = \lambda_3 = 0.1$, $\lambda_4 = -1$ and $\kappa = 8$. $\mathcal{V}_\lambda > 0$ in (a), while in (b) and (c) $\mathcal{V}_\lambda$ changes sign with increasing Higgs masses.

Acknowledgments

We would like to thank Borut Bajc, Ben Gripaios, Roberto Salerno and Goran Senjanovic for discussions. This work was supported by *Programme Hubert Curien, Volubilis, AI* n^0 : *MA/08/186*. We also acknowledge the LIA (*International Laboratory for Collider Physics - ILCP*) as well as the ICTP-IAEA Training Educational Program for partial support. The work of R.B. was supported by CSIC.

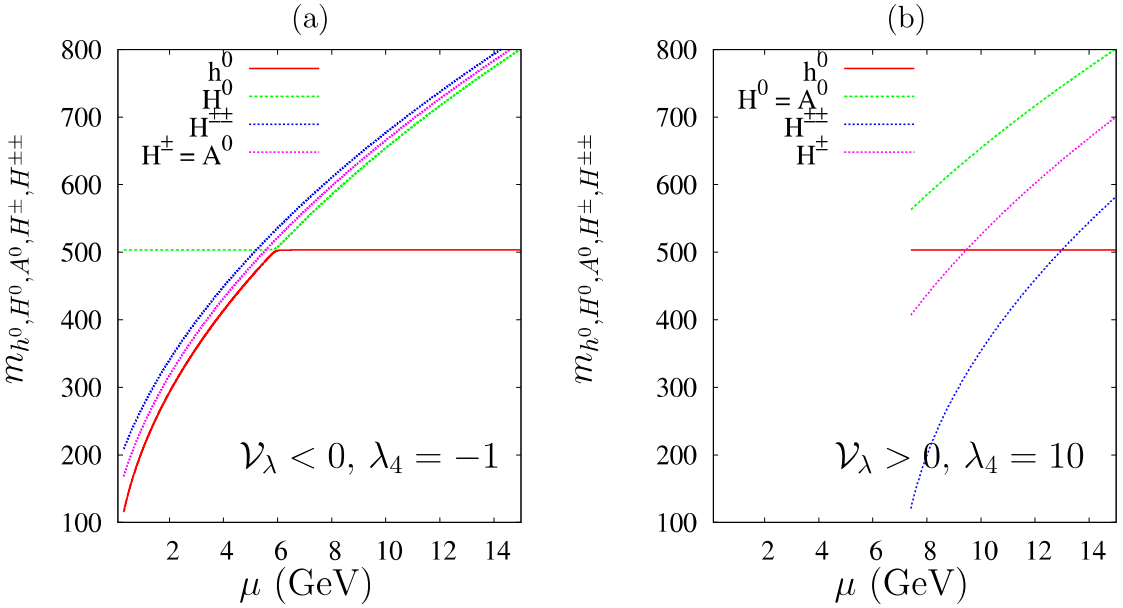

Figure 9: Higgs boson masses as a function of μ with $v_t = 1$ GeV, $\lambda = 8\pi/3$, $\lambda_1 = 0.5$, $\lambda_2 = \lambda_3 = 0.1$, for $\mathcal{V}_\lambda < 0$, $\lambda_4 = -1$ (left) and $\mathcal{V}_\lambda > 0$, $\lambda_4 = 10$ (right), we note that in both panels $m_{H^0} = m_{A^0}$.

Appendix A.

As stated in section 3, the positivity of $m^2_{h^0}$ constrains μ to lie in the range $\mu_- \leq \mu \leq \mu_+$ so as to satisfy Eq. (3.61). We give here the full expression for $\mu_\pm$:

$$\mu_\pm = \frac{\lambda v_d^2 + 8(\lambda_1+\lambda_4)v_t^2 \pm \sqrt{\lambda(\lambda v_d^4 + 16 v_t^2((\lambda_1+\lambda_4)v_d^2 + 4(\lambda_2+\lambda_3)v_t^2))}}{8\sqrt{2}v_t} \tag{A.1}$$

Note that due to the negative coefficient of μ^2 in Eq.(3.61), $\mu_\pm$ should always be real-valued otherwise Eq.(3.61) is not satisfied and h^0 is tachyonic for *all* values of μ. As can be seen from Eq. (A.1), this requirement leads in principle to an extra constraint on top of Eqs. (3.60 - 3.62), that is

$$\lambda(\lambda v_d^4 + 16 v_t^2((\lambda_1+\lambda_4)v_d^2 + 4(\lambda_2+\lambda_3)v_t^2)) \geq 0 \tag{A.2}$$

However, we show here that this extra constraint is automatically satisfied due to the BFB constraints: since $\lambda > 0$, cf. Eq. (6.1), it suffices to show that $(\lambda v_d^4 + 16 v_t^2((\lambda_1+\lambda_4)v_d^2 + 4(\lambda_2+\lambda_3)v_t^2)) \geq 0$. Now using the first inequality of Eq. (6.3) one obtains

$$\begin{aligned} \lambda v_d^4 + 16 v_t^2((\lambda_1+\lambda_4)v_d^2 + 4(\lambda_2+\lambda_3)v_t^2) &\geq (\lambda v_d^4 + 16 v_t^2(-\sqrt{\lambda(\lambda_2+\lambda_3)}v_d^2 + 4(\lambda_2+\lambda_3)v_t^2)) \\ &\geq (\sqrt{\lambda} v_d^2 - 8\sqrt{(\lambda_2+\lambda_3)}v_t^2)^2 \end{aligned} \tag{A.3}$$

that proves our statement.

Appendix B.

In this appendix we give the form of the Higgs potential in the field subspaces where only 2 or only 3 fields are non-vanishing, dubbed respectively 2-field and 3-field directions. We identify exhaustively 10 different directions for each of these two classes and give their corresponding BFB conditions.

The ten 2-field directions:

$$
\begin{aligned}
{}_2V^{(4)}_{\text{dir.1}} &= \frac{\lambda}{4}\left(|\phi^0|^2+|\phi^+|^2\right)^2 && \text{(B.1)}\\
{}_2V^{(4)}_{\text{dir.2}} &= (\lambda_2+\lambda_3)\,|\delta^{++}|^4+(\lambda_1+\lambda_4)\,|\delta^{++}|^2\,|\phi^+|^2+\frac{\lambda}{4}\,|\phi^+|^4 && \text{(B.2)}\\
{}_2V^{(4)}_{\text{dir.3}} &= (\lambda_2+\lambda_3)\,|\delta^{++}|^4+\lambda_1\,|\delta^{++}|^2\,|\phi^0|^2+\frac{\lambda}{4}\,|\phi^0|^4 && \text{(B.3)}\\
{}_2V^{(4)}_{\text{dir.4}} &= (\lambda_2+\frac{\lambda_3}{2})\,|\delta^{+}|^4+(\lambda_1+\frac{\lambda_4}{2})\,|\delta^{+}|^2\,|\phi^+|^2+\frac{\lambda}{4}\,|\phi^+|^4 && \text{(B.4)}\\
{}_2V^{(4)}_{\text{dir.5}} &= (\lambda_2+\frac{\lambda_3}{2})\,|\delta^{+}|^4+(\lambda_1+\frac{\lambda_4}{2})\,|\delta^{+}|^2\,|\phi^0|^2+\frac{\lambda}{4}\,|\phi^0|^4 && \text{(B.5)}\\
{}_2V^{(4)}_{\text{dir.6}} &= (\lambda_2+\frac{\lambda_3}{2})\,|\delta^{+}|^4+2\,(\lambda_2+\lambda_3)\,|\delta^{+}|^2\,|\delta^{++}|^2+(\lambda_2+\lambda_3)\,|\delta^{++}|^4 && \text{(B.6)}\\
{}_2V^{(4)}_{\text{dir.7}} &= (\lambda_2+\lambda_3)\,|\delta^{0}|^4+\lambda_1\,|\delta^{0}|^2\,|\phi^+|^2+\frac{\lambda}{4}\,|\phi^+|^4 && \text{(B.7)}\\
{}_2V^{(4)}_{\text{dir.8}} &= (\lambda_2+\lambda_3)\,|\delta^{0}|^4+(\lambda_1+\lambda_4)\,|\delta^{0}|^2\,|\phi^0|^2+\frac{\lambda}{4}\,|\phi^0|^4 && \text{(B.8)}\\
{}_2V^{(4)}_{\text{dir.9}} &= (\lambda_2+\lambda_3)\,|\delta^{0}|^4+2\,\lambda_2\,|\delta^{0}|^2\,|\delta^{++}|^2+(\lambda_2+\lambda_3)\,|\delta^{++}|^4 && \text{(B.9)}\\
{}_2V^{(4)}_{\text{dir.10}} &= (\lambda_2+\lambda_3)\,|\delta^{0}|^4+2\,(\lambda_2+\lambda_3)\,|\delta^{0}|^2\,|\delta^{+}|^2+(\lambda_2+\frac{\lambda_3}{2})\,|\delta^{+}|^4 && \text{(B.10)}
\end{aligned}
$$

$$
\begin{aligned}
&\text{direction } 1: \lambda>0 && \text{(B.11)}\\
&\text{directions 2 and 8}: \lambda>0,\ \lambda_2+\lambda_3>0,\ \lambda_1+\lambda_4+\sqrt{\lambda(\lambda_2+\lambda_3)}>0 && \text{(B.12)}\\
&\text{direcitons 3 and 7}: \lambda>0,\ \lambda_2+\lambda_3>0,\ \lambda_1+\sqrt{\lambda(\lambda_2+\lambda_3)}>0 && \text{(B.13)}\\
&\text{directions 4 and 5}: \lambda>0,\ \lambda_2+\frac{\lambda_3}{2}>0,\ \lambda_1+\frac{\lambda_4}{2}+\sqrt{\lambda(\lambda_2+\frac{\lambda_3}{2})}>0 && \text{(B.14)}\\
&\text{directions 6, 9 and 10}: \lambda_2+\lambda_3>0,\ \lambda_2+\frac{\lambda_3}{2}>0 && \text{(B.15)}
\end{aligned}
$$

The ten 3-field directions:

$$
\begin{aligned}
{}_3V^{(4)}_{\text{dir.1}} &= (\lambda_2+\lambda_3)|\delta^0|^4 + 2(\lambda_2+\lambda_3)|\delta^0|^2|\delta^+|^2 + (\lambda_2+\frac{\lambda_3}{2})|\delta^+|^4 + 2\,\lambda_2\,|\delta^0|^2\,|\delta^{++}|^2 \\
&\quad + 2(\lambda_2+\lambda_3)\,|\delta^+|^2\,|\delta^{++}|^2 + (\lambda_2+\lambda_3)\,|\delta^{++}|^4 \\
&\quad -\lambda_3\,\frac{\delta^{--}}{\delta^0\,(\delta^-)^2}|\delta^0|^2|\delta^+|^4 - \lambda_3\,\frac{\delta^0\,(\delta^-)^2}{\delta^{--}}\,|\delta^{++}|^2 \qquad \text{(B.16)} \\
{}_3V^{(4)}_{\text{dir.2}} &= (\lambda_2+\lambda_3)\,|\delta^0|^4 + 2(\lambda_2+\lambda_3)\,|\delta^0|^2\,|\delta^+|^2 + (\lambda_2+\frac{\lambda_3}{2})\,|\delta^+|^4 \\
&\quad + (\lambda_1+\lambda_4)\,|\delta^0|^2\,|\phi^0|^2 + (\lambda_1+\frac{\lambda_4}{2})\,|\delta^+|^2\,|\phi^0|^2 + \frac{\lambda}{4}\,|\phi^0|^4 \qquad \text{(B.17)} \\
{}_3V^{(4)}_{\text{dir.3}} &= (\lambda_2+\lambda_3)\,|\delta^0|^4 + 2(\lambda_2+\lambda_3)\,|\delta^0|^2\,|\delta^+|^2 + (\lambda_2+\frac{\lambda_3}{2})\,|\delta^+|^4 \\
&\quad + \lambda_1\,|\delta^0|^2\,|\phi^+|^2 + (\lambda_1+\frac{\lambda_4}{2})\,|\delta^+|^2\,|\phi^+|^2 + \frac{\lambda}{4}\,|\phi^+|^4 \qquad \text{(B.18)} \\
{}_3V^{(4)}_{\text{dir.4}} &= (\lambda_2+\lambda_3)\,|\delta^0|^4 + 2\,\lambda_2\,|\delta^0|^2\,|\delta^{++}|^2 + (\lambda_2+\lambda_3)\,|\delta^{++}|^4 \\
&\quad + (\lambda_1+\lambda_4)\,|\delta^0|^2\,|\phi^0|^2 + \lambda_1\,|\delta^{++}|^2\,|\phi^0|^2 + \frac{\lambda}{4}\,|\phi^0|^4 \qquad \text{(B.19)} \\
{}_3V^{(4)}_{\text{dir.5}} &= (\lambda_2+\lambda_3)\,|\delta^0|^4 + 2\,\lambda_2\,|\delta^0|^2\,|\delta^{++}|^2 + (\lambda_2+\lambda_3)\,|\delta^{++}|^4 \\
&\quad + \lambda_1\,|\delta^0|^2\,|\phi^+|^2 + (\lambda_1+\lambda_4)\,|\delta^{++}|^2\,|\phi^+|^2 + \frac{\lambda}{4}\,|\phi^+|^4 \qquad \text{(B.20)} \\
{}_3V^{(4)}_{\text{dir.6}} &= (\lambda_2+\lambda_3)\,|\delta^0|^4 + (\lambda_1+\lambda_4)\,|\delta^0|^2\,|\phi^0|^2 + \frac{\lambda}{4}\,|\phi^0|^4 \\
&\quad + \lambda_1\,|\delta^0|^2\,|\phi^+|^2 + \frac{\lambda}{2}\,|\phi^0|^2\,|\phi^+|^2 + \frac{\lambda}{4}\,|\phi^+|^4 \qquad \text{(B.21)} \\
{}_3V^{(4)}_{\text{dir.7}} &= (\lambda_2+\frac{\lambda_3}{2})\,|\delta^+|^4 + 2(\lambda_2+\lambda_3)\,|\delta^+|^2\,|\delta^{++}|^2 + (\lambda_2+\lambda_3)\,|\delta^{++}|^4 \\
&\quad + (\lambda_1+\frac{\lambda_4}{2})\,|\delta^+|^2\,|\phi^0|^2 + \lambda_1\,|\delta^{++}|^2\,|\phi^0|^2 + \frac{\lambda}{4}\,|\phi^0|^4 \qquad \text{(B.22)} \\
{}_3V^{(4)}_{\text{dir.8}} &= (\lambda_2+\frac{\lambda_3}{2})\,|\delta^+|^4 + 2(\lambda_2+\lambda_3)\,|\delta^+|^2\,|\delta^{++}|^2 + (\lambda_2+\lambda_3)\,|\delta^{++}|^4 \\
&\quad + (\lambda_1+\frac{\lambda_4}{2})\,|\delta^+|^2\,|\phi^+|^2 + (\lambda_1+\lambda_4)\,|\delta^{++}|^2\,|\phi^+|^2 + \frac{\lambda}{4}\,|\phi^+|^4 \qquad \text{(B.23)} \\
{}_3V^{(4)}_{\text{dir.9}} &= (\lambda_2+\frac{\lambda_3}{2})\,|\delta^+|^4 + (\lambda_1+\frac{\lambda_4}{2})\,|\delta^+|^2\,|\phi^0|^2 + \frac{\lambda}{4}\,|\phi^0|^4 \\
&\quad + (\lambda_1+\frac{\lambda_4}{2})\,|\delta^+|^2\,|\phi^+|^2 + \frac{\lambda}{2}\,|\phi^0|^2\,|\phi^+|^2 + \frac{\lambda}{4}\,|\phi^+|^4 \qquad \text{(B.24)} \\
{}_3V^{(4)}_{\text{dir.10}} &= (\lambda_2+\lambda_3)\,|\delta^{++}|^4 + \lambda_1\,|\delta^{++}|^2\,|\phi^0|^2 + \frac{\lambda}{4}\,|\phi^0|^4 \\
&\quad + (\lambda_1+\lambda_4)\,|\delta^{++}|^2\,|\phi^+|^2 + \frac{\lambda}{2}\,|\phi^0|^2\,|\phi^+|^2 + \frac{\lambda}{4}\,|\phi^+|^4 \qquad \text{(B.25)}
\end{aligned}
$$

The corresponding BFB conditions read:

$$\textbf{direction 1}: \; 2\lambda_2+\lambda_3>0 \wedge \lambda_2+\lambda_3>0 \wedge \Big(\lambda_3^2<4(\lambda_2+\lambda_3)^2 \vee \lambda_3<0\Big) \tag{B.26}$$

$$\begin{aligned}&\textbf{direction 2}: \\ &\lambda>0 \wedge \lambda_2+\lambda_3>0 \wedge 2\lambda_2+\lambda_3>0 \wedge \sqrt{\lambda(\lambda_2+\lambda_3)}+\lambda_1+\lambda_4>0 \wedge \Big(\Big(2\lambda(2\lambda_2+\lambda_3)>(2\lambda_1+\lambda_4)^2 \\ &\wedge\Big(\Big(\sqrt{2}\sqrt{\lambda_3(\lambda_2+\lambda_3)\Big((2\lambda_1+\lambda_4)^2-2\lambda(2\lambda_2+\lambda_3)\Big)}+2\lambda_2\lambda_4>2\lambda_1\lambda_3 \wedge \lambda_3<0\Big) \vee \\ &\Big(\frac{(2\lambda_2+\lambda_3)((2\lambda_1+\lambda_4)(2\lambda_1+3\lambda_4)-4\lambda(\lambda_2+\lambda_3))}{2\lambda_1+\lambda_4}>0 \wedge 2\lambda_1+\lambda_4<0\Big)\Big)\Big) \vee 2\lambda_1+\lambda_4>0\Big)\end{aligned} \tag{B.27}$$

$$\begin{aligned}&\textbf{direction 3}: \\ &\lambda>0 \wedge \lambda_2+\lambda_3>0 \wedge 2\lambda_2+\lambda_3>0 \wedge \sqrt{\lambda(\lambda_2+\lambda_3)}+\lambda_1>0 \wedge \Big(\Big(2\lambda(2\lambda_2+\lambda_3)>(2\lambda_1+\lambda_4)^2 \wedge \\ &\Big(\Big(2\lambda_1+\lambda_4<0 \wedge \frac{(2\lambda_2+\lambda_3)\Big(4\lambda(\lambda_2+\lambda_3)-4\lambda_1^2+\lambda_4^2\Big)}{2\lambda_1+\lambda_4}<0\Big) \vee \\ &\Big((\lambda_2+\lambda_3)(2\lambda_2+\lambda_3-2)>0 \wedge \sqrt{2}\sqrt{\lambda_3(\lambda_2+\lambda_3)\Big((2\lambda_1+\lambda_4)^2-2\lambda(2\lambda_2+\lambda_3)\Big)}>2\lambda_1\lambda_3 \\ &+2\lambda_4(\lambda_2+\lambda_3)\Big)\Big)\Big) \vee 2\lambda_1+\lambda_4>0\Big)\end{aligned} \tag{B.28}$$

$$\begin{aligned}&\textbf{direction 4}: \\ &\lambda>0 \wedge \lambda_2+\lambda_3>0 \wedge \sqrt{\lambda(\lambda_2+\lambda_3)}+\lambda_1+\lambda_4>0 \\ &\wedge\Big(\Big(\frac{(\lambda_2+\lambda_3)\Big(-\lambda\lambda_2^2+\lambda_1^2(\lambda_2-\lambda_3)+2\lambda_1\lambda_2\lambda_4\Big)}{\lambda_1\lambda_2}>0 \\ &\wedge\Big(\Big(\lambda_2>0 \wedge \lambda(\lambda_2+\lambda_3)>\lambda_1^2 \wedge \lambda_1<0\Big) \vee (\lambda_1>0 \wedge \lambda_3(2\lambda_2+\lambda_3)>0 \wedge \lambda_2<0)\Big)\Big) \\ &\vee(\lambda_1>0 \wedge \lambda_2>0) \vee \Big(\lambda(\lambda_2+\lambda_3)>\lambda_1^2 \wedge \lambda_3(2\lambda_2+\lambda_3)>0 \\ &\wedge\sqrt{\lambda_3(2\lambda_2+\lambda_3)\Big(\lambda(\lambda_2+\lambda_3)-\lambda_1^2\Big)}+\lambda_1\lambda_3+\lambda_4(\lambda_2+\lambda_3)>0\Big)\Big)\end{aligned} \tag{B.29}$$

$$\begin{aligned}&\textbf{direction 5}: \\ &\lambda>0 \wedge \lambda_2+\lambda_3>0 \wedge \sqrt{\lambda(\lambda_2+\lambda_3)}+\lambda_1>0 \wedge \\ &\Big(\Big(\frac{(\lambda_2+\lambda_3)\Big(\lambda\lambda_2^2+\lambda_1^2(\lambda_3-\lambda_2)+2\lambda_1\lambda_3\lambda_4+\lambda_4^2(\lambda_2+\lambda_3)\Big)}{\lambda_2(\lambda_1+\lambda_4)}<0 \wedge \\ &\Big((\lambda_3(2\lambda_2+\lambda_3)>0 \wedge \lambda_1+\lambda_4>0 \wedge \lambda_2<0) \vee \Big(\lambda_2>0 \wedge \lambda(\lambda_2+\lambda_3)>(\lambda_1+\lambda_4)^2 \\ &\wedge\lambda_1+\lambda_4<0\Big)\Big)\Big) \vee (\lambda_2>0 \wedge \lambda_1+\lambda_4>0) \vee \Big(\lambda(\lambda_2+\lambda_3)>(\lambda_1+\lambda_4)^2 \wedge \lambda_3(2\lambda_2+\lambda_3)>0 \\ &\wedge\sqrt{-\lambda_3(2\lambda_2+\lambda_3)\Big((\lambda_1+\lambda_4)^2-\lambda(\lambda_2+\lambda_3)\Big)}+\lambda_1\lambda_3>\lambda_2\lambda_4\Big)\Big)\end{aligned} \tag{B.30}$$

direction 6 :

$$\lambda > 0 \wedge \lambda_2 + \lambda_3 > 0 \wedge \sqrt{\lambda(\lambda_2 + \lambda_3)} + \lambda_1 > 0$$
$$\wedge\Big(\lambda_1 + \lambda_4 > 0 \vee \Big(\lambda(\lambda_2 + \lambda_3) > (\lambda_1 + \lambda_4)^2 \wedge \lambda_4 < 0\Big)\Big) \tag{B.31}$$

direction 7 :

$$\lambda > 0 \wedge 2\lambda_2 + \lambda_3 > 0 \wedge \lambda_2 + \lambda_3 > 0 \wedge \sqrt{\lambda(4\lambda_2 + 2\lambda_3)} + 2\lambda_1 + \lambda_4 > 0 \wedge \Big(\Big(\lambda(\lambda_2 + \lambda_3) > \lambda_1^2 \wedge$$
$$\Big(\Big(\lambda_1(2\lambda_2 + 3\lambda_3) + 2\lambda_4(\lambda_2 + \lambda_3) > \frac{2\lambda(\lambda_2 + \lambda_3)^2}{\lambda_1} \wedge \lambda_1 < 0\Big) \vee \sqrt{2}\sqrt{\lambda_3(\lambda_2 + \lambda_3)\Big(\lambda_1^2 - \lambda(\lambda_2 + \lambda_3)\Big)}$$
$$+\lambda_4(\lambda_2 + \lambda_3) > 0\Big)\Big) \vee \lambda_1 > 0\Big) \tag{B.32}$$

direction 8 :

$$\lambda > 0 \wedge 2\lambda_2 + \lambda_3 > 0 \wedge \lambda_2 + \lambda_3 > 0 \wedge \sqrt{\lambda(4\lambda_2 + 2\lambda_3)} + 2\lambda_1 + \lambda_4 > 0 \wedge$$
$$\Big(\Big(\lambda(\lambda_2 + \lambda_3) > (\lambda_1 + \lambda_4)^2 \wedge \Big(\Big(\sqrt{2}\sqrt{\lambda_3(\lambda_2 + \lambda_3)\Big((\lambda_1 + \lambda_4)^2 - \lambda(\lambda_2 + \lambda_3)\Big)} > \lambda_4(\lambda_2 + \lambda_3) \wedge \lambda_3 < 0\Big)$$
$$\vee\Big(2\lambda_1\lambda_2 + 3\lambda_1\lambda_3 + \lambda_3\lambda_4 > \frac{2\lambda(\lambda_2 + \lambda_3)^2}{\lambda_1 + \lambda_4} \wedge \lambda_1 + \lambda_4 < 0\Big)\Big)\Big) \vee \lambda_1 + \lambda_4 > 0\Big) \tag{B.33}$$

direction 9 :

$$\lambda > 0 \wedge 2\lambda_2 + \lambda_3 > 0 \wedge \sqrt{\lambda(4\lambda_2 + 2\lambda_3)} + 2\lambda_1 + \lambda_4 > 0$$
$$\wedge\Big(2\lambda(2\lambda_2 + \lambda_3) > (2\lambda_1 + \lambda_4)^2 \vee 2\lambda_1 + \lambda_4 > 0\Big) \tag{B.34}$$

direction 10 :

$$\lambda > 0 \wedge \lambda_2 + \lambda_3 > 0 \wedge \sqrt{\lambda(\lambda_2 + \lambda_3)} + \lambda_1 + \lambda_4 > 0 \wedge \Big(\lambda_1 > 0 \vee \lambda(\lambda_2 + \lambda_3) > \lambda_1^2 \vee \lambda_4 > 0\Big) \tag{B.35}$$

We emphasize that all the above BFB conditions are contained in the general solution given by Eqs. (6.1 - 6.3).

Appendix C.

For completeness we give in subsections C.1 and C.2 a partial list of the couplings in the DTHM that are relevant respectively to the discussion in section 8 and to the derivation of the results of section 5.

C.1 Higgs-gauge boson couplings & triple Higgs couplings

Shifting the neutral fields according to Eq. (2.26), and using the relations between the physical and non-physical state bases,

$$\begin{pmatrix} h \\ \xi^0 \end{pmatrix} = \mathcal{R}_\alpha \begin{pmatrix} h^0 \\ H^0 \end{pmatrix}, \qquad \begin{pmatrix} Z_1 \\ Z_2 \end{pmatrix} = \mathcal{R}_\beta \begin{pmatrix} G^0 \\ A^0 \end{pmatrix} \tag{C.1}$$

$$\begin{pmatrix} \phi^\pm \\ \delta^\pm \end{pmatrix} = \mathcal{R}_{\beta'} \begin{pmatrix} G^\pm \\ H^\pm \end{pmatrix} \tag{C.2}$$

whith $\mathcal{R}_\alpha, \mathcal{R}_\beta$ and $\mathcal{R}_{\beta'}$ as defined in Eqs.(2.12, 2.23), one extracts from the kinetic terms and the covariant derivatives, Eqs. (2.1, 2.2, 2.3), the couplings involving Higgs bosons and gauge bosons, and from the potential, Eq. (2.4), the triple Higgs couplings.

We list below some of the resulting Feynman rules and provide also approximate expressions in the limit of very small mixing between the triplet and doublet Higgs multiplets, (i.e $s_\alpha = \mathcal{O}(v_t^2/v_d^2)$, $c_{\alpha,\beta,\beta'} = 1 + \mathcal{O}(v_t^2/v_d^2)$, $s_\beta = 2v_t/v_d + \mathcal{O}(v_t^2/v_d^2)$ and $s_{\beta'} = \sqrt{2}v_t/v_d + \mathcal{O}(v_t^2/v_d^2)$).

$$h^0ZZ = +i\frac{g}{c_W}m_Z(c_\alpha c_\beta + 2s_\alpha s_\beta)g_{\mu\nu} \approx i\frac{g}{c_W}m_Z g_{\mu\nu} \tag{C.3}$$

$$H^0ZZ = -i\frac{g}{c_W}m_Z(s_\alpha c_\beta - 2c_\alpha s_\beta)g_{\mu\nu} \approx 4i\frac{g}{c_W}\frac{v_t}{v_d}m_Z g_{\mu\nu} \tag{C.4}$$

$$h^0W^+W^- = igc_W m_Z(c_\alpha c_\beta + s_\alpha s_\beta)g_{\mu\nu} \approx igm_W g_{\mu\nu} \tag{C.5}$$

$$H^0W^+W^- = -igm_W(s_\alpha c_\beta - c_\alpha s_\beta)g_{\mu\nu} \approx 2igm_W\frac{v_t}{v_d}g_{\mu\nu} \tag{C.6}$$

$$h^0A^0Z = -\frac{g}{2c_W}(c_\alpha s_\beta - 2c_\beta s_\alpha)(p_h - p_A)_\mu \approx -\frac{g}{c_W}\frac{v_t}{v_d}(p_h - p_A)_\mu \tag{C.7}$$

$$H^0A^0Z = \frac{g}{2c_W}(s_\alpha s_\beta + 2c_\alpha c_\beta)(p_H - p_A)_\mu \approx \frac{g}{c_W}(p_H - p_A)_\mu \tag{C.8}$$

$$\begin{aligned} h^0h^0H^0 &= i\,(\,(\frac{3}{2}\lambda c_\alpha^2 - \lambda_{14}^+)s_\alpha v_d - 6\lambda_{23}^+ c_\alpha s_\alpha^2 v_t + (c_\alpha^2 - 2s_\alpha^2)(\sqrt{2}c_\alpha\mu - \lambda_{14}^+(s_\alpha v_d + c_\alpha v_t))\,) \\ &\approx i\,(\,\sqrt{2}\mu + (3\lambda - 5(\lambda_1 + \lambda_4))v_t\,) + \mathcal{O}(v_t^2) \end{aligned} \tag{C.9}$$

$$h^0W^+H^- = i\frac{g}{2}(c_\alpha s_{\beta'} - \sqrt{2}s_\alpha c_{\beta'})(p_h - p_{H^-})_\mu \approx +i\frac{g}{\sqrt{2}}\frac{v_t}{v_d}(p_h - p_{H^-})_\mu \tag{C.10}$$

$$H^0W^+H^- = -i\frac{g}{2}(s_\alpha s_{\beta'} + \sqrt{2}c_\alpha c_{\beta'})(p_H - p_{H^-})_\mu \approx -i\frac{g}{\sqrt{2}}(p_H - p_{H^-})_\mu \tag{C.11}$$

$$A^0W^+H^- = \frac{g}{2}(\sqrt{2}c_{\beta'}c_\beta + s_{\beta'}s_\beta)(p_{A^0} - p_{H^-})_\mu \approx \frac{g}{\sqrt{2}}(p_{A^0} - p_{H^-})_\mu \tag{C.12}$$

$$Z_\mu W_\nu^+ H^- = gm_Z(c_\beta s_{\beta'} s_W^2 - \frac{s_\beta c_{\beta'}}{\sqrt{2}}(1 + s_W^2))g_{\mu\nu} \approx -\sqrt{2}g\frac{m_Z v_t}{v_d}g_{\mu\nu} \tag{C.13}$$

$$H^{++}H^-W_\mu^- = igc_{\beta'}(p_{H^{++}} - p_{H^-})_\mu \approx ig(p_{H^{++}} - p_{H^-})_\mu \tag{C.14}$$

$$H^{++}W_\mu^-W_\nu^- = -i\sqrt{2}g^2 v_t g_{\mu\nu} \tag{C.15}$$

$$H^{++}H^-H^- = -i(2\mu s_{\beta'}^2 + c_{\beta'}\,(\lambda_4\, s_{\beta'}\, v_d - \sqrt{2}\,\lambda_3\, c_{\beta'}\, v_t)) \tag{C.16}$$

$$H^{++}H^{--}VV' = 8ie_V e_{V'}g_{\mu\nu} \tag{C.17}$$

$$H^{++}H^{--}V = -2ie_V(p_{H^{++}} - p_{H^{--}})_\mu \tag{C.18}$$

$$H^+H^-VV' = 2ie_V e_{V'}\; g_{\mu\nu} \tag{C.19}$$

$$H^+H^-V = -ie_V(p_{H^+} - p_{H^-})_\mu \tag{C.20}$$

$$G^+G^-VV' = 2ie_V e_{V'}\; g_{\mu\nu} \tag{C.21}$$

$$G^+G^-V = -ie_V(p_{G^+} - p_{G^-})_\mu \tag{C.22}$$

where in Eqs. (C.17 - C.22) we denote by V and V' the γ or Z gauge boson, with the couplings satisfying $e_\gamma \equiv e$ and $e_Z \equiv e\cot 2\theta_W$. We also adopted the convention that all momenta are incoming at each vertex.

C.2 Quartic scalar couplings in the doublet-triplet basis

Here we give the complete list of Feynman rules for the quartic scalar couplings in the unrotated basis which were used in section 5 to determine the unitarity constraints:

$$
\begin{aligned}
&\delta^+\ \delta^+\ \delta^-\ \delta^- = -2i(2\lambda_2+\lambda_3) \quad , && Z_2\ Z_2\ \phi^-\ \phi^+ = -i(\lambda_1)\\
&\delta^+\ \delta^-\ \delta^{--}\ \delta^{++} = -2i(\lambda_2+\lambda_3) \quad , && Z_1\ Z_1\ \phi^-\ \phi^+ = -i\tfrac{1}{2}\lambda\\
&\delta^{++}\ \delta^{++}\ \delta^{--}\ \delta^{--} = -4i(\lambda_2+\lambda_3) \quad , && \phi^-\ \phi^-\ \phi^+\ \phi^+ = -i\lambda\\
&\delta^+\ \delta^+\ \delta^{--}\ Z_2 = \sqrt{2}\lambda_3 \quad , && \delta^+\ \delta^+\ \delta^{--}\ \xi^0 = i\sqrt{2}\lambda_3\\
&\delta^-\ \delta^-\ \delta^{++}\ Z_2 = -\sqrt{2}\lambda_3 \quad , && \delta^-\ \delta^-\ \delta^{++}\ \xi^0 = i\sqrt{2}\lambda_3\\
&\delta^-\ \delta^+\ Z_2\ Z_2 = -2i(\lambda_2+\lambda_3) \quad , && \delta^+\ Z_1\ \phi^-\ \xi^0 = \tfrac{\lambda_4}{2\sqrt{2}}\\
&Z_2\ Z_2\ Z_2\ Z_2 = -6i(\lambda_2+\lambda_3) \quad , && \delta^-\ Z_1\ \phi^+\ \xi^0 = \tfrac{-\lambda_4}{2\sqrt{2}}
\end{aligned}
$$

$$
\begin{aligned}
&\delta^{++}\ \delta^{--}\ Z_2\ Z_2 = -2i\lambda_2 \quad , && \delta^-\ \delta^+\ \xi^0\ \xi^0 = -2i(\lambda_2+\lambda_3)\\
&\delta^+\ \delta^-\ Z_1\ Z_1 = -\tfrac{i}{2}(2\lambda_1+\lambda_4) \quad , && \delta^{--}\ \delta^{++}\ \xi^0\ \xi^0 = -2i\lambda_2\\
&\delta^{++}\ \delta^{--}\ Z_1\ Z_1 = -i(\lambda_1) \quad , && Z_2\ Z_2\ \xi^0\ \xi^0 = -2i(\lambda_2+\lambda_3)\\
&Z_2\ Z_2\ Z_1\ Z_1 = -i(\lambda_1+\lambda_4) \quad , && Z_1\ Z_1\ \xi^0\ \xi^0 = -i(\lambda_1+\lambda_4)\\
&Z_1\ Z_1\ Z_1\ Z_1 = -\tfrac{3}{2}i\lambda \quad , && \phi^-\ \phi^+\ \xi^0\ \xi^0 = -i(\lambda_1)\\
&\delta^{++}\ \delta^-\ Z_1\ \phi^- = -\tfrac{\lambda_4}{2} \quad , && \xi^0\ \xi^0\ \xi^0\ \xi^0 = -6i(\lambda_2+\lambda_3)\\
&\delta^+\ \phi^-\ Z_1\ Z_2 = -\tfrac{i\lambda_4}{2\sqrt{2}} \quad , && \delta^-\ \delta^{++}\ \phi^-\ h = \tfrac{i\lambda_4}{2}\\
&\delta^+\ \delta^{--}\ \phi^+\ Z_1 = \tfrac{\lambda_4}{2} \quad , && \delta^+\ \phi^-\ Z_2\ h = -\tfrac{\lambda_4}{2\sqrt{2}}\\
&\delta^-\ \phi^+\ Z_2\ Z_1 = -\tfrac{i\lambda_4}{2\sqrt{2}} \quad , && \delta^+\ \delta^{--}\ \phi^+\ h = \tfrac{i\lambda_4}{2}\\
&\delta^-\ \delta^+\ \phi^+\ \phi^- = -\tfrac{i}{2}(2\lambda_1+\lambda_4) \quad , && \delta^-\ Z_2\ \phi^+\ h = \tfrac{\lambda_4}{2\sqrt{2}}\\
&\delta^{--}\ \delta^{++}\ \phi^+\ \phi^- = -i(\lambda_1+\lambda_4) \quad , && \delta^+\ \xi^0\ h\ \phi^- = -\tfrac{i\lambda_4}{2\sqrt{2}}\\
&\delta^-\ \phi^+\ \xi^0\ h = -\tfrac{i\lambda_4}{2\sqrt{2}} \quad , && Z_2\ Z_2\ h\ h = -i(\lambda_4+\lambda_1)\\
&\delta^-\ \delta^+\ h\ h = -\tfrac{i}{2}(2\lambda_1+\lambda_4) \quad , && Z_1\ Z_1\ h\ h = -i\tfrac{\lambda}{2}\\
&\delta^{--}\ \delta^{++}\ h\ h = -i(\lambda_1) \quad , && \phi^+\ \phi^-\ h\ h = -i\tfrac{\lambda}{2}\\
&h\ h\ \xi^0\ \xi^0 = -i(\lambda_1+\lambda_4) \quad , && h\ h\ h\ h = -i\tfrac{3\lambda}{2}
\end{aligned}
$$

One can read off from this list the μ-independent part of the triple scalar couplings, by making the substitutions $Z_1 \to -iv_d, h \to v_d$ or $Z_2 \to -iv_t, \xi^0 \to v_t$ (cf. Eq. (2.26)) in the appropriate vertices and modifying accordingly the symmetry factors for identical fields.

References

[1] Guido Altarelli. Status of Neutrino Masses and Mixing in 2010. 2010.

[2] Steven Weinberg. Baryon and Lepton Nonconserving Processes. *Phys. Rev. Lett.*, 43:1566–1570, 1979.

[3] M. Gell-Mann, P. Ramond, and Slansky R. . In *Supergravity*, ed. D. Freedman *et al.*, North-Holland, 1979.

[4] Tsutomu Yanagida. Horizontal gauge symmetry and masses of neutrinos. In Proceedings of the Workshop on the Baryon Number of the Universe and Unified Theories, Tsukuba, Japan, 13-14 Feb 1979.

[5] Rabindra N. Mohapatra and Goran Senjanovic. Neutrino mass and spontaneous parity nonconservation. *Phys. Rev. Lett.*, 44:912, 1980.

[6] W. Konetschny and W. Kummer. Nonconservation of Total Lepton Number with Scalar Bosons. *Phys. Lett.*, B70:433, 1977.

[7] T. P. Cheng and Ling-Fong Li. Neutrino Masses, Mixings and Oscillations in SU(2) x U(1) Models of Electroweak Interactions. *Phys. Rev.*, D22:2860, 1980.

[8] George Lazarides, Q. Shafi, and C. Wetterich. Proton Lifetime and Fermion Masses in an SO(10) Model. *Nucl. Phys.*, B181:287, 1981.

[9] J. Schechter and J. W. F. Valle. Neutrino Masses in SU(2) x U(1) Theories. *Phys. Rev.*, D22:2227, 1980.

[10] Rabindra N. Mohapatra and Goran Senjanovic. Neutrino Masses and Mixings in Gauge Models with Spontaneous Parity Violation. *Phys. Rev.*, D23:165, 1981.

[11] Robert Foot, H. Lew, X. G. He, and Girish C. Joshi. Seesaw Neutrino Masses Induced by a Triplet of Leptons. *Z. Phys.*, C44:441, 1989.

[12] Ernest Ma. Pathways to Naturally Small Neutrino Masses. *Phys. Rev. Lett.*, 81:1171–1174, 1998.

[13] Borut Bajc and Goran Senjanovic. Seesaw at LHC. *JHEP*, 08:014, 2007.

[14] Pavel Fileviez Perez. Renormalizable Adjoint SU(5). *Phys. Lett.*, B654:189–193, 2007.

[15] Pavel Fileviez Perez. Supersymmetric Adjoint SU(5). *Phys. Rev.*, D76:071701, 2007.

[16] A. Abada, C. Biggio, F. Bonnet, M. B. Gavela, and T. Hambye. Low energy effects of neutrino masses. *JHEP*, 12:061, 2007.

[17] Pavel Fileviez Perez, Tao Han, Gui-yu Huang, Tong Li, and Kai Wang. Neutrino Masses and the LHC: Testing Type II Seesaw. *Phys. Rev.*, D78:015018, 2008.

[18] Paramita Dey, Anirban Kundu, and Biswarup Mukhopadhyaya. Some consequences of a Higgs triplet. *J. Phys.*, G36:025002, 2009.

[19] Claude Amsler et al. Review of particle physics. *Phys. Lett.*, B667:1–1340, 2008.

[20] Mu-Chun Chen, Sally Dawson, and Tadas Krupovnickas. Higgs triplets and limits from precision measurements. *Phys. Rev.*, D74:035001, 2006.

[21] T. Blank and W. Hollik. Precision observables in SU(2) x U(1) models with an additional Higgs triplet. *Nucl. Phys.*, B514:113–134, 1998.

[22] Piotr H. Chankowski, Stefan Pokorski, and Jakub Wagner. (Non)decoupling of the Higgs triplet effects. *Eur. Phys. J.*, C50:919–933, 2007.

[23] Mu-Chun Chen, Sally Dawson, and C. B. Jackson. Higgs Triplets, Decoupling, and Precision Measurements. *Phys. Rev.*, D78:093001, 2008.

[24] Sidney R. Coleman. The Fate of the False Vacuum. 1. Semiclassical Theory. *Phys. Rev.*, D15:2929–2936, 1977.

[25] Curtis G. Callan, Jr. and Sidney R. Coleman. The Fate of the False Vacuum. 2. First Quantum Corrections. *Phys. Rev.*, D16:1762–1768, 1977.

[26] Marc Sher. Electroweak Higgs Potentials and Vacuum Stability. *Phys. Rept.*, 179:273–418, 1989.

[27] Abdul Wahab El Kaffas, Wafaa Khater, Odd Magne Ogreid, and Per Osland. Consistency of the Two Higgs Doublet Model and CP violation in top production at the LHC. *Nucl. Phys.*, B775:45–77, 2007.

[28] Thomas Appelquist and J.D. Bjorken. On weak interactions at high-energies. *Phys.Rev.*, D4:3726, 1971.

[29] John M. Cornwall, David N. Levin, and George Tiktopoulos. Derivation of Gauge Invariance from High-Energy Unitarity Bounds on the s Matrix. *Phys.Rev.*, D10:1145, 1974.

[30] Benjamin W. Lee, C. Quigg, and H.B. Thacker. Weak Interactions at Very High-Energies: The Role of the Higgs Boson Mass. *Phys.Rev.*, D16:1519, 1977.

[31] Shinya Kanemura, Takahiro Kubota, and Eiichi Takasugi. Lee-Quigg-Thacker bounds for Higgs boson masses in a two doublet model. *Phys. Lett.*, B313:155–160, 1993.

[32] Andrew G. Akeroyd, Abdesslam Arhrib, and El-Mokhtar Naimi. Note on tree-level unitarity in the general two Higgs doublet model. *Phys. Lett.*, B490:119–124, 2000.

[33] Mayumi Aoki and Shinya Kanemura. Unitarity bounds in the Higgs model including triplet fields with custodial symmetry. *Phys. Rev.*, D77:095009, 2008.

[34] Ilia Gogoladze, Nobuchika Okada, and Qaisar Shafi. Higgs Boson Mass Bounds in the Standard Model with Type III and Type I Seesaw. *Phys.Lett.*, B668:121–125, 2008.

[35] H.M. Pilkuhn. Relativistic Particle Physics. Springer-Verlag, 1979.

[36] M. Luscher and P. Weisz. Is There a Strong Interaction Sector in the Standard Lattice Higgs Model? *Phys.Lett.*, B212:472, 1988.

[37] William J. Marciano, G. Valencia, and S. Willenbrock. Renormalization group improved unitarity bounds on the Higgs boson and top quark masses. *Phys.Rev.*, D40:1725, 1989.

[38] A. G. Akeroyd and Cheng-Wei Chiang. Phenomenology of Large Mixing for the CP-even Neutral Scalars of the Higgs Triplet Model. *Phys. Rev.*, D81:115007, 2010.

[39] A. G. Akeroyd, Mayumi Aoki, and Hiroaki Sugiyama. Probing Majorana Phases and Neutrino Mass Spectrum in the Higgs Triplet Model at the LHC. *Phys. Rev.*, D77:075010, 2008.

[40] F. del Aguila and J. A. Aguilar-Saavedra. Distinguishing seesaw models at LHC with multi-lepton signals. *Nucl. Phys.*, B813:22–90, 2009.

[41] A. G. Akeroyd, Mayumi Aoki, and Hiroaki Sugiyama. Lepton Flavour Violating Decays tau to lll and mu to e gamma in the Higgs Triplet Model. *Phys. Rev.*, D79:113010, 2009.

[42] Takeshi Fukuyama, Hiroaki Sugiyama, and Koji Tsumura. Constraints from muon g-2 and LFV processes in the Higgs Triplet Model. *JHEP*, 03:044, 2010.

[43] A. G. Akeroyd and Cheng-Wei Chiang. Doubly charged Higgs bosons and three-lepton signatures in the Higgs Triplet Model. *Phys. Rev.*, D80:113010, 2009.

[44] S. T. Petcov, H. Sugiyama, and Y. Takanishi. Neutrinoless Double Beta Decay and $H^{\pm\pm} \to l'^{\pm} l^{\pm}$ Decays in the Higgs Triplet Model. *Phys. Rev.*, D80:015005, 2009.

[45] Takeshi Fukuyama, Hiroaki Sugiyama, and Koji Tsumura. Phenomenology in the Higgs Triplet Model with the A4 Symmetry. *Phys. Rev.*, D82:036004, 2010.

[46] A.G. Akeroyd, Cheng-Wei Chiang, and Naveen Gaur. Leptonic signatures of doubly charged Higgs boson production at the LHC. *JHEP*, 1011:005, 2010.

[47] E. Accomando et al. Workshop on CP Studies and Non-Standard Higgs Physics. 2006.

[48] A. G. Akeroyd. Higgs triplets at LEP-2. *Phys. Lett.*, B353:519–525, 1995.

[49] J. F. Gunion, C. Loomis, and K. T. Pitts. Searching for doubly charged Higgs bosons at future colliders. 1996.

[50] J. F. Gunion, R. Vega, and J. Wudka. Higgs triplets in the standard model. *Phys. Rev.*, D42:1673–1691, 1990.

[51] Chian-Shu Chen, Chao-Qiang Geng, and Dmitry V. Zhuridov. Searching for doubly charged Higgs bosons in Móller scattering by resonance effects at linear e^-e^- collider. *Eur. Phys. J.*, C60:119–124, 2009.

[52] Dilip Kumar Ghosh, Rohini M. Godbole, and Biswarup Mukhopadhyaya. Unusual charged Higgs signals at LEP-2. *Phys. Rev.*, D55:3150–3155, 1997.

[53] King-man Cheung, Roger J. N. Phillips, and Apostolos Pilaftsis. Signatures of Higgs triplet representations at TeV e+ e- colliders. *Phys. Rev.*, D51:4731–4737, 1995.

[54] Rohini Godbole, Biswarup Mukhopadhyaya, and Marek Nowakowski. Triplet Higgs bosons at e+ e- colliders. *Phys. Lett.*, B352:388–393, 1995.

[55] K. Huitu, J. Maalampi, A. Pietila, and M. Raidal. Doubly charged Higgs at LHC. *Nucl. Phys.*, B487:27–42, 1997.

[56] G. Azuelos, K. Benslama, and J. Ferland. Prospects for the search for a doubly-charged Higgs in the left-right symmetric model with ATLAS. *J. Phys.*, G32:73–92, 2006.

[57] Vernon D. Barger, H. Baer, Wai-Yee Keung, and R. J. N. Phillips. Decays of Weak Vector Bosons and t Quarks into Doubly Charged Higgs Scalars. *Phys. Rev.*, D26:218, 1982.

[58] A. G. Akeroyd and Mayumi Aoki. Single and pair production of doubly charged Higgs bosons at hadron colliders. *Phys. Rev.*, D72:035011, 2005.

[59] P. Achard et al. Search for doubly charged Higgs bosons at LEP. *Phys. Lett.*, B576:18–28, 2003.

[60] G. Abbiendi et al. Search for doubly charged Higgs bosons with the OPAL detector at LEP. *Phys. Lett.*, B526:221–232, 2002.

[61] J. Abdallah et al. Search for doubly charged Higgs bosons at LEP2. *Phys. Lett.*, B552:127–137, 2003.

[62] V. M. Abazov et al. Search for doubly-charged Higgs boson pair production in the decay to $\mu^+\mu^+\mu^-\mu^-$ in $p\bar{p}$ collisions at $\sqrt{s} = 1.96$ TeV. *Phys. Rev. Lett.*, 93:141801, 2004.

[63] V. M. Abazov et al. Search for pair production of doubly-charged Higgs bosons in the $H^{++}H^{--} \to \mu^+\mu^+\mu^-\mu^-$ final state at D0. *Phys. Rev. Lett.*, 101:071803, 2008.

[64] Darin E. Acosta et al. Search for doubly-charged Higgs bosons decaying to dileptons in $p\bar{p}$ collisions at $\sqrt{s} = 1.96$ TeV. *Phys. Rev. Lett.*, 93:221802, 2004.

[65] T. Aaltonen et al. Search for Doubly Charged Higgs Bosons with Lepton-Flavor-Violating Decays involving Tau Leptons. *Phys. Rev. Lett.*, 101:121801, 2008.

[66] Julia Garayoa and Thomas Schwetz. Neutrino mass hierarchy and Majorana CP phases within the Higgs triplet model at the LHC. *JHEP*, 03:009, 2008.

[67] M. Kadastik, M. Raidal, and L. Rebane. Direct determination of neutrino mass parameters at future colliders. *Phys. Rev.*, D77:115023, 2008.

[68] T. Rommerskirchen and T. Hebbeker. Study of pair-produced doubly charged Higgs bosons with a four-muon final state with the CMS detector. *J. Phys.*, G33:N47–N66, 2007.

[69] Eung Jin Chun, Kang Young Lee, and Seong Chan Park. Testing Higgs triplet model and neutrino mass patterns. *Phys. Lett.*, B566:142–151, 2003.

[70] Ping Ren and Zhi-zhong Xing. Interference bands in decays of doubly-charged Higgs bosons to dileptons in the minimal type-II seesaw model at the TeV scale. *Phys. Lett.*, B666:48–56, 2008.

[71] P. Achard et al. Search for charged Higgs bosons at LEP. *Phys. Lett.*, B575:208–220, 2003.

[72] J. Abdallah et al. Search for charged Higgs bosons at LEP in general two Higgs doublet models. *Eur. Phys. J.*, C34:399–418, 2004.

[73] Anindya Datta and Amitava Raychaudhuri. Mass bounds for triplet scalars of the left-right symmetric model and their future detection prospects. *Phys. Rev.*, D62:055002, 2000.

[74] J. Abdallah et al. Searches for neutral Higgs bosons in extended models. *Eur. Phys. J.*, C38:1–28, 2004.

[75] J. A. Aguilar-Saavedra and G. C. Branco. Probing top flavour-changing neutral scalar couplings at the CERN LHC. *Phys. Lett.*, B495:347–356, 2000.

[76] M. Beneke et al. Top quark physics. 2000.

[77] J. A. Aguilar-Saavedra. Top flavor changing neutral coupling signals at a linear collider. *Phys. Lett.*, B502:115–124, 2001.

[78] J. A. Aguilar-Saavedra. Top flavor-changing neutral interactions: Theoretical expectations and experimental detection. *Acta Phys. Polon.*, B35:2695–2710, 2004.

[79] K Nakamura et al. Review of particle physics. *J.Phys.G*, G37:075021, 2010.